Design, construction and testing of a photoactivatable and diffusive protein network in Saccharomyces cerevisiae

Bury, A.E.

Publication date
2019

Document Version
Final published version

License
Other

Design, construction and testing of a photoactivatable and diffusive protein network in *Saccharomyces cerevisiae*

Aleksandra E. Bury

Design, construction and testing of a photoactivatable and diffusive protein network in *Saccharomyces cerevisiae*

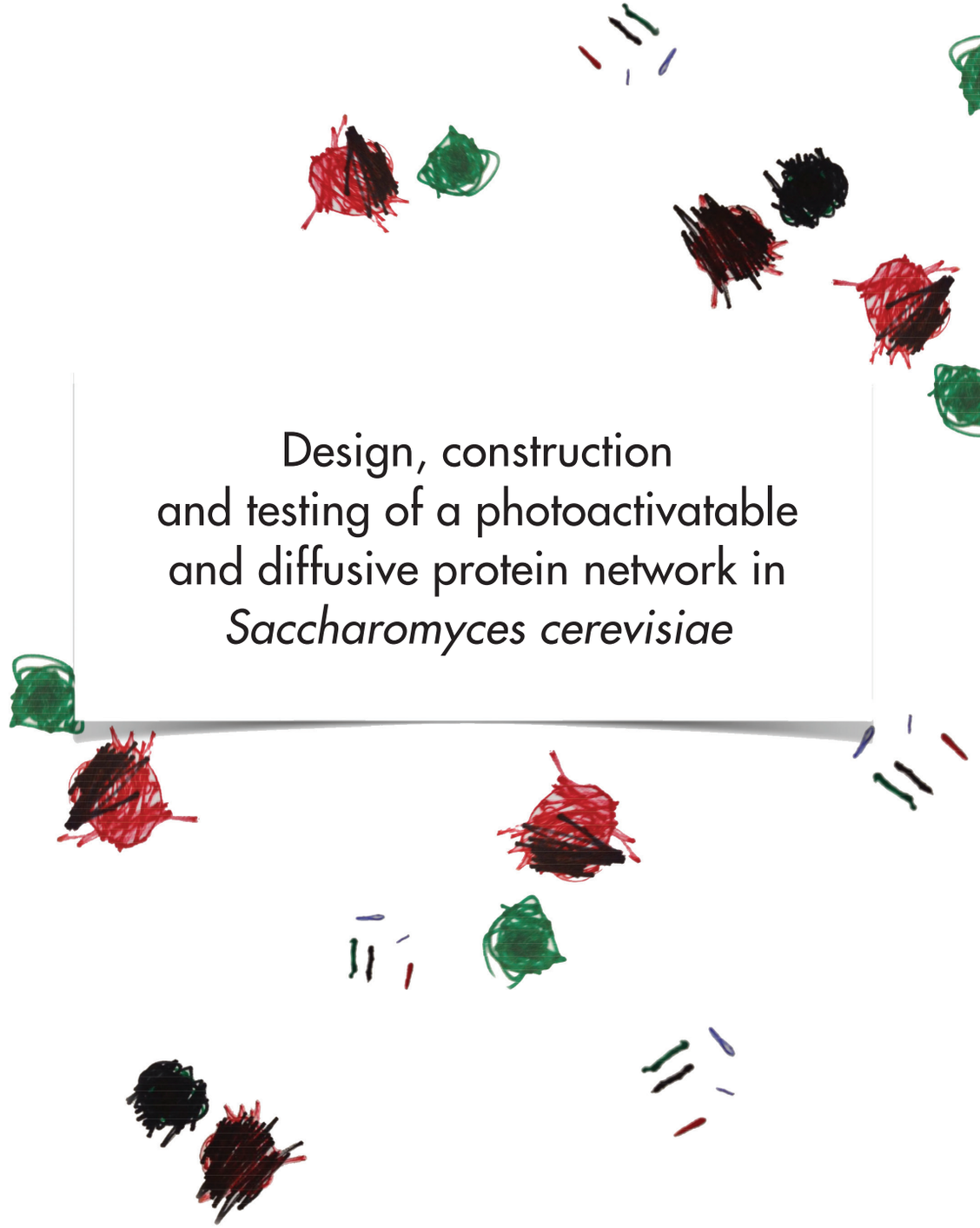

Aleksandra E. Bury

Design, construction and testing of a photoactivatable and diffusive protein network in *Saccharomyces cerevisiae*.

Aleksandra Ewa Bury

Design, construction and testing of a photoactivatable and diffusive protein network in *Saccharomyces cerevisiae*

Aleksandra Bury

The research reported in this thesis was carried out in the Molecular Microbial Physiology Group of the Swammerdam Institute for Life Sciences, Faculty of Science, University of Amsterdam, Amsterdam, the Netherlands. This work is part of the research program "Spatial design of biochemical regulation networks (SPAT)" with project number 110, which is financed by the Netherlands Organisation for Scientific Research (NWO) through the Foundation for Fundamental Research on Matter (FOM).

Cover: Schematic drawing of the *Saccharomyces cerevisiae* and *Bacillus subtillis* cells observed in the light microscope by H. Pilat, May, 2017.

Cover design: G.J. Pilat

Printed by: Off Page

Design, construction and testing of a photoactivatable and diffusive protein network in *Saccharomyces cerevisiae*

ACADEMISCH PROEFSCHRIFT

ter verkrijging van de graad van doctor

aan de Universiteit van Amsterdam

op gezag van de Rector Magnificus

prof. dr. ir. K.I.J. Maex

ten overstaan van een door het College voor Promoties ingestelde

commissie, in het openbaar te verdedigen in de Agnietenkapel

op 3 april 2019, te 10.00 uur

door

Aleksandra Ewa Bury

geboren te Myszków

Promotiecommissie:

Promotor: Prof. Dr. K.J. Hellingwerf	Universiteit van Amsterdam
Copromotor: Dr. F. Branco dos Santos	Universiteit van Amsterdam

Overige leden:

Prof. Dr. A. Möglich	Universität Bayreuth, Germany
Prof. Dr. A. M. Dogterom	Technische Universiteit Delft
Prof. Dr. J. T. M. Kennis	Vrije Universiteit Amsterdam
Dr. M. A. Hink	Universiteit van Amsterdam
Dr. G. J. Smits	Universiteit van Amsterdam
Prof. Dr. L. W. Hamoen	Universiteit van Amsterdam

Faculteit der Natuurwetenschappen, Wiskunde en Informatica

Table of Contents

1 General introduction

Bury AE, Hellingwerf KJ

1.1 Microbiology: single cells, the basic units of life

The basic unit of life is the (single) cell, be it of prokaryotic or eukaryotic nature, although meaningful higher forms of organization, up to level of Gaia, can be defined. All basic attributes of life, i.e. growth, reproduction, adaptation to changes in the environment, and evolution, are observable – and can be engineered – already at this basic level. [1] Such engineering is key in a society that aims at supporting a growing world population in a sustainable way, to allow exploitation of the exquisite specificity and efficiency of biocatalysis in so-called cell-factories. [2, 3]

The majority of this engineering is aimed at inventing and selecting new-, and optimizing existing, metabolic pathways. [4, 5] Nevertheless, ultimately, such metabolic engineering will have to be complemented with adjustment of the signal-transduction network (components) of the engineered cell (factory). To be able to do this rationally, a thorough understanding of the signal transduction processes is required. This study was initiated to contribute to this latter aspect.

1.2 Signal transduction systems, and networks, in pro- and eukaryotic organisms

Fluctuating and/or oscillating environmental conditions (i.e. physical parameters and concentrations of key molecules) make it necessary for cells to adjust; mostly through adjustment of the level of gene expression, and occasionally via the adjustment of enzyme activity. From this it follows that information about these changing conditions has to be transferred across the cell envelope, and in eukaryotic cells, often across an organelle membrane barrier. To facilitate this signal transfer, both prokaryotic and eukaryotic cells are equipped with a plethora of dedicated signal transduction systems. In prokaryotes the most abundant systems are: the one- and two-component systems, the cyclic-di-GMP responsive systems, quorum sensing systems (responding e.g. to homo-serine lactones or short peptides) and various types of (protein) kinases (for reviews see [6, 7]). Eukaryotic cells make use of the same basic types of signal transduction system see e.g. [8, 9], be it often with less redundancy), but have expanded their repertoire considerably. In lower eukaryotes, like *Saccharomyces cerevisiae*, these are first of all the RAS/cAMP pathways and the MAP kinase pathways. In higher eukaryotes one finds an even more expanded repertoire, with e.g. tyrosine kinases, Toll-like receptors, steroid receptors, proteins of the apoptotic Bcl2/Bax family, p53, and transcriptional activators of the NFκB, Fos, and Myc families.[10]

In prokaryotes many signal transduction components function in rather linear-, and isolated, signal transduction pathways that relate a single signal straightforwardly to a particular response. It seems that the most typical signal transduction system in these organisms, the so-called two-component systems (for more detail on these systems, see paragraph 1.4 below), have explicitly evolved, and been wired, to display particularly this very aspect. [11] With an explicitly high redundancy, however, of signal transfer systems of one particular kind (like two-component systems, homo-serine-lactone based quorum sensing systems and cyclic-di-GMP based systems), these linear pathways may start to laterally interact, to form a signal transduction network. Network properties are identifiable particularly in the MAP kinase pathways in lower eukaryotes in yeast and e.g. in the photosensory receptor networks in algae and plants. These network properties form a formidable challenge for (i) detailed understanding of these networks, even with the help of advanced forms of mathematical/computational analyses, and (ii) their heteterologous and/or orthogonal expression. Interestingly, such networks may bestow neural-like characteristics on their owners. [7]

1.3 How spatial heterogeneity and cytoplasmic diffusion may influence the regulatory function of signal transduction networks

The inside of the every cell is now generally considered as a crowded environment. [12] Here, the term 'crowded' is used in the meaning to describe the fact that not only the concentration of single compound could be high, but that there are many additional molecules that jointly occupy a significant fraction of the total volume of the cells (up to about 20-30 %). Crowding has an effect on the rates of biochemical reactions and the positioning of their thermodynamic equilibrium. The effect on the reaction rates can be two-fold: First of all, crowding reduces the molecular diffusion rates; the more, the bigger the molecules are. Hence bimolecular reaction rates will slow down. Nevertheless, the crowding increases thermodynamic activity, which tends to increase reaction rates. The net effect of these two opposing trends will depend on the nature and specifics of each reaction. The equilibrium of a reaction is affected by favouring macromolecular association. [13] Initially the concept of crowding was received with considerable scepticism in the biochemical community. Meanwhile, however, a lot has changed. Newly developed methods gave more insight into the crowded intracellular milieu, but quantitatively the molecular crowding still stays poorly understood. A simple way to characterize the degree of molecular crowding is to analyse the

viscosity of a solution, which may be estimated from the diffusion coefficient of a simple probe such as a nanoparticle, organic dye or fluorescent protein. [14–16] Studies in model systems for macromolecular diffusion in the intracellular environment, have revealed that protein diffusion deviates from simple diffusion in dilute systems. Artificial systems that mimic the crowded environment of a cell e.g. are concentrated solutions of globular proteins or random-coil structured polymers. For example, the diffusion of a protein in dextran solution can be described as 'subdiffiusive', where the diffusive exponent α is smaller than 1. The magnitude of this anomalous exponent decreases continuously with increasing concentrations and molecular weight of the 'obstacles' (i.e. the dextran). [17] Besides mathematical prediction of crowding and of the diffusion constant of molecules in a crowded environment, it is also possible to measure how crowded it is in a specific cell. Liu et. al. have reported on a probe that allows sensing of the macromolecular crowding. They designed this probe based on the mCitrine (yellow fluorescent protein, YFP) and the mCeurelean3 (cyan fluorescent protein, CFP). The two fluorescent proteins are connected via a flexible linker and form a FRET (Forster Resonance Energy Transfer) pair. Crowding induces the compression of the two fluorescent proteins, which then can be quantified by measuring their FRET efficiency.[18, 19] Another tool to quantitatively analyze the effect of macromolecular crowding was introduced by Gnutt et al. They synthesized a synthetic probe, based on polyethylene glycol (PEG), a highly soluble, inert, and biocompatible random-coil polymer. The PEG was functionalized by adding the end-groups Atto488 and Atto565, to allow measurement of the mean end-to-end distance of the functionalized PEG by FRET [20], and from that the degree of crowding can be calculated.

As alluded to above, the interior of living cells is now generally considered to be a highly crowded environment, and scientists are actively investigating the effect of this crowding on the functioning of the cellular machinery. Accordingly, it was shown that the crowded intracellular milieu causes 'anomalous diffusion' of proteins, [21] which affects the functioning of biochemical networks. Diffusion of transcription factors can e.g. increase the noise in gene expression. [21] Its effect, via its effect on diffusion, can also be noticed in the characteristics of protein-protein interactions, in which restricted diffusion of proteins can reduce concentration fluctuations.[21–23]

Crowding and diffusion will also have an effect on cellular signalling, particular in those aspects where protein/protein interactions are crucial. An example of this are the phosphorylation-based signal transduction pathways, also referred to as two component

signal transduction pathways, which are commonly utilized by both pro- and eukaryotic micro-organisms. The core of the two component signal transduction pathway is the directed phosphoryl-transfer from a histidine kinase to the cognate response regulator. These systems are described in detail further below. [24] To prevent (unwanted) cross-talk between separate phosphoryl-transfer pathways, a few potential strategies can be foreseen. Taking as an example the MAP kinase signalling pathways, which are evolutionary conserved signalling modules common in many intracellular signalling pathways in eukaryotic organisms, including fungi and yeast. [25] Potential strategies to prevent cross talk in the crowded environment of a yeast cell are: (i) direct interactions between two components in the pathway [26] and (ii) binding components from a single pathway together thorough a scaffold protein. [27] (iii) And also cross-pathway inhibition is possible; this takes place when activity of one pathway is inhibited by output from another pathway. These three mechanisms are very often complemented by 'kinetic isolation', which takes place when one pathway is activated by pulsed input, while another pathway is activated by a slowly, but steadily increasing input signal. [28, 29] These mechanisms ensure that only the relevant response is induced by a very specific power spectrum of stimuli.

1.4 Optogenetics: Triggering signal transduction processes/networks with light/photons

Because of the complex nature of cellular signal transduction networks, and the so far unresolved role of (anomalous) diffusion therein, it is crucial to have the ability to locally and dynamically activate such a network, and analyse the effects of this type of activation in comparison with global activation of the same network. Such local activation can be achieved with microfluidics, [30, 31], especially in the time domain, but with much more precision and variation with light. With lasers, LEDs, light guides and lenses, light can be delivered to live cells with utmost precision with respect to wavelength and intensity, and its temporal- and spatial dimension. With respect to the latter aspect even the diffraction limit can be broken by making use of multiple excitations and/or multi-photon effects (compare e.g. STORM microscopy). [32] These possibilities of control, together with developments in genomics and molecular genetics, have led to the emergence of a new field of research in the life sciences: Optogenetics, an approach in which light is used to control a biological process in a live organism, via an orthogonal, genetically encoded, light-switchable protein. [33] Hence, optogenetics increases the range and degree of control of biological processes,

relative to chemical approaches. [34] Moreover, inexpensive microcontrollers and light emitting diodes (LEDs) are sufficient to create quantitatively precise and dynamically reproducible optical input signals, in ensembles of cells cultured in batch, as well as in single cells. [35]

Over the past decade, light-switchable proteins from phototrophic- and chemotrophic bacteria, eukaryotic micro-organisms and plants, have been engineered for synthetic control of processes in many organisms. These proteins can be switched from their (equilibrium) dark state to a metastable light state by a specific illumination regime with light ranging from the ultraviolet to the near-infrared, dependent on the specific photoactive protein selected (see figure 2). Subsequently, they revert spontaneously back to the ground state thermally in the dark [36], with a rate characteristic for each specific protein. In table 1 we present a few of the examples of the use of light-switchable proteins in *E. coli*, cyanobacteria, yeast, mammalian cells, and brain and liver of mice.

The first use of a broad beam of blue light to evoke action potentials in *Aplysia* ganglion cells was reported by Fork in 1971. [37] But in this study the biological target of the blue photons was unknown. Since that time many groups have tried to optimize illumination-based methods to control neural activity, with the aim to develop a method that is minimally invasive and temporarily precise. [38, 39] Genetically encoded optical control of neuronal activity was finally achieved in 2005 by Boyden et all [40], via selective expression of channelrodopsin 2 in selected parts of the brain and using light to induce and control the generated ion fluxes and action potentials in the mouse brain. So far, a subclass of the rhodopsins, i.e. the channelrhodopsins, that function as photoactivated ion channels in green algae like *Chlamydomonas*, have most widely been used to regulate neuronal activity in different animal model systems. The toolkit of optogenetics, however, is rapidly expanding: By now, also other (bacterial) rhodopsins and photoreceptors from the LOV- and BLUF families have proven to be versatile opotgenetic tools. The advantages of members of the latter two families are that their members are quite small (i.e. about 10 to 14 kDa), and utilize a flavin, which is endogenously synthesized, as their chromophore (which spontaneously incorporates itself into the apoprotein).

Another approach of using light sensitive proteins as an optogenetic tool is to use engineered fusion proteins, like the light activated PA-Rac [41] protein or the light modulated DNA binding protein, LovTAP. [42] Fusion of Rac1 with a LOV2 domain from *Avena sativa* results in a photoactivatable Rac1 fusion protein. Rac1 is a key GTPase, regulating actin

cytoskeleton dynamics in metazoan cells. The LOV domain sterically blocks interactions of Rac1 with its effector (the PAK protein), until irradiation unwinds the helix linking LOV with Rac1, and allows the Rac1 to interact with the PAK. [41]

A light modulated DNA binding optogenetic device can also be obtained by fusing a LOV domain to the Trp repressor from *E. coli*, i.e. a LovTAP construct. Illumination of this fusion protein with blue light causes selective binding to the Trp operator in selected DNA sequences, and protects those sequences from nuclease digestion. [42] For details and more examples of engineered light dependent fusion proteins: see table 1.

1.5 How to link input- and output domains in signal transduction proteins

Designing engineered photoreceptors, by fusion of a light-sensing domain to an output domain, while being derived from non-cognate proteins, is a recently developed tool in the optogenetics field. Before the final product, in the form of a light dependent signal transduction protein, will be available, however, e.g. for application in cell biology or neurobiology, the design principles and strategies for this coupling need to be understood. The design process can be divided into several steps: The first choice is about the photochemical requirements of the photosensor domain. This includes the spectral region to be used for photoreceptor activation (figure 1), reversibility of the photocycle, rate of the reversion to the ground state, and its photostability during continued illumination. Besides that, the requirements for the genetic encoding need to be fulfilled. This includes the optimization of the encoding DNA sequence, through optimization of codon usage, and use of promoters of different strength and with expression specific for a selected cell type, as well as correct subcellular location, which often can be ensured through translation signals. [43, 44]

Table 1. Some examples of optogenetic application of light-switchable proteins.

Organism of origin	Light-switchable protein domain	Effector domain	Organism/tissue in which it is functional	Function of the light-switchable fusion protein	Ref.
Chlamydomonas reinhardtii	ChR2 – channel-rhodopsin 2	Expression of the opsin in brain cells	Mammalian brain	Can be used to evoke single spikes or defined trains of action potentials over a range of frequencies	[45]
Avena sativa	LOV2 (phototropin 1)	Rac1	Metazoan cells	GTPase regulating actin cytoskeletal dynamics, polarized cell movement PA-Rac1	[41]
Avena sativa	LOV2	*E. coli* Trp repressor	*In vitro* study	Light activated DNA binding, LovTAP	[42]
Cyanobacteria	*Synechocystis* phytochrome Cph1	Intracellular histidine kinase domain of EnvZ	*E. coli*	Control of gene expression	[46]
Beggiatoa sp.	BLUF	Adenylate cyclase	*E. coli, Xenopus* oocytes, rat hippocampal pyramidal cells *Drosophila* CNS	Control of the cAMP concentration in cells	[47, 48]
Bacillus subtilis	YtvA LOV domain	FixL histidine kinase domain of *B. japonicum*	*E. coli*	Light-dependent gene expression	[33]
Synechocystis sp. PCC6803	Green-light sensing histidine kinase CcaS	The promotor of *cpcG2*,	Cyanobacteria	Green-light-regulated gene expression system	[49]
Arabidopsis thaliana	FKF1	GIGANTEA (G1)	Mammalian cells	Light-activated dimerization	[50]
Arabidopsis thaliana	phyA and phyB	PIF3	Yeast cells	Light-switchable gene promoter system	[51]
Arabidopsis thaliana	cryptochrome 2	Helix-loop-helix protein *Arabidopsis* CIB1	Mammalian cells	Protein dimerization	[52]
Arabidopsis thaliana,	GIGANTEA and the LOV domain of FKF1	Programmable zinc finger transcription factors	Human cells	Control synthetic zinc finger transcription factor activity	[53]

In the covalent linkage of a sensor domain and effector domain, the sensor domain is usually N-terminal to the effector domain. It has long been known that the linkers between domains play an important role [54, 55] in signal transduction. [33, 43] The design of light dependent signal transduction pathways, with a LOV domain as the light sensing domain, has been described already in several publications. [56, 57] One of the pioneering works in this direction was the design of a LovTAP fusion protein. Photoactivation of the LOV2 domain from *Avena sativa* induces the unfolding of its C-terminal Jα helix. This was utilized in the design of a light-controllable DNA binding protein, in the form of a fusion protein composed of an N-terminal LOV domain with the Trp repressor from *E. coli*. Illumination with the blue light triggers its selective binding to the Trp operator (in its genome) and protects it from nuclease digestion. [42]

Another approach was taken in the design of the PA-Rac1 fusion, mentioned above. The strategy used for this protein was to restrict access to the active site of the effector domain by the dark state of the light-sensitive domain. Illumination then causes unfolding of the Jα helix of the LOV domain and makes the active site of the Rac1 domain accessible. [41] In the design and characterization of the set of YF(n) fusion proteins, Möglich et. al. showed that the length and the heptad periodicity of the Jα helix is crucial for proper propagation of the signal from the light sensing domain (here the LOV domain of YtvA from *Bacillus subtilis*) to the histidine kinase domain of FixL from *Bradyhrizobium jabonicum*. [33, 58] The authors suggest that light absorption in the LOV domain leads to a rotation within the coiled coil structure of the linker domain, which causes the necessary conformational changes within the kinase domain. This coiled coil structure would be formed by parallel dimerization of the – covalently linked - signalling helices. The authors identify a highly conserved DIT motif in the LOV domain, just upstream of the Jα helix, important for this rotary movement. It is important to not disturb the hydrophobic/hydrophilic pattern in the linker between the LOV domain and the kinase domain with changes in the length of the linker, except for multiples of the 7 amino acids repeat sequence, except for single amino acid insertion or deletion. [33]

1.6 Sensory photoreceptors: classes, photochemistry and function

Photoreceptors are widely spread through all Kingdoms of Life. These are proteins that have the ability to sense light (i.e. photons) and send the information of the presence of these stimuli into a diverse range of effectors. [59, 60] Typically, photoreceptor proteins bind a

small molecule, called chromophore, which is able to change its conformation after light absorption. Effectors, either intrinsic or extrinsic to the photoreceptor protein itself, regulate a plethora of output functions, including the physiological effects that underlie circadian rhythms, altered (mostly increased) gene expression (e.g. of virulence factors, light-harvesting antenna proteins and even photoreceptor proteins), and phototropism and protective stress responses. Based on the chemical nature of the chromophore involved, different classes of photoreceptors are distinguished. The most important families are the rhodopsins, the phytochromes, the xanthopsins, the cryptochromes, the phototropins, and the BLUF proteins. In the phytochromes, the xanthopsins and the rhodopsins the photochemical transformation of the respective chromophore (i.e. a linear tetrapyrrole, *p*-coumaric acid and retinal, respectively) is *trans/cis* (or: E/Z) isomerization. Cryptochromes, phototropins (or: LOV domains) and BLUF domains/proteins utilise a flavin as their chromophore, i.e. FMN in LOV domains and FAD in cryptochromes and BLUF domains. For cryptochromes and BLUF proteins, light-induced electron transfer initiates signalling, while the photochemistry of the LOV domains is based on cysteinyl adduct formation between the C4 from the aromatic ring of the flavin and a nearby, fully conserved, cysteine. [61] The chemical structure of each chromophore – in interaction with its protein environment – dictates the colours of light that it can absorb. Figure 1 shows the spectral sensitivity of the above mentioned photoreceptor families.

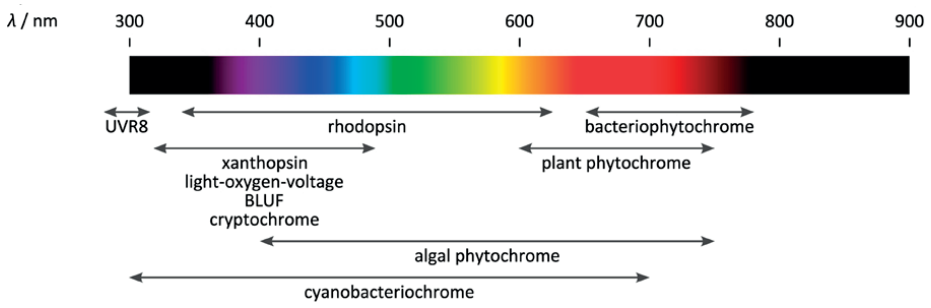

Figure 1. Spectral sensitivity of photoreceptors. The spectral sensitivity of sensory photoreceptors ranges from the UV to the near-infrared region of the electromagnetic spectrum.[62]

Light-oxygen-voltage (LOV) domains/proteins are part of the phototropin family. Phototropins are the most common in plants, where they can initiate photomorphogenesis, including leaf orientation, stomatal opening and chloroplast relocation. Genes that encode a LOV domain were also identified in fungi, algae and bacteria. The LOV domain has the classical PER–ARNT–SIM (PAS) fold, consisting of a five-stranded antiparallel β-sheet (Aβ, Bβ, Gβ, Hβ and Iβ) and helical connector elements (Cα, Dα, Eα and Fα). LOV domains regulate a large and diverse number of processes, in most cases initiated by the initial photochemistry of cysteinyl adduct formation. [63] Significantly, a recent study has shown that signal transduction in a LOV domain is also possible even when it lacks the conserved cysteine residue.[64] The direct effect of cysteinyl adduct formation is protonation of the N5 atom in the flavin ring. This in turn promotes flip of the nearby glutamine residue, which then results in changes in the hydrogen bonding network surrounding the Flavin chromphore. In the LOV domains that lack the conserved cysteinyl residue photoactivation leads to formation of the FMN neutral semiquinone, which also then leads to protonation of the N5 atom within the flavin ring and the subsequent glutamine-flip. [64, 65] These results imply that cysteine-deletion mutants of LOV domains cannot be taken as 'dark controls' in studies of their functional activity *in vivo*.

The bacterial LOV domains are mostly coupled with a histidine kinase domain; their second most common function is regulation of the synthesis and hydrolysis of cyclic di-GMP. Other LOV-domain containing signalling proteins include LOV-STAS proteins (sulphate transporter anti-σ antagonist), LOV-HTH (helix-turn-helix) proteins, that function as transcription factors, and the LOV-SpoIIE proteins (sporulation stage II protein E). [63]
In this study, two light-sensitive protein domains were used for the construction of an orthogonal optogenetic system in the cytoplasm of the yeast *Saccharomyces cerevisiae*, i.e. the LOV domains of the LovK protein from *Caulobacter crescentus* and the LOV domain of the YtvA protein from *Bacillus subtilis*. The general characteristics of these two domains will be discussed in the next two sections below.

1.6.1 **LovK: domain organization, signal transduction.**

LovK is a light sensitive histidine kinase involved in the general stress response of *Caulobacter crescentus.* [66] It consists of two domains: an N-terminal LOV domain that shows the classical characteristics of the LOV domains of the phototropin family and a C-terminal histidine kinase domain. Light, through LovK, modulates *C. crescentus* holdfast

production and attachment to abiotic surfaces. [67] The dark-state of LovK shows the typical flavin absorption maximum at 447 nm. Activation with blue light triggers formation of the adduct between Cys70 and the C4(a) atom of FMN, which then activates phosphorylation of the C-terminal domain histidine kinase domain. The life time of recovery of the activated state, i.e. the conversion of the adduct state back to the dark state, is about 120 min. [68]

1.6.2 YtvA: domain organization, and mechanism of signal transduction in the stress response of *B. subtilis*

YtvA is a photoreceptor involved in the general stress response, based on stressosome activation, in the abundant soil bacterium *Bacillus subtilis*. With this response *B. subtilis* is able to respond to a wide range of moderate stresses in an integrated way. [69] YtvA was identified as the first prokaryotic protein containing a LOV domain. [70] The LOV domain in YtvA is located at the N-terminus of the protein. Its C-terminal part is composed of a STAS (sulphate transporter anti-σ antagonist) domain. The LOV domain binds FMN as its chromophore. Blue light absorption causes formation of an adduct between Cys62 and the C4(a) atom of the FMN ring system. This reaction can be followed spectroscopically, by the disappearance of the dark-state absorption peak at 488 nm, and appearance of a new peak with a maximum at 390 nm. The recovery life time of the LOV domain of YtvA is about 43 min at 25°C. [71]

Although *Bacillus subtilis* is not a phototropic bacterium, evidence has been provided that visible (i.e. blue) light can activate YtvA and through that the general stress response of this organism in wild type cells. [72, 73] Under physiological conditions light enhances the response to salt stress. Furthermore, increased expression of YtvA sensitises *B. subtilis* to blue light in the activation of the general stress response. [73]

1.7 Two component signal transduction pathways: constituent components and *in vivo* functioning

Two component signal transduction systems play a crucial role in the processing of information about the extracellular environment (and intracellular events), particularly in the cells of prokaryotes and lower eukaryotes. This includes processing of information transfer across the cell envelope as well as further processing of information in the cytoplasm and cytoplasmic organelles (particularly the nucleus). [74, 75] The total number of these signal

transducing proteins encoded in a particular genome tends to increase with genome size. [75] It was shown that about one third of the histidine kinases encoded in the genome of bacteria do not contain a transmembrane domain. This suggests that a minor part of the histidine kinases serve as intracellular sensors. Based on this classification two types of bacteria were introduced. The extrovert, which are very much oriented towards sensing of the outer environment and the introvert, which are more focused on maintaining their intracellular homeostasis. [74]

The abundance of two component signal transduction pathways differs between prokaryotic and eukaryotic (micro)organisms. Among the prokaryotic genomes there is a wide variety of two component systems, varying from zero for *Mycoplasma genitalium* up to several dozen in some soil bacteria and cyanobacteria. [76] In contrast, in eukaryotic genomes way less two component systems were identified. For example the genome of *S. cerevisae* encodes only a single system, which is of the phospho-relay type (SLN1-YPD1-SSK1, SKN7; see further below). [77] This system plays a role in osmoregulation. The pathogenic fungus *Candida albicans* has at least two histidine kinases, involved in osmoregulation (CASLN1) and hyphal development (COS1/CANIK1), respectively. [78, 79] The classical sequence of events in a two component signal transduction pathway is the phosphorylation of a conserved histidine within the histidine kinase (HK) domain and transfer of this phosphoryl group to the conserved aspartate within the cognate response regulator (RR) which is the effector protein, i.e. this phosphorylation leads to structural change in a second domain of the protein that alters interaction with its target protein or target DNA sequence. This type of signal transduction system is particularly abundant in bacteria. The two phosphorylated amino acids, particularly the phospho-histidine, but also the phospho-apartate has a high free energy of hydrolysis, making them excellent candidates for driving a flux of phosphoryl groups from ATP, via the phosphorylated histidine to the aspartate side chain. [80]

Surprisingly, it is also possible to transfer the phosphate group from the phosphorylated aspartate to a second histidine. [81] This happens in so-called 'phospho-relay systems', which comprise almost 25 % of all two-component signal transduction pathways and are particularly abundant in cells of lower eukaryotes. The domain arrangement of these systems is very diverse: They function on the basis of the involvement of four rather than two protein domains. All four domains can be contained in one single protein, but examples also are known in which each domain is expressed as a separate protein. These phospho-relay systems

thus make use of a phophoryl-transfer (Hpt) domain, plus an extra receiver domain. Often, the specificity for their cognate partners of these Hpt domains is rather low, which then allows for the branching of signal transfer and cross-talk between adjacent phospho-transfer pathways. [76]

The architecture of the histidine kinase proteins shows significant conservation in the catalytic core domain, which is often located at the C-terminus of the protein. The N-terminal domain usually is the signal input domain and shows a high (sequence/structure) variety within the two component systems. Within the catalytic core of the kinase domain, which is located in the cytoplasm, several conserved motifs can be distinguished. C-terminally are the ATP binding and the catalytic domain (CA) that are well conserved within the HK family. At the N-terminal side of the domain is the phosphorylation- and dimerization domain (DHp). The DHp domain contains the conserved histidine, whereas the CA domain carries the catalytic activity that is required to transfer the phosphoryl group from the ATP to conserved histidine. The N-terminal sensing domain is often located at the extracellular side of the cytoplasmic membrane, and is responsible for sensing one or more of a wide variety of stimuli, including small molecules, light, turgor pressure, cell envelope stress, redox potential, and electrochemical gradients. [24, 80] These sensing domains are usually linked to the kinase domains via long (transmembrane) α-helices, that are often organized in the form of a coiled-coil structure. [76] Dimers of these membrane-embedded sensory kinases are then thought to relay signals into the cells via mutual rotation of the sensory domains upon binding of a signalling molecule or activation by a photon. [82–85]

1.7.1 **Osmotic stress response in baker yeast**

The osmo-sensing system in the budding yeast *Saccharomyces cerevisiae* involves multiple sensors. By consequence, the information regarding (the absence of) osmostress initially is transmitted through parallel pathways; eventually it reaches the MAP-kinase-kinase-kinase (MAPKKK) Pbs2 that phosphorylates the Hog1 protein. One of these sensors is the transmembrane histidine kinase Sln1, which is part of a phospho-relay type two component signal transduction system. [86, 87] Another sensor is Sho1, that transmits a signal via the integral membrane protein Opy2 to Cdc42 and Ste20, to then activate the MAPKKK Ste11, with the assistance of Ste50. Ste11 phosphorylates Pbs2, that in turn phosphorylates Hog1. [88, 89] Phosphorylated Hog1 translocates to the nucleus. There, it can phosphorylate at least three transcription factors (i.e. Sko1, Hot1, and Smp1), and in this way osmotic stress

modulates the transcription of hundreds of genes. [88–90] Figure 2 shows an overview of the MAP kinase network in budding yeast. [91]

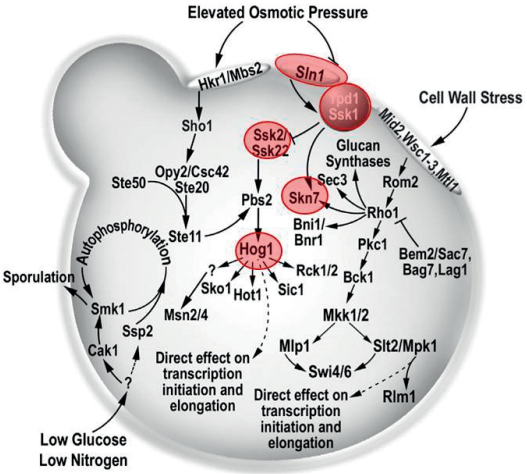

Figure 2. The *S. cerevisiae* Hog1, Mpk1/Slt2 and Smk1 MAP kinase pathways. In red components of the Sln1 pathway are indicated. Adapted from [91].

The Sln1 histidine protein kinase consists of an N-terminal domain associated with the plasma membrane, followed by two typical domains of a two-component system: the histidine kinase domain (HK) with the conserved histidine H576, and the response regulator domain (R1) with the conserved aspartate D1144. Both residues are transiently phosphorylated during osmo-signalling, initiated by phosphoryl transfer from ATP. In the steady state of physiological conditions, the conserved H576 residue is moderately phosphorylated. An increase in this level of phosphorylation occurs after application of a stress that causes weakening of the cell wall. In contrast, conditions that cause a reduction of the cell turgor lead to accumulation of the Sln1 in its non-phosphorylated form (presumably through activation of intrinsic phosphatase activity).

The wall stress leads to phosphorylation of the Ssk1 and Skn7 response regulators via transfer of the phosphoryl group through the Ypd1 phosphoryl-transfer protein. Phosphorylation of Ssk1 renders it inactive in its role in the Hog1 pathway. Phosphorylation of Skn7 leads to activation of Skn7-dependent genes, such as the mannosyl-transferase, OCH1. Osmotic stress leads to lowering of the kinase activity of Sln1 therefore accumulation

of the kinase domain of Sln1 in the dephosphorylated form. This causes de-phosphorylation of the Ssk1 response regulator, which can interact with and activate Ssk2 and the Ssk22 kinases of the Hog1 pathway. Phosphorylation of Hog1 leads to its translocation into nucleus and activation of the genes responsible for osmotic-stress regulation. Sln1 is in the cytoplasm membrane. [86, 87, 92] Figure 3 shows the schematic flow of the phosphoryl groups in Sln1 pathway.

The Sln1 system of *S. cerevisiae* seems well-fitted as a target for an optogenetic approach, i.e. the introduction of an engineered histidine kinase of which the activity can be modulated with light. If such a system can be constructed, it may prove useful in subsequent studies on the consequences of local activation of signal transduction networks in the eukaryotic cytoplasm.

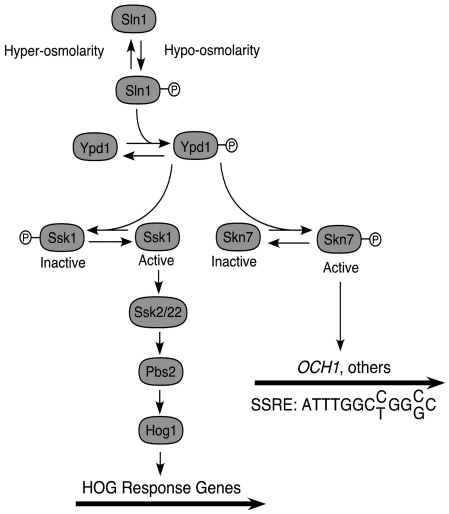

Figure 3. Schematic drawing of the flow of phosphoryl groups through the Sln1 pathway of *Saccharomyces cerevisiae*. Sln1 branch of the HOG pathway. [92]

1.8 Scope and outline of this thesis

The primary goal of the work presented in this thesis was to provide a unique tool that may prove useful in increasing our understanding of the mechanism of cytoplasmic diffusion in signal transduction in eukaryotic cells, in the form of a chimeric, light-addressable, cytoplasmic signal transduction device in the yeast *Saccharomyces cerevisiae*. Such a device

can be composed of a photo-sensory receptor domain translationally fused to a signal-dependent kinase domain. Such a device may prove to be useful for localized excitation of a cytoplasmic signal transduction network in the cytoplasm of a eukaryotic cell. In chapter 2 we further characterize the *in vivo* redox transitions of a flavin-containing photo-sensory receptor domain for such a chimeric device. Chapter 3 describes designing and functional characterization of the intended chimera: a light-sensitive histidine protein kinase, derived from the Sln1 kinase of *S. cerevisiae,* translationally fused in a coiled-coil motif with the LOV domain of the stressosome component YtvA from *Bacillus subtilis*. In chapter 4 we describe tests that show the *in vivo* functionality of this light-sensitive histidine protein kinase. This orthogonal photo-transduction system can be used to either activate or repress gene expression in *S. cerevisiae*, depending on the specific promotor targeted. Furthermore, it can be used to initiate nuclear accumulation of a selected signal transduction protein. In chapter 5 we go into detail on one of the methods for functional testing of these histidine protein kinases: the Phos-tag method for the detection of the phosphorylated form of a response regulator. In chapter 6, in a general discussion, the results of this study are placed in the context of recent developments in the field.

References

1. Madigan MT, Martinko JM, Bender KS, Buckley DH, Stahl DA, Brock T (2015) Brock Biology of Microorganisms, 15th ed. Pearson Education Limited, Global Edition
2. Chaudhary AK, Na D, Lee EY (2015) Rapid and high-throughput construction of microbial cell-factories with regulatory noncoding RNAs. Biotechnol Adv 33:914–930 . doi: 10.1016/j.biotechadv.2015.05.009
3. Delvigne F, Pêcheux H, Tarayre C (2015) Fluorescent Reporter Libraries as Useful Tools for Optimizing Microbial Cell Factories: A Review of the Current Methods and Applications. Front Bioeng Biotechnol 3:147 . doi: 10.3389/fbioe.2015.00147
4. Bar-Even A, Salah Tawfik D (2013) Engineering specialized metabolic pathways—is there a room for enzyme improvements? Curr Opin Biotechnol 24:310–319 . doi: 10.1016/j.copbio.2012.10.006
5. Stephanopoulos G (2012) Synthetic Biology and Metabolic Engineering. ACS Synth Biol 1:514–525 . doi: 10.1021/sb300094q
6. Bourret RB, Borkovich KA, Simon MI (1991) Signal Transduction Pathways Involving Protein Phosphorylation in Prokaryotes. Annu Rev Biochem 60:401–441 . doi: 10.1146/annurev.bi.60.070191.002153
7. Hellingwerf KJ, Postma PW, Tommassen J, Westerhoff HV (1995) Signal transduction in bacteria: phospho-neural network(s) in Escherichia coli? FEMS Microbiol Rev 16:309–21
8. Mull RW, Harrington A, Sanchez LA, Tal-Gan Y (2018) Cyclic Peptides that Govern Signal Transduction Pathways: From Prokaryotes to Multi-Cellular Organisms. Curr Top Med Chem 18:625–644 . doi: 10.2174/1568026618666180518090705
9. Launer-Felty KD, Strobel SA (2018) Enzymatic synthesis of cyclic dinucleotide analogs by a promiscuous cyclic-AMP-GMP synthetase and analysis of cyclic dinucleotide responsive riboswitches. Nucleic Acids Res 46:2765–2776 . doi: 10.1093/nar/gky137
10. Engelberg D, Perlman R, Levitzki A (2014) Transmembrane signaling in Saccharomyces cerevisiae as a model for signaling in metazoans: State of the art after 25years. Cell. Signal.
11. Yoshida M, Ishihama A, Yamamoto K (2015) Cross talk in promoter recognition between six NarL-family response regulators of *Escherichia coli* two-component system. Genes to Cells 20:601–612 . doi: 10.1111/gtc.12251
12. Minton AP (2001) The Influence of Macromolecular Crowding and Macromolecular Confinement on Biochemical Reactions in Physiological Media*. doi: 10.1074/jbc.R100005200
13. Ellis RJ (2001) Macromolecular crowding: obvious but underappreciated. Trends Biochem Sci 26:597–604 . doi: S0968-0004(01)01938-7 [pii]
14. Kalwarczyk T, Zie-Bacz N, Bielejewska A, Zaboklicka E, Koynov K, Szyma J-D, Wilk A, Patkowski A, Jacek ||, Nski G, Urgen Butt H-J, Hozyst R (2011) Comparative Analysis of Viscosity of Complex Liquids and Cytoplasm of Mammalian Cells at the

Nanoscale. doi: 10.1021/nl2008218
15. Kao Y-T, Zhu X, Min W Protein-flexibility mediated coupling between photoswitching kinetics and surrounding viscosity of a photochromic fluorescent protein
16. Möller CB, Eckert T, Loman A, Org Enderlein J, Richtering W (2009) Dual-focus fluorescence correlation spectroscopy: a robust tool for studying molecular crowding. doi: 10.1039/b812289j
17. Banks DS, Fradin C (2005) Anomalous diffusion of proteins due to molecular crowding. Biophys J. doi: 10.1529/biophysj.104.051078
18. Liu B, Åberg C, van Eerden FJ, Marrink SJ, Poolman B, Boersma AJ (2017) Design and Properties of Genetically Encoded Probes for Sensing Macromolecular Crowding. Biophys J. doi: 10.1016/j.bpj.2017.04.004
19. Morikawa TJ, Fujita H, Kitamura A, Horio T, Yamamoto J, Kinjo M, Sasaki A, Machiyama H, Yoshizawa K, Ichimura T, Imada K, Nagai T, Watanabe TM (2016) Dependence of fluorescent protein brightness on protein concentration in solution and enhancement of it. doi: 10.1038/srep22342
20. Gnutt D, Gao M, Brylski O, Heyden M, Ebbinghaus S Macromolecule Biophysics Hot Paper Excluded-Volume Effects in Living Cells. doi: 10.1002/anie.201409847
21. ten Wolde PR, Mugler A (2014) Importance of crowding in signaling, genetic, and metabolic networks. Int Rev Cell Mol Biol 307:419–442 . doi: 10.1016/B978-0-12-800046-5.00012-6 [doi]
22. Kwon S, Cho HW, Kim J, Sung BJ (2017) Fractional Viscosity Dependence of Reaction Kinetics in Glass-Forming Liquids. Phys Rev Lett 119:87801 . doi: 10.1103/PhysRevLett.119.087801 [doi]
23. Sadati M, Nourhani A, Fredberg JJ, Qazvini NT (2014) Glass-like dynamics in the cell and in cellular collectives. Wiley Interdiscip Rev Biol Med 6:137–149 . doi: 10.1002/wsbm.1258 [doi]
24. Gao R, Stock AM (2009) Biological insights from structures of two-component proteins. Annu Rev Microbiol 63:133–154 . doi: 10.1146/annurev.micro.091208.073214
25. Saito H (2010) Regulation of cross-talk in yeast MAPK signaling pathways. Curr. Opin. Microbiol.
26. Bardwell L (2006) Mechanisms of MAPK signalling specificity. Biochem Soc Trans 34:837–41 . doi: 10.1042/BST0340837
27. Dard N, Peter M (2006) Scaffold proteins in MAP kinase signaling: more than simple passive activating platforms. BioEssays 28:146–156 . doi: 10.1002/bies.20351
28. Schwartz MA, Madhani HD (2004) Principles of MAP Kinase Signaling Specificity in *Saccharomyces cerevisiae*. Annu Rev Genet 38:725–748 . doi: 10.1146/annurev.genet.39.073003.112634
29. Hao N, Behar M, Parnell SC, Torres MP, Borchers CH, Elston TC, Dohlman HG (2007) A systems-biology analysis of feedback inhibition in the Sho1 osmotic-stress-response pathway. Curr Biol 17:659–667 . doi: S0960-9822(07)01021-4 [pii]
30. Dusseiller MR, Niederberger B, Städler B, Falconnet D, Textor M, Vörös J (2005) A

novel crossed microfluidic device for the precise positioning of proteins and vesicles. Lab Chip 5:1387 . doi: 10.1039/b509957a

31. Kou S, Pan L, van Noort D, Meng G, Wu X, Sun H, Xu J, Lee I (2011) A multishear microfluidic device for quantitative analysis of calcium dynamics in osteoblasts. Biochem Biophys Res Commun 408:350–355 . doi: 10.1016/J.BBRC.2011.04.044
32. Bates M, Jones SA, Zhuang X (2013) Stochastic optical reconstruction microscopy (STORM): a method for superresolution fluorescence imaging. Cold Spring Harb Protoc 2013:498–520 . doi: 10.1101/pdb.top075143
33. Möglich A, Ayers RA, Moffat K (2009) Design and signaling mechanism of light-regulated histidine kinases. J Mol Biol 385:1433–1444 . doi: 10.1016/j.jmb.2008.12.017
34. Gautier A, Gauron C, Volovitch M, Bensimon D, Jullien L, Vriz S (2014) How to control proteins with light in living systems. Nat Chem Biol 10:533–541 . doi: 10.1038/nchembio.1534 [doi]
35. Schierling B, Pingoud A (2012) Controlling the DNA cleavage activity of light-inducible chimeric endonucleases by bidirectional photoactivation. Bioconjug Chem 23 (6):1105–1109
36. Pathak GP, Vrana JD, Tucker CL (2013) Optogenetic control of cell function using engineered photoreceptors. Biol Cell 105:59–72 . doi: 10.1111/boc.201200056
37. Fork RL (1971) Laser stimulation of nerve cells in Aplysia. Science 171:907–8
38. Miesenböck G, Kevrekidis IG (2005) Optical imaging and control of genetically designated neurons in functioning circuits. Annu Rev Neurosci 28:533–563 . doi: 10.1146/annurev.neuro.28.051804.101610
39. Kramer RH, Chambers JJ, Trauner D (2005) Photochemical tools for remote control of ion channels in excitable cells. Nat Chem Biol 1:360–5
40. Boyden ES, Zhang F, Bamberg E, Nagel G, Deisseroth K Millisecond-timescale, genetically targeted optical control of neural activity. doi: 10.1038/nn1525
41. Wu YI, Frey D, Lungu OI, Jaehrig A, Schlichting I, Kuhlman B, Hahn KM (2009) A genetically encoded photoactivatable Rac controls the motility of living cells. Nature 461:104–108 . doi: 10.1038/nature08241
42. Strickland D, Moffat K, Sosnick TR Light-activated DNA binding in a designed allosteric protein
43. Möglich A, Moffat K (2010) Engineered photoreceptors as novel optogenetic tools. Photochem Photobiol Sci 9:1286 . doi: 10.1039/c0pp00167h
44. Ziegler T, Möglich A (2015) Photoreceptor engineering. Front Mol Biosci 2:30 . doi: 10.3389/fmolb.2015.00030 [doi]
45. Zhang F, Wang L-P, Boyden ES, Deisseroth K Channelrhodopsin-2 and optical control of excitable cells. doi: 10.1038/NMETH936
46. Levskaya A, Chevalier AA, Tabor JJ, Simpson ZB, Lavery LA, Levy M, Davidson EA, Scouras A, Ellington AD, Marcotte EM, Voigt CA (2005) Synthetic biology: engineering Escherichia coli to see light. Nature 438:441–442 . doi: nature04405 [pii]
47. Ryu M-H, Moskvin O V, Siltberg-Liberles J, Gomelsky M (2010) Natural and engineered photoactivated nucleotidyl cyclases for optogenetic applications. J Biol

Chem 285:41501–8 . doi: 10.1074/jbc.M110.177600
48. Stierl M, Stumpf P, Udwari D, Gueta R, Hagedorn R, Losi A, Gärtner W, Petereit L, Efetova M, Schwarzel M, Oertner TG, Nagel G, Hegemann P (2011) Light modulation of cellular cAMP by a small bacterial photoactivated adenylyl cyclase, bPAC, of the soil bacterium Beggiatoa. J Biol Chem 286:1181–8 . doi: 10.1074/jbc.M110.185496
49. Abe K, Miyake K, Nakamura M, Kojima K, Ferri S, Ikebukuro K, Sode K (2014) Engineering of a green-light inducible gene expression system in Synechocystis sp. PCC6803. Microb Biotechnol 7:177–183 . doi: 10.1111/1751-7915.12098 [doi]
50. Yazawa M, Sadaghiani AM, Hsueh B, Dolmetsch RE (2009) Induction of protein-protein interactions in live cells using light. Nat Biotechnol 27:941–945 . doi: 10.1038/nbt.1569 [doi]
51. Shimizu-Sato S, Huq E, Tepperman JM, Quail PH (2002) A light-switchable gene promoter system. Nat Biotechnol 20:1041–1044 . doi: 10.1038/nbt734 [doi]
52. Kennedy MJ, Hughes RM, Peteya LA, Schwartz JW, Ehlers MD, Tucker CL (2010) Rapid blue-light-mediated induction of protein interactions in living cells. Nat Methods 7:973–975 . doi: 10.1038/nmeth.1524 [doi]
53. Polstein LR, Gersbach CA (2012) Light-Inducible Spatiotemporal Control of Gene Activation by Customizable Zinc Finger Transcription Factors. J Am Chem Soc. doi: 10.1021/ja3065667
54. Ottemann KW, Xiao W, Yeon-Kyun S, Koshland DEJ (1999) A Piston Model for Transmembrane Signaling of the Aspartate Receptor. Science 285:1751–1754. doi: 10.1126/science.285.5434.1751
55. Yu D, Ma X, Tu Y, Lai L (2015) Both piston-like and rotational motions are present in bacterial chemoreceptor signaling. Sci Rep 5:8640 . doi: 10.1038/srep08640
56. Crosson S, Rajagopal S, Moffat K (2003) The LOV domain family: photoresponsive signaling modules coupled to diverse output domains. Biochemistry 42:2–10. doi: 10.1021/bi026978l
57. Halavaty AS, Moffat K (2007) N- and C-terminal flanking regions modulate light-induced signal transduction in the LOV2 domain of the blue light sensor phototropin 1 from Avena sativa. Biochemistry 46:14001–14009 . doi: 10.1021/bi701543e
58. Möglich A, Moffat K (2010) Engineered photoreceptors as novel optogenetic tools. Photochem Photobiol Sci 9:1286–1300 . doi: 10.1039/c0pp00167h [doi]
59. Purcell EB, Crosson S (2008) Photoregulation in prokaryotes. Curr Opin Microbiol 11:168–178 . doi: 10.1016/j.mib.2008.02.014
60. Glantz ST, Carpenter EJ, Melkonian M, Gardner KH, Boyden ES, Wong GK, Chow BY (2016) Functional and topological diversity of LOV domain photoreceptors. Proc Natl Acad Sci U S A 113:E1442-51 . doi: 10.1073/pnas.1509428113
61. van der Horst MA, Hellingwerf KJ (2004) Photoreceptor proteins, "star actors of modern times": a review of the functional dynamics in the structure of representative members of six different photoreceptor families. Acc Chem Res 37:13–20 . doi: 10.1021/ar020219d
62. Ziegler T, Möglich A (2015) Photoreceptor engineering. Front Mol Biosci 2:30 . doi: 10.3389/fmolb.2015.00030

63. Herrou J, Crosson S (2011) Function, structure and mechanism of bacterial photosensory LOV proteins. Nat Rev 9:713–723 . doi: 10.1038/nrmicro2622; 10.1038/nrmicro2622
64. Yee EF, Diensthuber RP, Vaidya AT, Borbat PP, Engelhard C, Freed JH, Bittl R, Möglich A, Crane BR (2015) Signal transduction in light-oxygen-voltage receptors lacking the adduct-forming cysteine residue. Nat Commun 6:10079 . doi: 10.1038/ncomms10079
65. Suzuki H, Okajima K, Ikeuchi M, Noguchi T (2008) LOV-Like Flavin-Cys Adduct Formation by Introducing a Cys Residue in the BLUF Domain of TePixD. J Am Chem Soc 130:12884–12885 . doi: 10.1021/ja805363u
66. Foreman R, Fiebig A, Crosson S (2012) The LovK-LovR two-component system is a regulator of the general stress pathway in Caulobacter crescentus. J Bacteriol 194:3038–3049 . doi: 10.1128/JB.00182-12; 10.1128/JB.00182-12
67. Lori C, Kaczmarczyk A, de Jong I, Jenal U (2018) A Single-Domain Response Regulator Functions as an Integrating Hub To Coordinate General Stress Response and Development in Alphaproteobacteria. MBio 9:e00809-18 . doi: 10.1128/mBio.00809-18
68. Purcell EB, McDonald CA, Palfey BA, Crosson S (2010) An analysis of the solution structure and signaling mechanism of LovK, a sensor histidine kinase integrating light and redox signals. Biochemistry 49:6761–6770 . doi: 10.1021/bi1006404
69. van der Steen JB, Hellingwerf KJ (2015) Activation of the General Stress Response of Bacillus subtilis by Visible Light. Photochem Photobiol 91:1032–1045 . doi: 10.1111/php.12499
70. Losi A, Gartner W (2011) The Evolution of Flavin-Binding Photoreceptors: An Ancient Chromophore Serving Trendy Blue-Light Sensors. Annu Rev Plant Biol. doi: 10.1146/annurev-arplant-042811-105538
71. Losi A, Polverini E, Quest B, Gartner W (2002) First evidence for phototropin-related blue-light receptors in prokaryotes. Biophys J 82:2627–2634 . doi: S0006-3495(02)75604-X
72. Suzuki N, Takaya N, Hoshino T, Nakamura A (2007) Enhancement of a σB-dependent stress response in Bacillus subtilis by light via YtvA photoreceptor. J Gen Appl Microbiol 53:81–88 . doi: 10.2323/jgam.53.81
73. Avila-Perez M, Hellingwerf KJ, Kort R (2006) Blue light activates the sigmaB-dependent stress response of Bacillus subtilis via YtvA. J Bacteriol 188:6411–6414 . doi: 10.1128/JB.00716-06
74. Egbert MD (2013) Bacterial Chemotaxis: Introverted or Extroverted? A Comparison of the Advantages and Disadvantages of Basic Forms of Metabolism-Based and Metabolism-Independent Behavior Using a Computational Model. PLoS One. doi: 10.1371/journal.pone.0063617
75. Galperin MY (2005) A census of membrane-bound and intracellular signal transduction proteins in bacteria: Bacterial IQ, extroverts and introverts. BMC Microbiol. doi: 10.1186/1471-2180-5-35
76. Stock AM, Robinson VL, Goudreau PN (2000) Two-component signal transduction.

Annu Rev Biochem 69:183–215
77. Maeda T, Wurgler-Murphy SM, Saito H (1994) A two-component system that regulates an osmosensing MAP kinase cascade in yeast. Nature 369:242–245 . doi: 10.1038/369242a0
78. Nagahashi S, Mio T, Ono N, Yamada-Okabe T, Arisawa M, Bussey H, Yamada-Okabe H (1998) Isolation of CaSLN1 and CaNIK1, the genes for osmosensing histidine kinase homologues, from the pathogenic fungus Candida albicans. Microbiology 144 (Pt 2):425–32 . doi: 10.1099/00221287-144-2-425
79. Alex LA, Korch C, Selitrennikoff CP, Simon MI (1998) COS1, a two-component histidine kinase that is involved in hyphal development in the opportunistic pathogen Candida albicans. Proc Natl Acad Sci U S A 95:7069–73
80. Gao R, Mack TR, Stock AM (2007) Bacterial response regulators: versatile regulatory strategies from common domains. Trends Biochem Sci 32:225–234 . doi: S0968-0004(07)00058-8
81. Appleby JL, Bourret RB (1998) Proposed signal transduction role for conserved CheY residue Thr87, a member of the response regulator active-site quintet. J Bacteriol 180:3563–9
82. Okada T, Ernst OP, Palczewski K, Hofmann KP (2001) Activation of rhodopsin: new insights from structural and biochemical studies. Trends Biochem Sci 26:318–24
83. Kandori H (2015) Ion-pumping microbial rhodopsins. Front Mol Biosci 2:52 . doi: 10.3389/fmolb.2015.00052
84. Ames P, Parkinson JS (1988) Transmembrane signaling by bacterial chemoreceptors: E. coli transducers with locked signal output. Cell 55:817–26
85. Hulko M, Berndt F, Gruber M, Linder JU, Truffault V, Schultz A, Martin J, Schultz JE, Lupas AN, Coles M (2006) The HAMP Domain Structure Implies Helix Rotation in Transmembrane Signaling. Cell 126:929–940 . doi: 10.1016/j.cell.2006.06.058
86. Posas F, Wurglermurphy S, Maeda T, Witten E, Thai T, Saito H (1996) Yeast HOG1 MAP Kinase Cascade Is Regulated by a Multistep Phosphorelay Mechanism in the SLN1-YPD1-SSK1 -Two-Component- Osmosensor. Cell 86:865–875 . doi: 10.1016/S0092-8674(00)80162-2
87. Li S, Dean S, Li Z, Horecka J, Deschenes RJ, Fassler JS (2002) The eukaryotic two-component histidine kinase Sln1p regulates OCH1 via the transcription factor, Skn7p. Mol Biol Cell 13:412–424 . doi: 10.1091/mbc.01-09-0434
88. Lee KS, Irie K, Gotoh Y, Watanabe Y, Araki H, Nishida E, Matsumoto K, Levin DE (1993) A yeast mitogen-activated protein kinase homolog (Mpk1p) mediates signalling by protein kinase C. Mol Cell Biol 13:3067–75
89. Maayan I, Engelberg D (2009) The yeast MAPK Hog1 is not essential for immediate survival under osmostress. FEBS Lett 583:2015–2020 . doi: 10.1016/j.febslet.2009.05.014
90. Clotet J, Escoté X, Adrover MÀ, Yaakov G, Garí E, Aldea M, de Nadal E, Posas F (2006) Phosphorylation of Hsl1 by Hog1 leads to a G2 arrest essential for cell survival at high osmolarity. EMBO J 25:2338–2346 . doi: 10.1038/sj.emboj.7601095
91. Engelberg D, Perlman R, Levitzki A (2014) Transmembrane signaling in

Saccharomyces cerevisiae as a model for signaling in metazoans: State of the art after 25 years. Cell Signal 26:2865–2878 . doi: 10.1016/J.CELLSIG.2014.09.003

92. Levin DE (2005) Cell wall integrity signaling in Saccharomyces cerevisiae. Microbiol Mol Biol Rev 69:262–91 . doi: 10.1128/MMBR.69.2.262-291.2005

2 On the *in vivo* redox state of flavin-containing photosensory receptor proteins.

Bury AE, Hellingwerf KJ

Abstract:
Measured values of the redox midpoint potential of flavin-containing photoreceptor proteins range from physiologically very negative values, i.e., < -300 mV (compared to the calomel electrode) for some LOV domains, to slightly positive values for some cryptochromes. The actual intracellular redox potential of several key physiological electron-transfer intermediates, like the nicotinamide dinucleotides, particularly in chemoheterotrophic bacteria, may be varying beyond these two values, and are subject to physiological- and environmental regulation. The photochemical activity of photoreceptor proteins containing their flavin chromophore in the reduced, and in the fully oxidized form, is very different. We therefore have addressed the question whether or not the functioning of these flavin-containing photosensory receptors *in vivo* is subject to redox regulation. Here we provide further evidence for the overlap of the ranges of the redox midpoint potential of the flavin in a specific photoreceptor protein and the redox potential of key intracellular redox-active metabolites, and demonstrate that the redox state and photochemical activity of LOV domains can be recorded *in vivo* in *Escherichia coli*. Significantly, so far *in vivo* reduction of LOV domains under physiological conditions could not be detected. The implications of these observations are discussed.

This chapter has been published as:
Bury A, Hellingwerf KJ. 2014 On the in vivo redox state of flavin-containing photosensory receptor proteins. Methods Mol Biol. 2014 1146:177-90

2.1 Introduction

Three families of photosensory receptor proteins exist that contain a flavin derivative (*i.e.* FMN or FAD) as their light-sensitive chromophore: The LOV- and BLUF-domain-containing proteins and the Cryptochromes (see refs [1, 2] for a review). Of these, the family of the LOV domains is the most widely distributed, to the extent that several subclasses are identifiable. [3] The family of the Cryptochromes is difficult to delimit because it is difficult to separate members from a family of nucleic acid repair proteins, the photolyases. [4] In a previous publication we have addressed the issue of the electrochemical midpoint potential (*i.e.* the Em') of the flavin chromophore in representatives of these three families of photosensory receptors [5] and found that this Em' value increases from LOV domains, via BLUF domains to Cryptochromes, in the range from < -300 to close to zero, [6] relative to the calomel electrode.

More recently, Crosson and co-workers [7] reported on the midpoint potential of the LOV domain of LovK, a photosensory protein histidine kinase from *Caulobacter crescentus* which has been implicated in the regulation of cellular adhesion, and several of its truncated derivatives. Crucial in their observations was that the measured midpoint potentials range from -258 for the full-length protein, to -303 mV for one of the truncated fragments (*i.e.* the fragment that contains the 138 N-terminal amino acids of the protein, which includes the entire LOV domain, but not its associated linker to the kinase domain [7]). These results imply that one would expect that the LOV domain of full-length LovK sensory kinase is subjected to physiological redox regulation by redox-active compounds from the cytoplasmic environment in which it is located. This is because the redox potential of the most dominant cytoplasmic redox-mediating couple, NADH/NAD+, in a typical chemoheterotrophic eubacterium like *Escherichia coli,* varies from ~ -320 mV under strict anaerobic conditions, to values close to -200 mV when these cells encounter fully aerobic conditions. [8, 9] For other organisms this range may be slightly (*i.e.* because of the range of cellular compartments that are present), but not very, different because of the physiological role that the NAD+/NADH couple has in compartments and cells of different origin. Other redox couples in the cell may be at dis-equilibrium (*i.e.* more negative) with the NAD+/NADH couple, like the NADP+/NADPH couple, because of the presence of an energy linked transhydrogenase, [10] but such complications will not be further discussed. If a LOV domain with a potential in the range of that of LovK (*i.e.* LOV domain with a relatively high midpoint potential; see above) is present in a cell in which the redox potential of the NAD+/NADH couple varies

significantly through transitions in the physiological- or metabolic state of the cell, one may then expect that the redox state of its flavin moiety will change accordingly. We have therefore further characterized the redox midpoint potential of the LOV domain of LovK, and investigated whether reducing conditions in the cytoplasm of *Escherichia coli*, achieved by incubating cells under stringently anaerobic conditions, would lead to conversion of the flavin of LovK into its reduced state, thereby taking the LOV domain of YtvA from *B. subtilis* as a reference. [11] Surprisingly, we have not been able to find evidence of such a physiology-driven flavin reduction of these LOV domains.

2.2 Materials and methods

2.2.1 Materials

Xanthine oxidase (from bovine milk), methylviologen, phenosafranin, safranin O, flavin mononucleotide, buffers and general chemicals were bought from Sigma–Aldrich Co, St. Louis, MO, USA. Glucose oxidase (lyophilized) was supplied by Roche Products Ltd. (Hertfordshire, UK), and Argon gas (Argon 5.0 Instrument; >99.99% pure) was provided by Praxair (Vlaardingen, The Netherlands).

2.2.2 Bacterial strains and construction of plasmids

The bacterial strains, plasmids, and primers that were used in this investigation have been listed in Table 1. *Escherichia coli* Xll-blue was used as the intermediate cloning host for plasmids prior to transformation of *E. coli* M15. Transformants were selected on LB agar plates, containing 100 μg/mL ampicillin or 100 μg/mL ampicillin plus 25 μg/mL kanamycin, after their overnight incubation at 37°C. The *lovK* gene was amplified by using chromosomal DNA from *Caulobacter crescentus* FC19 as the template and part of the primers shown in Table 1. Truncated derivatives of this gene (*i.e.* 1 – 138 and 1 – 156; numbers refer to amino acids of the full length LovK sequence) were amplified with the PCR technique, digested with BamHI and HindIII, and ligated into the pQE30 vector. A gene encoding the STAS domain of YtvA from *Bacillus subtilis* was amplified by using chromosomal DNA from *B. subtilis* PB2 and the primers shown in Table 1. Gene splicing by the overlap extension procedure was used to construct LovK-STAS fusion proteins. [12] The resulting PCR products were cloned into the pQE30 vector and transformed into *E. coli* M15, in order to obtain overexpression strains.

Table 1. Strains, plasmids, and primers used in this investigation

Strain, plasmid or primer	Relevant genotype, characterization, or primer sequences	Ref, source, or construction
Strains:		
E. coli M15		
E. coli Xl1-blue		
Plasmids:		
pQE30		
Primers:		
LovK_R_A	5' GCTTGGT CACGTCCACCTGCGAGC 3'	This study
LovK_R_B	5' GTTGAAAGCTGCTGCAGACCGTCGC 3'	This study
YtvA_F_A	5'GGACGTGACCAAGCAAAAAGAATATGAAAAGCT TCTCG3'	This study
YtvA_F_B	5' GCAGCAGCTTTCAACTCCTATTGTCCCG3'	This study
pQE30LovKbaHFW	5' CCCGGATCCATGGAAGACTATTCGGATCGC 3'	This study
pQE30YtvARV	5'GGGGTCGACTTACATAATCGGAAGCACTTTAAC G 3'	[13]
pQE30LovKRV	5' CCCAAGCTTCTATTGCGTCCCATTGATGGGCA 3'	This study
pQE30LovK138RV	5'CCCAAGCTTGTCGGTCACGTCCACCT 3'	This study
pQE30LovK156RV	5' CCCAAGCTTCATCTGCTGCAGACCGT 3'	This study
pQE30YtvAFW	5'CCCGGATCCATGGCTTTTCAATCATTTGGG 3'	[13]

2.2.3 **Overexpression and purification of the flavoproteins**

Flavoproteins, and various domain combinations thereof, were overexpressed in *E. Coli* growing in Production Broth medium [Tryptone (20 g/L; Becto and Dickson Company), Yeast Extract (10 g/L; Scharlab S.L.), Glucose (5 g/L; Dextro energy GmbH Co. KG), NaCl (5 g/L; Sigma-Aldrich), and K2HPO4 (8.7 g/L; Merck)], supplemented with 100 µg/ml ampicillin and 25 µg/ml kanamycin. Overnight grown pre-cultures, inoculated with a single colony from a fresh plate of the same medium, were diluted into fresh medium at 37 °C and were allowed to grow for an additional 1.5 to 2 h with vigorous shaking. When OD600 of these cultures reached 0.6, overexpression of the heterologous product was induced by sterile addition of isopropyl β-D-thiogalactopyranoside (IPTG) to a final concentration of 0.1 mM. At this point the temperature was lowered to 30 °C and growth was allowed to continue with vigorous shaking for approximately 16 hours in darkness. Then cells were harvested by centrifugation and were lysed by sonication in 50 mM Tris-HCl buffer pH = 8, plus 10 mM NaCl, and an EDTA-free protease inhibitor cocktail (complete, EDTA-free, provided by Roche). The recombinant proteins were purified from the resulting cell-free extracts in a twostep procedure: Affinity chromatography on a HisTrap FF column (GE Healthcare, 5 mL

column) and anion exchange chromatography on a ResQ column (GE Healthcare, 6 ml column volume).

2.2.4 **Measurement of redox midpoint potentials**

Redox midpoint potentials were determined with the procedure based on the use of xanthine/xanthine oxidase as the electron donor developed by Massey, [14] as described in Arents *et al*. [5] The midpoint potential of all proteins included in this study was measured with both safranin O and with phenosafranin as the indication dye. Complete reduction of a protein sample typically took between two and three hours.

2.2.5 **Spectroscopy**

UV/visible spectra were recorded using an HP8453 UV/visible diode array spectrophotometer (Hewlett-Packard Nederland BV, Amstelveen, NL) for purified protein (domains), or a SPECORD 210PLUS double beam UV/visible spectrometer (Analytik Jena, Jena, Germany), equipped with a 1 cm quartz cuvette, for analyses in intact cells (*i.e. in vivo*). To monitor the kinetics of thermal recovery of the ground state of the photoreceptor proteins, spectra were recorded at 60 s intervals. For *in vivo* measurements, cells were precultured overnight in PB medium, with the appropriate antibiotics, at 37 °C, with vigorous shaking. Pre-cultures were diluted 100 times in the same medium, and grown until their OD600 reached a value of ~ 0.6. At this point IPTG was added to a final concentration of 0.1 mM, and the temperature was lowered to 30 °C. Cultures were then incubated under these conditions for another 16 hours. After harvesting the cells (through centrifugation), cell pellets were re-suspended in 20 mM Tris-HCl buffer pH = 8 (in a volume equivalent to three times the wet weight of the pellet). For *in vivo* measurements of the redox transition of a LOV domain, cell-samples were diluted 4 times in 20 mM Tris-HCl buffer pH = 8, and flushed with argon in a screw-cap cuvette wrapped with aluminium foil. Then argon-flushed solutions of glucose and glucose oxidase were added. Next, a reducing agent was added and the measurements with the SPECORD 210PLUS were initiated.

2.3 Results

2.3.1 Choice of protein domains and design of fusion proteins

Because Crosson and colleagues reported quite some variation in the redox midpoint potential between full-length LovK and several truncated LOV-domain fragments, [7] we decided to first look into the effect of variation of the linker to the LOV domain on the flavin midpoint potential. For this we purified (via heterologous overexpression in *Escherichia coli*; see Materials and Methods) full-length LovK, as well as its truncated derivatives LovK1-138 and LovK1-156. In addition, we generated two fusion proteins, LovK-STAS A and LovK-STAS B. The STAS domain (for: sulfate transport anti-sigma factor antagonist) is the C-terminal effector domain of YtvA, a photo-sensory stress protein from *Bacillus subtilis,* which contains an N-terminal LOV domain that mediates light perception. [11, 13, 15] Significantly, in both YtvA and in LovK, the N-terminal LOV domain is linked to the respective effector domain through a helical linker structure (often referred to as Jα helix [16]) that presumably forms a coiled/coil structure in the functionally active dimers of both proteins. [13, 17] These fusion proteins were designed via sequence alignment of the two full-length proteins in the linker region (figure 1A). In LovK-STAS A the LOV domain from LovK1-138 is connected to the STAS domain (128-256) from YtvA, such that the Jα linker from YtvA is retained. LovKSTAS B comprises 156 residues from LovK which are connected to the 146th residue of YtvA, *i.e.* the N-terminus of its STAS domain. LovK-STAS B therefore contains the linker region of LovK (*i.e.* a covalent peptide linkage of residue 127 of YtvA to 139 of LovK). In the selection of the fusion sites care was taken not to disturb the hepta-helical pattern that is typical for coiled/coil structures (compare ref [18]). The two fusion proteins were overexpressed in, and purified from, the heterologous overexpression host *Escherichia coli* M15. Recording of their light/dark difference spectra *in vitro* showed the expected features (figure 1B) and recovery rates (data not shown). As the expression levels achieved under these conditions are relatively high (in the order of 0.3 to 0.8 mg protein per g dry weight of cells), we tried to analyze their UV/visible spectra also *in vivo*. For this we made use of the SPECORD 210PLUS, a spectrophotometer in which the sample cell is placed very close to the light detector, so that artefacts by light scattering are minimized. Spectra recorded accordingly (figure. 1C) clearly revealed the heterologously expressed LOV domains. Furthermore, their observed peak-height, corrected for light scattering, is consistent with the yield of purified protein obtained. Illumination of these *E. coli* cells with 450 nm light from a blue LED for several minutes led to complete bleaching of the (oxidized) flavin

features from these spectra. This is confirmed by the shape of the difference spectra, taken of cells prior to, and after illumination (figure 1D). This shows that both fusion proteins are fully functional with respect to photosensory activity also *in vivo*, be it that LovK-STAS B appears to be slightly sensitive to intracellular proteolysis. Analysis of recovery rates *in vivo* is complicated by simultaneous settling of the cells during the measurement. These aspects will therefore be addressed elsewhere. Both fusion proteins were also expressed in *B. subtilis*. No functional activity, however, could be detected in the general stress response of this organism that could be ascribed to these chimeras, in contrast to a fusion protein composed of the LOV domain of YtvA and the STAS domain of RsbRA. [19] Generally, expression levels of the LOV-domain containing proteins that we have studied, are lower in the Gram-positive organism than in *E. coli*; for this reason we have limited our *in vivo* characterization to *E. coli*.

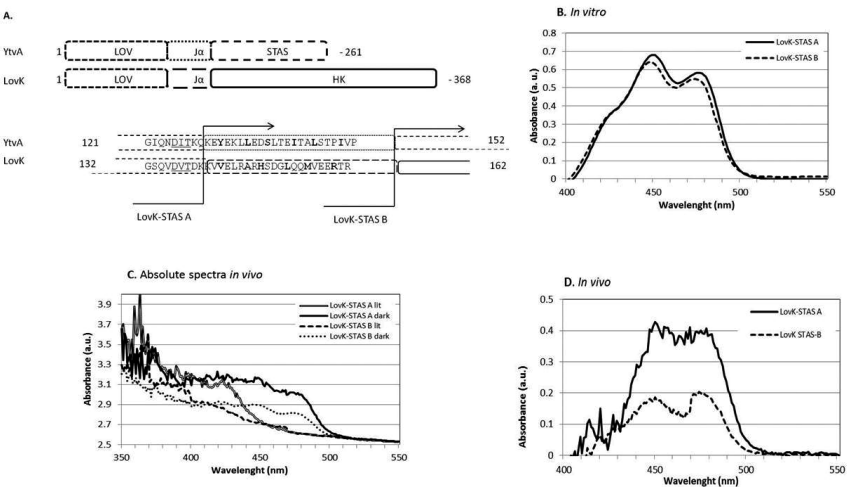

Figure 1. Characterization of LOV/STAS fusion proteins. A. Schematic drawing of the LOVK-STAS A/B domains used in this study; B. *In vitro* difference spectra of LovK-STAS A and LovK-STAS B; C. Absolute spectra of the LovK-STAS A and LovK-STAS B proteins *in vivo*; D. Dark-minus-light absorption difference spectra of the LovK-STAS A and LovK STAS B proteins *in vivo*.

2.3.2 **Redox midpoint potential measurements**

All redox midpoint potential measurements were carried out under exactly the same conditions as described in Arents *et al*. [5] Full UV/visible absorption spectra of the visible color changes in the reaction mixture during the reducing titration were recorded. For all measurements just two indicator dyes, safranin and phenosafranin were used (figure 2A-D). The midpoint potentials of these dyes are -252 mV and -289 mV, respectively. Figures 2E and 2F show plots of the ratio of the oxidized/reduced form of the flavin and the indicator dye used in the reaction. Based on such plots it is possible to calculate the redox midpoint potential of the flavoproteins, based on the known redox midpoint potential of the respective dye. During the reductive titrations with purified proteins no formation of the semiquinone intermediate was observed.

Surprisingly, close inspection of the midpoint potential values obtained showed small, but significant, differences in the values of the midpoint potentials measured with the two indicator dyes for all constructs (see Table 2). Nearly all actual values for the midpoint potential of the series of LOV domains, derived from measurements with phenosafranin as the indicator dye, are higher than values calculated with safranin as the indicator dye (up to 48 mV, but notice that there is significant spread in these values). On average, values determined with phenosafranin are 18 mV more positive than those determined with safranin, which is measurably higher than the standard error of the mean of the measurement of the individual domains, 7 or 8 mV for safranin and phenosafranin respectively (Table 2). Nevertheless, based on these separate values we could calculate average values for the midpoint potential of every investigated construct. The average midpoint potentials for LovKSTAS A and LovK-STAS B are -274 mV and -287 mV, respectively. For the truncated LovK constructs the midpoint potential gradually increases from -287 mV for full-length LovK, via -284 mV for LovK1-156 to -272 mV for LovK1-138. The midpoint potential determined for YtvA in this investigation (-305 mV) is not significantly different from the value reported earlier (-307 mV; ref [5]).

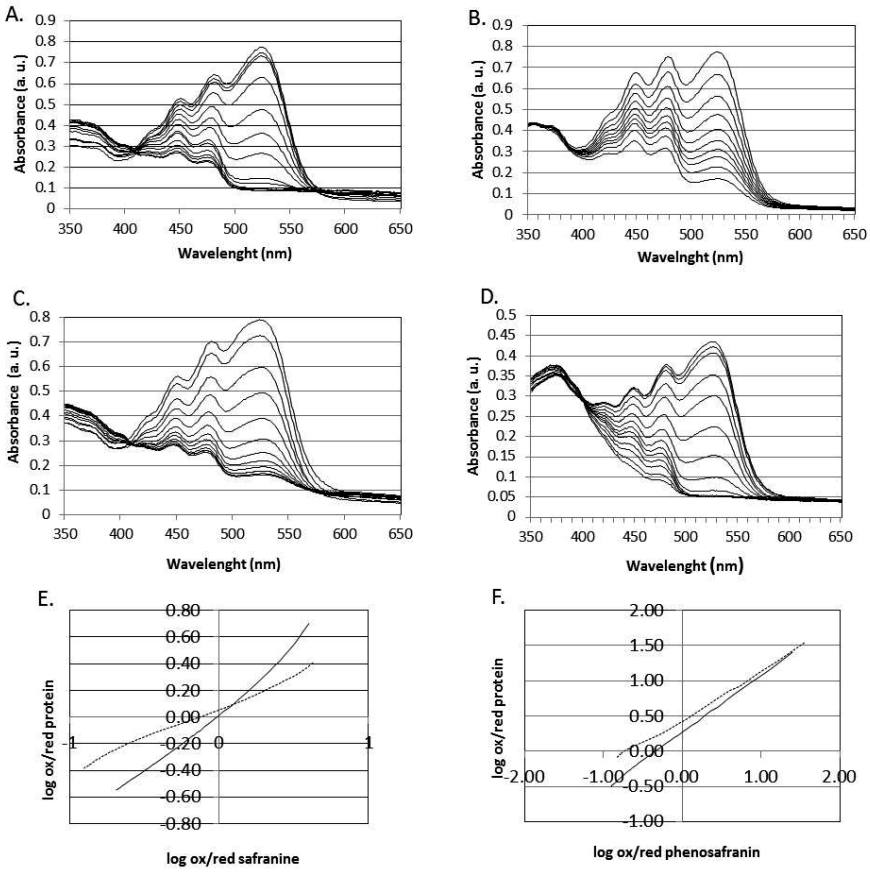

Figure 2. Spectral recording and data evaluation of the color changes in the reaction mixture during the reducing titration with xanthine/xanthine oxidase. Spectra were taken at 60 s intervals, but only every 20th spectrum is shown. A. Full-length LovK titrated with phenosafranin; B. LovK-STAS A with phenosafranin, C. Full-length LovK with safranin, D. LovK-STAS A with safranin. E, F. Plot of the redox potential of the LovK-STAS A (solid line) and full-length LovK (dashed line) versus: E. safranin and: F. phenosafranin. Such plots allow a straightforward calculation of the respective midpoint potentials.

Table 2. Overview of the redox midpoint potentials of the LOV domains studied in this investigation. Values are given in mV relative to the calomel electrode.

Flavoprotein	Em in pH 8 with safranin (S)	Em in pH 8 with phenosafranin (PS)	ΔEm Em(PS) – Em(S)	Standard deviation:	
				safranin	pheno-safranin
LovK-STAS A Av: -274	-295	-272	23	7	6
	-283	-268	15		
	-284	-261	23		
LovK-STAS B Av: -287	-305	-257	48	8	6
	-295	-266	29		
	-311				
LovK (1-368) Av: -287	-291	-285	6	9	11
	-304	-270	34		
LovK (1-156) Av: -284	-293	-276	17	2	7
	-295	-276	19		
	-292	-276	16		
	-297	-263	34		
LovK (1-138) Av: -272	-270	-272	-2	7	11
	-285	-248	37		
	-285	-268	17		
	-283	-263	20		
FMN	-209	-213	-4		
YtvA Av: -305	-313	-296	17		
Average			18	7	8

2.3.3 **On the redox state of LovK *in vivo***

(a) Specificity of the *in vitro* Reduction of the LOV Domain of LovK.

To better understand the factors that determine the *in vivo* redox state of the LOV domain(s) we first studied the specificity of their reduction *in vitro*. To this end, LOV-domain containing protein solutions were incubated with sodium dithionite, NADH or methylviologen. All solutions were flushed with argon before mixing. Of these three compounds only sodium dithionite (Em' = -660 mV) did reduce the LOV domain of LovK under anaerobic conditions (figure 3). Glucose and glucose oxidase were added to the reaction mixtures to remove remaining traces of oxygen. It is clear from these data (*i.e.* the broad peak in the range between 550 and 700 nm) that dithionite in this case does give rise to very pronounced flavosemiquinone formation. Addition of equimolar amounts of NADH did not reduce this LOV domain, as was also observed by Crosson and co-workers. [7] A 25-

fold increase of the NADH concentration in the reaction mixture did not lead to reduction of the LOV domain either. Also, addition of 10 µM methyl viologen (Em' = -449 mV) did not reduce the LOV domain *in vitro*, despite the reduction seen *in vivo* (see further below). When all these different reductants, including the (pheno)safranin dyes, are combined, this – as expected – does lead to the observation that the LOV domain is reduced first, followed by the NAD+.

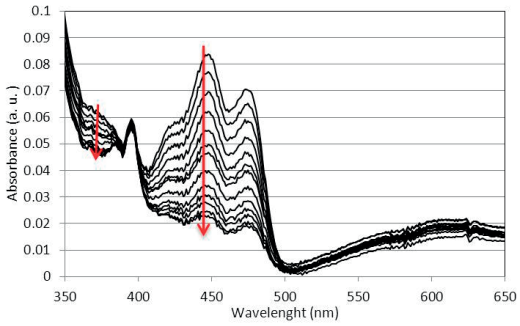

Figure 3. Reduction of the LovK-LOV domain with 10 µM sodium dithionite *in vitro* under anaerobic conditions in the presence of glucose and glucose oxidase. The arrows indicate increasing time and increasing degree of reduction.

(b) *In vivo* Reduction of the LOV domain of LovK.

As the LovK1-138 construct has the highest midpoint potential of the ones we have studied in this investigation (Table 2), this latter construct was the prime target for further *in vivo* studies. We first tested the effect of addition of a range of reducing agents to cells that overexpress this LOV domain: methyl viologen, benzyl viologen, sodium dithionite, sodium borohydride and riboflavin. Of these compounds, methyl viologen, sodium dithionite and sodium borohydride (for the examples of methyl viologen and sodium dithionite: see figure 4) can chemically reduce the LOV domain of LovK, as can clearly be seen in difference spectra of cells before and after addition of these reductants, in spite of the noise particularly at the high-energy shoulder of the flavin difference spectrum. Addition of benzyl viologen as the reductant to intact cells of *E. coli* led to only a transient reduction of the LOV domain,

whereas with riboflavin an appreciable amount of flavin semiquinone was formed (data not shown). In contrast, chemical reduction of the LOV domain from YtvA was not possible with any of these latter reducing agents. Shifting growing *E. coli* cells from aerobic- to anaerobic conditions will lower the midpoint potential of the cytoplasm considerably, by lowering of the redox potential of the NADH /NAD+ couple. [8, 9] We therefore tried to record spectra of strictly anaerobically grown LovK-producing *E. coli* cells. For this cells were cultivated in 250 ml bottles filled to the top with medium. Bottles were incubated at 37 °C, with slow stirring, for approximately 20 hours. After that cells were transferred anaerobically to a cuvette and spectra were recorded after flushing with argon for half an hour. These conditions, however, did not lead to sufficient level of LOV-domain overexpression to allow identification of the absorbance band of the LOV domain in the UV/visible spectra. Therefore, *E. coli* M15/pQE30(LovK1-138) was grown aerobically, to achieve maximal overexpression levels of LovK1-138, and after concentrating the cells through centrifugation, UV/visible spectra were recorded (figure 5). Next, cells were kept under anaerobic conditions by flushing the suspension with argon for 5 h in the presence of glucose. We could not detect any change in the spectra of the cells after this incubation under anaerobic conditions, neither with the LOV domain from LovK nor with the one from YtvA (figure 5); in contrast a reduction was achieved when in addition dithionite plus methylviologen (data not shown).

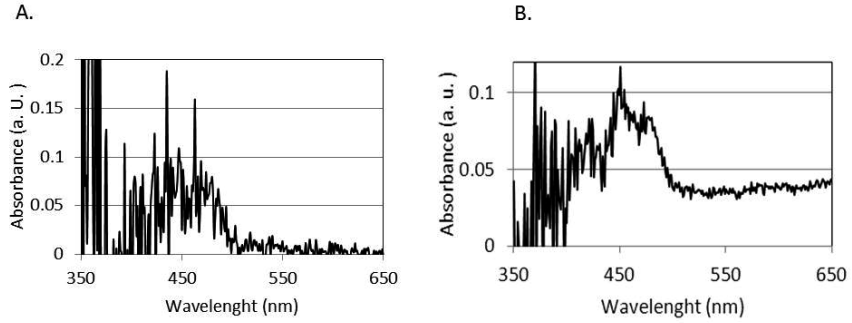

Figure 4. Difference spectra of the chemical reduction of the LOV domain of LovK *in vivo* with: A. 10 µM methyl viologen, B. 10 µM sodium dithionite.

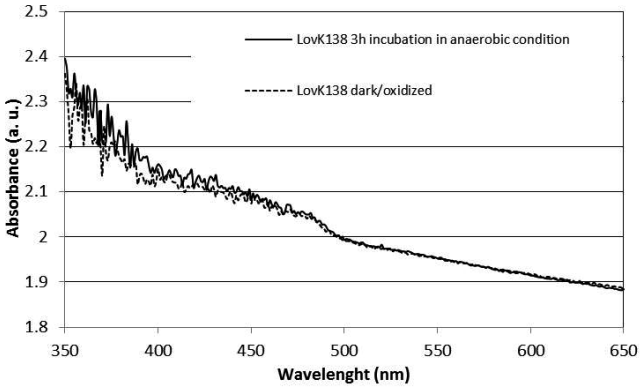

Figure 5. Comparison of i*n vivo* $LovK_{1-138}$ spectra between aerobic and anaerobic conditions.

2.4 Discussion

The data reported here for the redox midpoint potential of LovK, and some of its truncated fragments, differs slightly from the values reported by Crosson and co-workers. [7] The most notable are the differences for the midpoint potential of the full-length LovK protein and LovK1-138, *i.e*. -287 and -272 mV, as reported here, and -258 and -303 mV as reported in the study of Purcell *et al*. [7] However, as the latter study does not indicate which specific indicator dye was used for which protein, nor what the typical standard deviation was in their assays, it is difficult to pinpoint the reason(s) for these differences. Although not observed in our previous study, [5] here we did observe a slight but significant difference in the apparent redox midpoint potential of the set of analyzed proteins, as a function of the specific indicator dye that was used. We attribute this to a difference in reactivity of the two indicator dyes with the respective proteins, rather than to a kinetic disequilibrium caused by too high rates of electron input via the xanthine/xanthine oxidase system. [5] Because of the relatively small differences in the values reported by the two indicator dyes used here, we nevertheless think that it is relevant to calculate the averaged midpoint potential for the various proteins/domains (see Table 2). The observed range of absorption maxima of the purified proteins (447 to 449 nm; data not shown) is too small to allow a conclusion to be drawn as to whether or not the correlation between wavelength of maximal absorbance and redox midpoint potential, that we reported in our previous study, [5] is also visible in the data of the series of protein domains studied here. Overall, the LOV domain of the LovK derivatives

tends to have a higher midpoint potential than the LOV domain of YtvA derivatives (Table 2). This is not paralleled by generally higher values for the photocycle recovery rate of the LOV domain of LovK [3, 7, 13] as might have been expected on the basis of a better flavin accessibility from the aqueous phase. [20] Another trend that can be extracted from the average values of the midpoint potential of the proteins analyzed in Table 2 is the increase one observes in the midpoint potential when the authentic linker helix of the LOV domain of LovK is replaced by a heterologous one, or when the linker region is truncated. The conversion of a LOV domain *in vivo* from its oxidized to the chemically reduced state is readily observed upon the addition of a strong, non-physiological, electron donor like dithionite (figure 4). But it is important to note that the use of a UV/visible spectrometer with the photo-detection cells positioned as close as possible to the measurement cuvette is crucial in order to be able to make such observations. All attempts, however, to show a similar oxidized-to-reduced transition under physiological conditions so far failed. We therefore think that, if physiologically relevant, redox regulation of light-sensing LOV domains will only occur under very extreme conditions. A major contributing factor in this probably is the absence of suitable physiological redox mediators that can equilibrate the redox state of the flavin in the LOV domain with the ambient redox potential (of NAD+/NADH) in the cytoplasm. Yet other flavin-containing blue light photoreceptor proteins exist, like cryptochromes and photolyases, that have a significantly more positive midpoint potential than the LOV domains ([21, 22]; in particular the cryptochromes). Intracellular reduction of photolyases is readily observed. [23] It therefore remains an interesting challenge to resolve whether or not for the crypotochromes one is able to observe an integration of redox- and light-signalling in a single signalling receptor protein.

References

1. van der Horst MA, Hellingwerf KJ (2004) Photoreceptor proteins, “star actors of modern times”: a review of the functional dynamics in the structure of representative members of six different photoreceptor families. Acc Chem Res 37:13–20 . doi: 10.1021/ar020219d
2. Möglich A, Yang X, Ayers RA, Moffat K (2010) Structure and function of plant photoreceptors. Annu Rev Plant Biol 61:21–47 . doi: 10.1146/annurev-arplant-042809-112259
3. Losi A, Gartner W (2011) The Evolution of Flavin-Binding Photoreceptors: An Ancient Chromophore Serving Trendy Blue-Light Sensors. Annu Rev Plant Biol. doi: 10.1146/annurev-arplant-042811-105538
4. Sancar A (2004) Photolyase and cryptochrome blue-light photoreceptors. Adv Protein Chem 69:73–100 . doi: 10.1016/S0065-3233(04)69003-6
5. Arents JC, Perez MA, Hendriks J, Hellingwerf KJ (2011) On the midpoint potential of the FAD chromophore in a BLUF-domain containing photoreceptor protein. FEBS Lett 585:167–172 . doi: 10.1016/j.febslet.2010.11.035
6. Balland V, Byrdin M, Eker AP, Ahmad M, Brettel K (2009) What makes the difference between a cryptochrome and DNA photolyase? A spectroelectrochemical comparison of the flavin redox transitions. J Am Chem Soc 131:426–427 . doi: 10.1021/ja806540j
7. Purcell EB, McDonald CA, Palfey BA, Crosson S (2010) An analysis of the solution structure and signaling mechanism of LovK, a sensor histidine kinase integrating light and redox signals. Biochemistry 49:6761–6770 . doi: 10.1021/bi1006404
8. Canovas M, Sevilla A, Bernal V, Leal R, Iborra JL (2006) Role of energetic coenzyme pools in the production of L-carnitine by Escherichia coli. Metab Eng 8:603–618 . doi: 10.1016/j.ymben.2006.06.002
9. Alexeeva S, Hellingwerf KJ, de Mattos MJT (2003) Requirement of ArcA for redox regulation in Escherichia coli under microaerobic but not anaerobic or aerobic conditions. J Bacteriol 185:204–209
10. Jackson JB (1991) The proton-translocating nicotinamide adenine dinucleotide transhydrogenase. J Bioenerg Biomembr 23:715–741
11. Avila-Perez M, Hellingwerf KJ, Kort R (2006) Blue light activates the sigmaB-dependent stress response of Bacillus subtilis via YtvA. J Bacteriol 188:6411–6414 . doi: 10.1128/JB.00716-06
12. Horton RM, Hunt HD, Ho SN, Pullen JK, Pease LR (1989) Engineering hybrid genes without the use of restriction enzymes: gene splicing by overlap extension. Gene 77:61–68
13. Avila-Perez M, Vreede J, Tang Y, Bende O, Losi A, Gartner W, Hellingwerf K (2009) In vivo mutational analysis of YtvA from Bacillus subtilis: mechanism of light activation of the general stress response. J Biol Chem 284:24958–24964 . doi: 10.1074/jbc.M109.033316

14. Messey V (1990) A simple method for the determination of redox potentials. Flavins and Flavoproteins 1990, Walter de Gruyter, Berlin (1991) 59–66
15. Gaidenko TA, Kim TJ, Weigel AL, Brody MS, Price CW (2006) The blue-light receptor YtvA acts in the environmental stress signaling pathway of Bacillus subtilis. J Bacteriol 188:6387–6395 . doi: 10.1128/JB.00691-06
16. Harper SM, Neil LC, Gardner KH (2003) Structural basis of a phototropin light switch. Science 301:1541–1544 . doi: 10.1126/science.1086810
17. Jurk M, Dorn M, Schmieder P (2011) Blue flickers of hope: secondary structure, dynamics, and putative dimerization interface of the blue-light receptor YtvA from Bacillus subtilis. Biochemistry 50:8163–8171 . doi: 10.1021/bi200782j
18. Möglich A, Ayers RA, Moffat K (2009) Design and signaling mechanism of light-regulated histidine kinases. J Mol Biol 385:1433–1444 . doi: 10.1016/j.jmb.2008.12.017
19. van der Steen JB, Avila-Perez M, Knippert D, Vreugdenhil A, van Alphen P, Hellingwerf KJ (2012) Differentiation of function among the RsbR paralogs in the general stress response of Bacillus subtilis with regard to light perception. J Bacteriol 194(7):1708–1716 . doi: 10.1128/JB.06705-11
20. Alexandre MT, Arents JC, van Grondelle R, Hellingwerf KJ, Kennis JT (2007) A base-catalyzed mechanism for dark state recovery in the Avena sativa phototropin-1 LOV2 domain. Biochemistry 46:3129–3137 . doi: 10.1021/bi062074e
21. Gindt YM, Schelvis JP, Thoren KL, Huang TH (2005) Substrate binding modulates the reduction potential of DNA photolyase. J Am Chem Soc 127:10472–10473 . doi: 10.1021/ja051441r
22. Sokolowsky K, Newton M, Lucero C, Wertheim B, Freedman J, Cortazar F, Czochor J, Schelvis JP, Gindt YM (2010) Spectroscopic and thermodynamic comparisons of Escherichia coli DNA photolyase and Vibrio cholerae cryptochrome 1. J Phys Chem 114:7121–7130 . doi: 10.1021/jp102275r
23. Brettel K, Byrdin M (2010) Reaction mechanisms of DNA photolyase. Curr Opin Struct Biol 20:693–701 . doi: 10.1016/j.sbi.2010.07.003

3 Design and functional characterization of the hybrid light dependent yeast histidine kinase, Light-Oxygen-Voltage (LOV)-Sln1.

Bury AE, Hellingwerf KJ

Abstract:
Phosphorylation plays a critical role in facilitating signal transduction in prokaryotic and low eukaryotic organisms. Here we describe the light regulated histidine kinases. These were designed by the helical alignment of the α-helical linker of the LOV (light-oxygen-voltage) domain of YtvA from *Bacillus subtilis* with the α-helical linker of the histidine-protein kinase domain of the Sln1 kinase of the phospho-relay system for osmoregulation of *Saccharomyces cerevisiae*. *In vitro*, illumination with blue light inhibits/stimulate the ATP-dependent phosphorylation of these hybrid kinases.

A condensed version of this chapter has been published as:
Bury A, Hellingwerf KJ. 2018 Design, characterization and *in vivo* functioning of a light-dependent histidine protein kinase in the yeast Saccharomyces cerevisiae. AMB Express. 2018 Apr 2;8(1):53

3.1 Introduction

In this chapter the design and functional *in vitro* characterization of light-dependent histidine kinase fusion proteins is described. This can be achieved e.g. by fusion of the LOV domain from e.g. YtvA from *Bacillus subtilis* with the histidine kinase domain of the Sln1 histidine kinase from *Saccharomyces cerevisiae*. The choice of these two domains is dictated by (i) the research history with YtvA within the Molecular Microbial Physiology Group, which amongst others has shown that this particular LOV domain will be relatively insensitive to alterations in the redox potential in its surroundings (for further detail: see Chapter 2) and (ii) the application we have in mind for future studies with this fusion protein (*i.e.* light activation of a signal-transduction responses in the eukaryotic (yeast) cytoplasm; the Sln1 protein is responsible for the osmotic stress response in yeast cells). Sln1 histidine kinase consists of a plasma membrane-associated domain, followed by two separate domains: the histidine kinase domain (HK) with the conserved histidine H576, and the response regulator domain (R1) with the conserved aspartate D1144, which both are phosphorylated during the phosphoryl transfer reaction (for details see figure 1A). Under physiological conditions the conserved H576 residue is moderately phosphorylated. Hyper-phosphorylation occurs, however, after a stress that causes weakening of the cell wall. In contrast, conditions causing a reduction of the cell turgor lead to accumulation of the Sln1 kinase in non-phosphorylated form (presumably through activation of intrinsic phosphatase activity). Phosphoryl groups from the conserved histidine are transferred to the conserved aspartate (D1144) within the R1 domain. In the next step the phosphoryl group is transferred to the conserved histidine (H64) in Ypd1, the phosphoryl-transfer domain of this phospho-relay system, and finally to D554 and D427 in the receiver domains of the Ssk1 and Skn7 response regulators, respectively. [1, 2] Here we demonstrate the functionality of a fusion proteins composed of the LOV domain of YtvA and the histidine kinase domain of Sln1 in light-sensitivity of the phosphoryl flux through the Sln1 kinase. By properly engineering the point of fusion between the two domains, as well as of the linker domain, fusion proteins can be obtained in which illumination with blue light either increases or decreases the level of activation of the 'fusion kinase'. For the composition of the domains see figure 1.

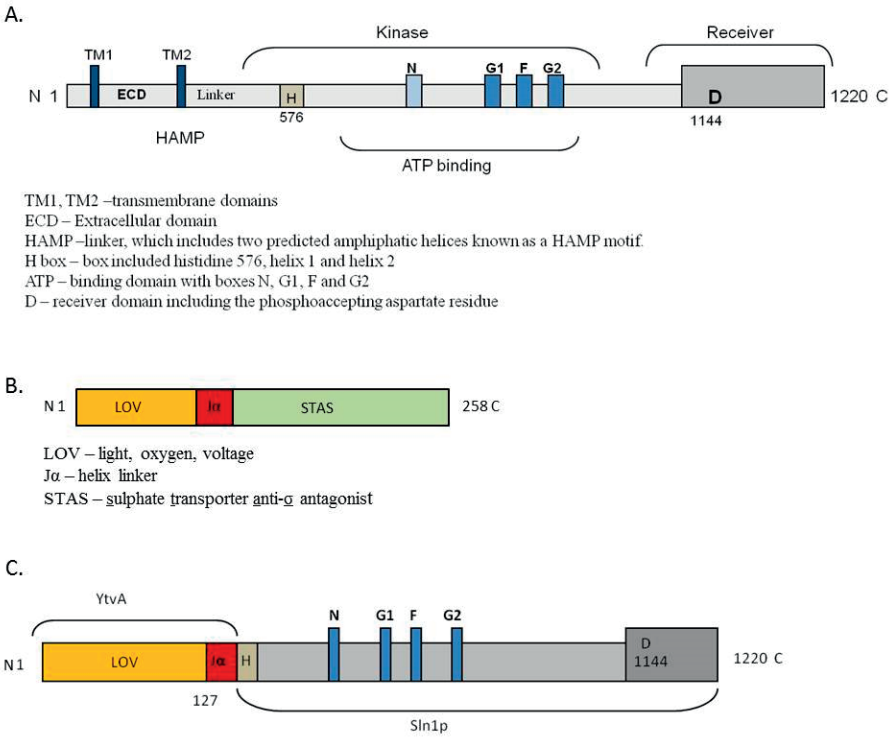

Figure 1. Panel A: Components of the Sln1 histidine kinase from *S. cerevisiae*. Panel B: Components of the YtvA protein from *B. subtilis*. Panel C. Overall design of the LOV-Sln1 fusion protein.

3.1.1 **Designing of the light stimulated histidine kinase**

To generate the LOV-domain/histidine-kinase domain fusion protein, the plasma membrane associated domain of the Sln1 kinase was replaced with the LOV domain of YtvA. It was shown by others that N-terminal of the conserved histidine H576 a sequence-identifiable coiled-coil secondary structure is present in the Sln1 protein (see figure 1A). [3] Following the idea's developed in Möglich et al. [4] we aligned the coiled-coil structures of the Jα helix of the LOV domain and the coiled-coil structure of the Sln1 kinase and we designed a number of fusion proteins (referred to as C#) that would be expected to show light-activation and/or de-activation of kinase activity (see table 2). [5] Aligning the two proteins/domains was straightforward because the hepta-helical (see figure 2) sequence feature was straightforwardly identifiable in both proteins.

Of the newly designed fusion proteins C1 consists of the LOV domain plus the J_α helix from YtvA, and the HK- and R1 domains of Sln1, starting from the 567th amino acid of the Sln1 part (for further detail see figure 1B and 2A). C2 consists of the LOV domain from YtvA and the HK-R1 part, starting from the 538th amino acid of Sln1 which means that the coiled coil linker structure is fully derived from Sln1. C5 consists of 127 amino acids of the LOV domain from YtvA, which means that there is a switch-over between the two proteins just after the DIT motif [6, 7] in the Jα region of the LOV domain of YtvA. The C6 construct, just as C5, consists of 127 amino acids from the LOV domain, but however, with an important difference in the coiled-coil structure compared to the C5 construct: After 13 amino acids into the coiled-coil structure one extra amino acid was added. This position was selected based on an alignment of the coiled-coil structures of the two proteins. This insertion of a single amino acid is expected to allow a change in the light/dark activity ratio of this construct. Another construct, called C8, consists of 132 amino acids of the LOV domain from YtvA, connected to the coiled-coil structure of the Sln1 histidine kinase. Details about the construction of the C1 to C11 fusion proteins are summarized in table 2.

A.

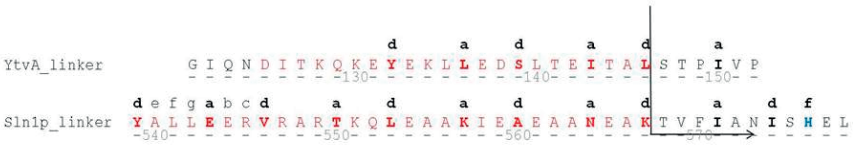

B.

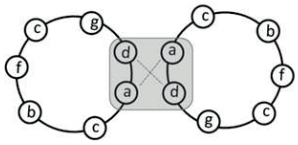

Figure 2. Panel A: Alignment of the coiled coil structures from Sln1 and YtvA. The point of switching from the Jα to Sln1 in the C1 construct is indicated by the arrow. Panel B: Schematic, helical, diagram of a coiled coil structure. [3]

As in the C1 construct light-inhibition of kinase activity was observed, we also tried to generate constructs with light-stimulated kinase activity. Such light-stimulated kinase activity was e.g. reported for the YF constructs described in Möglich et al. [7] Their YF1 construct is composed of the LOV domain from YtvA (#1 to 127) fused to the kinase domain of FixL (# 258 to 505), i.e. it derives its helical linker from FixL. We therefore first composed the triple-fusion protein C9, consisting of the LOV domain of YtvA (# 1 to 127), the linker helix of FixL (# 259 to 281) and the histidine kinase- plus response regulator domain from Sln1 (# 567 to 1221). Phosphorylation assays, however, showed that this construct did not display any measurable kinase activity (see table 2). The C10 and C11 constructs were then designed, to conserve the sequence around the DIT motif of YtvA, and to expand it to the DITKQ motif. Accordingly, C10 was designed, and also C11, with the deletion of one amino acid downstream of the DITKQ motif (figure 2A). The TKQ motif was identified in the Sln1 histidine kinase too and therefore the YtvA sequence was linked to the kinase domain with optimal conservation of the coiled/coil structure.

3.1.2 **Activity tests for protein kinases**

Protein phosphorylation events are catalysed by protein kinases that transfer the γ-phosphoryl group from a nucleoside triphosphate, usually ATP, to the side chain of an amino acid residue in a substrate protein. [8] Protein histidine phosphorylation was discovered to occur in protein extracts from [^{32}P]P_i-labelled bovine mitochondria by Boyer et al. in 1962. [9] After that the corresponding protein kinases were discovered (for a review see [10]). Histidine (protein) kinases are the most common in bacteria, fungi and plants [8], while in higher eukaryotes mainly serine/threonine and tyrosine kinases play a crucial role in many biological processes. [8, 11, 12]

Detection of kinase activity maybe be achieved in several different ways (see figure 3). Radiometric assays are among the earliest used for detection of kinase activity, and generally, these methods also offer detection with the highest level of sensitivity. These assays utilize ATP, radiolabeled on the γ-phosphate group (generally with ^{32}P or ^{33}P). In a kinase reaction, the radioisotope is transferred from ATP to the acceptor molecule, and the rate of product formation can be quantified by measuring the extent of isotope incorporation in the product molecules. [13, 14]

Based on the (non-radioactive) ATP depletion the kinase activity can be measured by quantifying the remaining amount of unreacted ATP, using luminescent detection coupled to

a luciferase assay. The luminescence signal is proportional to the amount of ATP present and is inversely correlated with kinase activity. As the kinase reaction proceeds, less and less ATP will be available for coupling to the luciferase assay, so the overall readout is a decreasing signal. [15, 16]

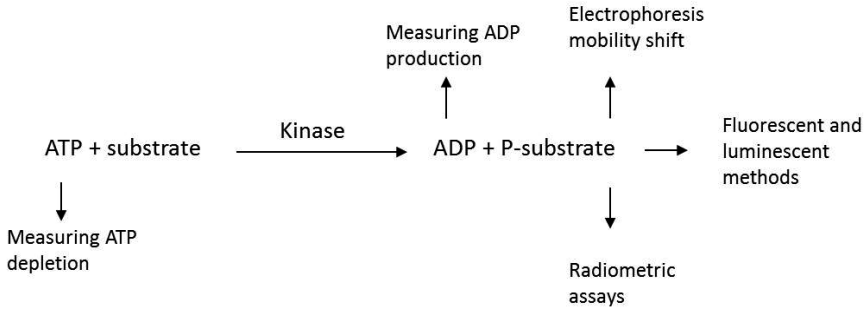

Figure 3. Overview of some methods for detection of (protein) kinase activity. Based on a kinase-catalyzed reaction, enzyme activity can be detected by either measuring ATP consumption, ADP formation or phospho-product formation. [14, 15]

ADP accumulation can be detected – after quenching of the phosphorylation reaction - by a coupled enzyme reaction involving pyruvate kinase, pyruvate oxidase, horseradish peroxidase, and a fluorogenic substrate. [17] Pyruvate kinase catalyzes – with high affinity - the transfer of the phosphate group from phosphoenolpyruvate to ADP, resulting in the formation of ATP and pyruvate. Pyruvate is then oxidized by pyruvate oxidase to form hydrogen peroxide, which is in turn utilized in the oxidation peroxidase to generate resorufin. The concentration of resorufin is determined by measuring fluorescence emission at 590 nm after excitation at 530 nm, with increasing signal corresponding to increasing ADP concentrations. [15, 17]

A more recently developed method is based on the shift in electrophoretic mobility that is caused by phosphorylation of the target protein during electrophoresis in poly-acrylamide gels that contain a dinuclear Mn^{2+} complex covalently linked to the poly-acrylamide, loosely referred to as a 'Pos-tag'. [18]The principle behind this method is that phosphorylated proteins move slower in SDS-PAGE than do the corresponding non-phosphorylated molecules, because the phosphoryl group interacts with the Mn^{2+} Phos-tag ligand in the gel. [19]

Fluorescence and luminescence methods for detecting kinase activity can be based on binding of a phosphorylated peptide substrate by an antibody that specifically recognizes the phosphorylated form of the target protein. However, this method requires a high chemical stability of the phosphorylated protein/peptide. So far, no antibodies are available that recognize proteins phosphorylated on an aspartate side chain. For convenient detection fluorescence energy transfer can be achieved by bringing in close proximity the peptide substrate labeled with e.g. a FRET acceptor molecule and phospho-specific antibody labeled with a fluorescence donor molecule. Phosphorylation allows for bringing the donor and acceptor molecules close enough together to generate the FRET signal. [15, 20, 21] Many commercially available kinase assays are based on this principle (for details see [14, 15]).
Because of the high instability of the phosphorylated histidine and previous experience of the other group working on the Sln1 pathway phosphorylation (A.West, private conversation, data not published) the method of choice is the radioactive labeling of the phosphoprotein with ^{32}P, which seems to be the most robust and sensitive among the others.

3.2 Materials and methods

3.2.1 Expression and purification of the proteins

All proteins were overexpressed in *E. coli* growing in Production Broth medium [Tryptone (20 g/L; Becto and Dickson Company), Yeast Extract (10 g/L; Scharlab S.L.), Glucose (5 g/L; Dextro energy GmbH Co. KG), NaCl (5 g/L; Sigma-Aldrich), and K_2HPO_4 (8.7 g/L; Merck)], supplemented with 100 µg/ml ampicillin and 25 µg/ml kanamycin. Overnight grown pre-cultures, inoculated with a single colony from a fresh agar plate made of the same medium, were diluted into fresh medium at 37°C and were allowed to grow for an additional 1.5 to 2 h with vigorous shaking. When OD_{600} of these cultures reached 0.6, overexpression of the heterologous protein product was induced by sterile addition of isopropyl β-D-thiogalactopyranoside (IPTG) to a final concentration of 0.1 mM. At this point the temperature was lowered to 25°C and growth was allowed to continue with vigorous shaking for approximately 16 hours in darkness. Then cells were harvested by centrifugation and subsequently lysed by sonication in 50 mM Tris-HCl buffer pH = 8, plus 10 mM NaCl, and an EDTA-free protease inhibitor cocktail (complete, EDTA-free, provided by Roche), 10% (v/v) glycerol, lysozyme, DNase, and RNase, were added. The recombinant proteins were purified from the resulting cell-free extracts in a two-step procedure: Affinity

chromatography on a HisTrap FF column (GE Healthcare, 5 mL column) followed by anion exchange chromatography on a ResQ column (GE Healthcare, 6 ml column volume). Table 1 shows the list of the overexpression vectors used in this study.

Table 1. Plasmids used in this study

Strain or plasmid	Characteristics	Source or reference
pAB009	pQE30 overexpression vector for the C1 protein	This study
pAB010	pQE30 overexpression vector for the C2 protein	This study
pAB025	pQE30 overexpression vector for the C5protein	This study
pAB026	pQE30 overexpression vector for the C6 protein	This study
pAB014	pQE30 overexpression vector for the C8 protein	This study
pAB022	pQE30 overexpression vector for the C9 protein	This study
pAB023	pQE30 overexpression vector for the C10 protein	This study
pAB024	pQE30 overexpression vector for the C11 protein	This study
pAB011	pQE30 overexpression vector for the Ypd1 protein	This study

3.2.2 *In vitro* assay of the extent and rate of phosphorylation of the hybrid histidine protein kinases and of phosphoryl transfer from Sln1 kinase- to the Ypd1 phosphoryl transfer domain

Kinase activity assays were carried out after slight modification of established procedures [1]: 30 µM of the specific histidine protein kinase was incubated with 1 to 5 mM cold ATP, after mixing of the latter with 3300 Ci/mmol of [γ-^{32}P]-ATP. All reactions were carried out in a buffer containing 50 mM Tris.HCl pH = 8, 100 mM KCl, 15 mM $MgCl_2$, 2 mM DTT and 20 % (v/v) glycerol in a total volume of 0.1 to 1 ml in Eppendorf tubes. Time-series samples were taken between 0 and 120 minutes. Samples were immediately mixed with 4x concentrated stop buffer. This concentrated stop buffer contains 0.25 M Tris.HCl pH = 8.8 % (w/v) SDS, 40 % (v/v) glycerol, 40 mM EDTA, 0.008 % (w/v) bromophenol blue and 4 mM β-mercapto-ethanol. For the phosphoryl transfer experiments histidine kinases were first autophosphorylated for one hour in the dark, after which Ypd1 was added to the sample in a molar ratio of 1:2. Time-series samples were taken between 1 and 120 minutes. Samples were immediately mixed with the stop buffer, just as described above. The same volume of the

samples (15 µl) were analyzed on 10 % (w/v) SDS PAGE gels, which were then exposed to a GE healthcare screen. Screens were scanned with a Typhoon Fla 7000 system and the resulting data files were saved as .tiff files. Image Quant software was used for the quantification of the intensity of the different bands. The standard curve equation was calculated based on the standards spotted on the paper and their decay in time. Based on the standard curve equation, kinase concentration and time of the reaction the intensity of the bands was converted to nmoles P/nmole kinase/h.Kinase phosphorylation experiments and phosphoryl transfer experiments were conducted in the dark, with minimal red background light [22], or under constant illumination from blue Light Emitting Diodes (LEDs with λ^{max} = 464 nm) with an incident light intensity of 200 µEinstein·m^2·s^{-1}.

3.3 Results

3.3.1 Photochemistry of the LOV-Sln1 fusion protein

The absorption spectrum of a typical LOV domain in the near-UV/visible range shows two major bands with maxima around 370 and 450 nm. To check for unimpaired photochemistry of the LOV domain in one of the LOV-Sln1 fusion proteins, the latter was assayed by measuring light-induced absorbance changes indicative of adduct formation. Figure 3A shows the steady state dark- and light-induced spectrum of the LOV-Sln1 C1 construct. Loss of absorption in the 450 nm band with some increase in the UV region are characteristic of formation of the flavin–cysteinyl adduct. The time course of the spontaneous dark recovery, to the ground state, after interruption of the blue-light excitation of the C1 fusion histidine kinase, is presented in the figure 3B. A mono-exponential fit of these data leads to the conclusion that the half-time of the recovery of the ground state of the LOV domain in this fusion protein is 144 min., which is comparable to the rate of recovery of the LOV domain in YtvA. [23]

All designed LOV-Sln1 constructs showed photochemistry similar to that presented for the C1 construct.

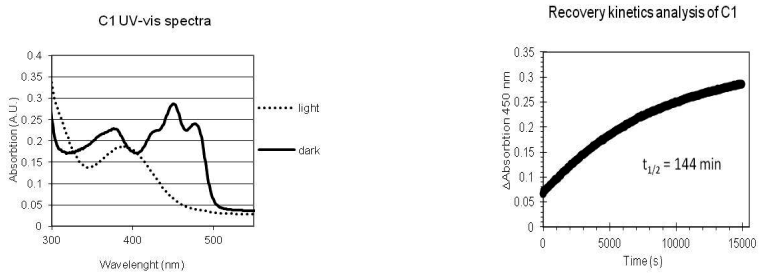

Figure 3. Photochemistry and dynamics of the thermal decay of the LOV-Sln1 C1 fusion histidine kinase. A. UV–vis absorbance spectra of the C1 fusion histidine kinase. B. Spontaneous dark recovery to the ground state after blue-light excitation of the C1 fusion histidine kinase.

3.3.2 **Light influence on the kinase activity**

The helical linker regions of YtvA and Sln1 were aligned according to the identifiable hepta-helical pattern of the coiled-coil structure that presumably is present in both of them, and joined in several different ways (table 2 and figure 2A), i.e. with preservation of the Jα- helix from either protein completely, or partially conserved; with or without insertion of extra amino acids to translationally shift the hepta-helical pattern, and with or without conservation of the position of the crucial DIT motif of the LOV domain of YtvA and of the phosphorylatable histidine of the Sln1 kinase domain.

The resulting hybrid kinases, with the truncated Sln1 kinase domain as a reference, were assayed for kinase activity in the dark with the classical kinase assay based on the use of ^{32}P[ATP]. Other assays, e.g. based on inorganic phosphate release, were tested too, but turned out to be less suited. Of all the kinase domains tested, only the truncated reference domain and the C1 and C6 fusion proteins showed considerable auto-phosphorylation activity, in the order of 0.38 and 0.24 nmolP/g protein/minute for the latter two, respectively, at saturating concentrations of the nucleotide substrate (i.e. 5 mM; see [1]) and 30 µM of the specific histidine protein kinase (domain). Next, we tested a possible difference between this activity, and the corresponding activity in saturating amounts of blue light (for further experimental detail: see Materials and Methods). These assays revealed that significant differences in activity, when assayed in light and dark, were only observed for the fusion protein C1 (while a very small difference was observed for C6, see table 2). Figure 4A shows differences in the

phosphorylation level of the phosphorylated LOV-Sln1. The former, i.e. C1, in spite of its slightly lower maximal activity than C10, was therefore selected for further experiments. Significantly, for both hybrid kinases it turned out that illumination lowered their activity. In subsequently designed fusion proteins (e.g. C11) it turned out to be possible also to observe significant light-stimulation of kinase activity (see table 2 and figure 7). However, as for our subsequent *in vivo* experiments (see chapter 4) the light-inhibition of kinase activity was most valuable, these latter constructs have not been further characterized.

Table 2. Details of the design and *in vitro* activity of a series of LOV::Sln1 histidine kinase fusion proteins.

Construct name	Numbers of amino acid from YtvA	Numbers of amino acid from Sln1	Initial rate of phosphorylation in the dark	Initial rate of phosphorylation in the light	Ratio
C1	YtvA (1-146)	Sln1HKR1 (567-1221)	0.18	0.08	2.25
C2	YtvA (1-127)	Sln1HKR1 (538-1221)	0.08	0.08	1
C5	YtvA (1-127)	Sln1HKR1 (536-1221)	0.03	0.03	1
C6	YtvA (1-127)	Sln1HKR1 (536-1221) ↓549H	0.08	0.09	0.9
C8	YtvA (1-132)	Sln1HKR1 (540-1221)	0.01	0.01	1
C9	YtvA (1-127) FixL (259-281)*	Sln1HKR1 (567-1221)	n.d	n.d	n.d
C10	YtvA (1-129)	Sln1HKR1 (553-1221)	0.20	0.16	1.3
C11	YtvA (1-129)	Sln1HKR1 (554-1221)	0.11	0.21	0.5

*: this sequence from the hepta-helical signature domain of the coiled-coil structure of FixL was inserted in-between the sequences of LOV-domain of YtvA and the kinase domain of Sln1p. n.d.: not determined; n.a.: not available.

Besides their autophosphorylation activity, several of the hybrid kinases were also tested for activity in an assay that measures phosphoryl transfer from the kinase/response-regulator domain of Sln1 to the phosphoryl-transfer domain of the Sln1 phosphorelay system, i.e. Ypd1 (see figure 4B). All constructs except C9 were active in this assay; however, because we did not have a rapid-quench system available we could not time-resolve this process, and

therefore not meaningfully differentiate between the different hybrid kinases with respect to this activity

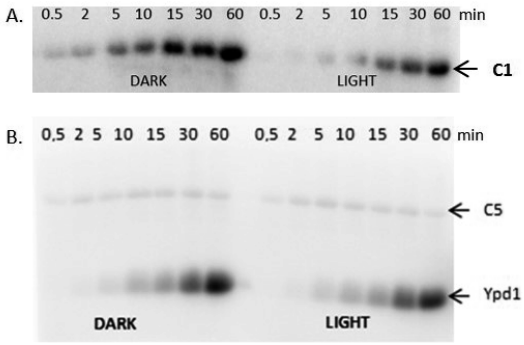

Figure 4. Autoradiographs of the *in vitro* autophosphorylation of the C1 in the dark and light conditions (panel A) and *in vitro* phosphoryl transfer from C5 to Ypd1in the dark and light conditions (panel B) in the dark and in the light.

For the C1 light-modulatable histidine protein kinase we then characterized the kinetic basis of its light sensitivity. Time-course phosphorylation experiments in a time window of 120 minutes, with a wide range of nucleotide concentrations, revealed that in most experiments the increase in the degree of phosphorylation of the kinase was approximately proportional with time during the first 30 minutes (figure 5).

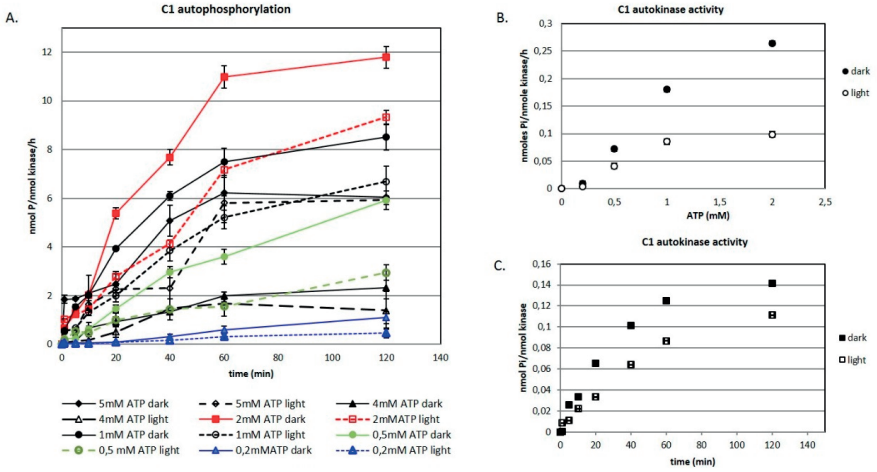

Figure 5. A. Kinetics of the incorporation [^{32}Pi] into the C1 histidine kinase protein. [γ-^{32}P]-ATP was used as the phosphoryl group donor. Reaction mixtures were incubated either in the presence of light (open symbols, dashed lines) or in the dark (filled symbols, full lines). Analysis of the amount of phosphorylated protein was carried out as described in Materials and Methods. B. The ATP-concentration dependence of the rate of incorporation of [^{32}Pi] into the C1 histidine kinase fusion protein. Values calculated based on the slope of the corresponding kinetics curves (see panel A). C. Auto-phosphorylation of the C1 LOVSln1HKR1 fusion proteins in the presence of 1mM of ATP. Error bars indicate standard deviations calculated from three independent biological experiments. If the error bar is not visible it means it is smaller than the corresponding symbol.

From these data, the dependency of the rate of autophosphorylation of the C1 kinase on the concentration of ATP was then plotted against the nucleotide concentration from 0 to 2 mM (figure 5B). This analysis revealed that under both assay conditions (i.e. in the light and in the dark) the half-maximal rate of phosphorylation is observed at about 0.5 mM ATP, while the maximal rate of phosphorylation (V_{max}) is lowered with more than 50 % in the presence of saturating amounts of blue light (figure 5C). We do not refer to Km values here because under both conditions the rate of phosphorylation appears to be dependent on the nucleotide concentration in a slightly sigmoidal way, which may well be due to allosteric regulation of the kinase activity. This latter point, however, was not further investigated

because of the relatively large error in the measurements of the rate of phosphorylation. In contrast to previously presented results in the case of the C11 construct it was possible to observe significant light-stimulation of kinase activity (see table 2 and figure 6).

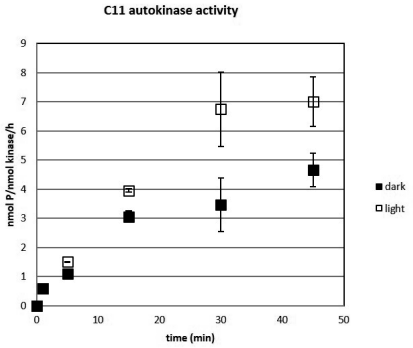

Figure 6. Effect of illumination on the auto-phosphorylation of the C11 LOVSln1HKR1 fusion protein in the presence of 1mM of ATP. Error bars indicate standard deviations calculated from two independent biological experiments. If the error bar is not visible it means it is smaller than the corresponding symbol.

3.4 Discussion

The fusion proteins described in this study of which the activity can be modulated by blue-light illumination were designed following work reported by the group of Moffat, Möglich and co-workers [4, 7, 24]. Their approach is based on the identification of the boundaries of the independently folded domains in signal-transduction proteins like FixL, YtvA, etc., and of the helices linking them. These linker helices often form a coiled/coil tertiary structure in dimers of the corresponding signal transduction proteins. Coiled/coil structures, besides their α-helical nature, display a seven- (hepta-) amino acid repeat structure, with a hydrophobic side chain at each 4^{th}- and 7^{th}-position. [25] This repeat structure then provides a rationale for domain swapping to make new functionalities via fusion proteins. A light modulatable histidine kinase can then be constructed by swapping sequences within these linker domains in such a way that the stability of the independently folded domains is not affected by the swap. Therefore, the coiled/coil linker helices, identified in YtvA and in Sln1, were aligned

on the basis of the hepta-helical repeat motif that is identifiable in both of them (figures 2A, B). [3, 7] This alignment shows that the YtvA sequence, (directly) following the conserved DIT motif (amino acids #125 to 127, which are key to signal transduction within the YtvA protein (for review: see [26]) can be fused with a non-cognate kinase domain. The Sln1 kinase domain qualifies for such a swap in the region just upstream the phosphorylatable histidine of the kinase (i.e. amino acids # 512 to 540).

Based on the above considerations we designed the C1 construct, in which the upstream sequences, including the linker helix of Sln1, are replaced by the LOV domain plus Jα helix from YtvA. Constructs C2, C5 and C6 instead have the LOV domain fused to the Sln1 kinase domain directly after the conserved DIT motive. They differ among each other in the length of the helical linker of the Sln1 domain (see table 2), which will have an influence on the total length of the coiled/coil structure. In the C8 construct the part contributed by YtvA has been extended with 6 amino acids, as an attempt to enhance the difference in kinase activity between light and dark, following Möglich's design of the YF2 construct. [7]

As in the C1 construct light-inhibition of kinase activity was observed, we then also tried to design constructs with light-stimulated kinase activity. Such light-stimulated kinase activity was e.g. reported for the YF constructs described in Möglich et al. [7] Their YF1 construct is composed of the LOV domain from YtvA (#1 to 127) fused to the kinase domain of FixL (# 258 to 505), i.e. it derives its helical linker from FixL. We therefore first composed the triple-fusion protein C9, consisting of the LOV domain of YtvA (# 1 to 127), the linker helix of FixL (# 259 to 281) and the histidine kinase- plus response regulator domain from Sln1 (# 567 to 1221). Phosphorylation assays, however, showed that this construct did not display any measurable kinase activity (table 2). Two constructs were then designed, to conserve the sequence around the DIT motif of YtvA, and to expand it to the DITKQ motif. Accordingly, C10 was designed, and also C11, with the deletion of one amino acid downstream of the DITKQ motif (figure 2A). The TKQ motif was identified in the Sln1 histidine kinase too and therefore the YtvA sequence was linked to the kinase domain with optimal conservation of this domain and the coiled/coil structure. Of these two constructs, indeed C11 shows considerable light-activation of kinase activity in the auto-phosphorylation assay (table 2).

The results of tests of the *in vivo* activity if the C1 fusion kinase will be presented in Chapter 4.

References

1. Fassler JS, West AH (2010) Genetic and biochemical analysis of the SLN1 pathway in Saccharomyces cerevisiae. Methods Enzymol 471:291–317 . doi: 10.1016/S0076-6879(10)71016-8 [doi]
2. Posas F, Wurgler-Murphy S, Maeda T, Witten E, Thai T, Saito H (1996) Yeast HOG1 MAP kinase cascade is regulated by a multistep phosphorelay mechanism in the SLN1-YPD1-SSK1 two-component osmosensor. Cell 86:865 <last_page> 875 . doi: 10.1016/S0092-8674(00)80162-2
3. Tao W, Malone CL, Ault AD, Deschenes RJ, Fassler JS (2002) A cytoplasmic coiled-coil domain is required for histidine kinase activity of the yeast osmosensor, SLN1. Mol Microbiol 43:459–473 . doi: 2757 [pii]
4. Möglich A, Moffat K (2007) Structural basis for light-dependent signaling in the dimeric LOV domain of the photosensor YtvA. J Mol Biol 373:112–126 . doi: S0022-2836(07)00967-9
5. Möglich A, Yang X, Ayers RA, Moffat K (2010) Structure and function of plant photoreceptors. Annu Rev Plant Biol 61:21–47 . doi: 10.1146/annurev-arplant-042809-112259
6. Yee EF, Diensthuber RP, Vaidya AT, Borbat PP, Engelhard C, Freed JH, Bittl R, Möglich A, Crane BR (2015) Signal transduction in light-oxygen-voltage receptors lacking the adduct-forming cysteine residue. Nat Commun 6:10079 . doi: 10.1038/ncomms10079
7. Möglich A, Ayers RA, Moffat K (2009) Design and signaling mechanism of light-regulated histidine kinases. J Mol Biol 385:1433–1444 . doi: 10.1016/j.jmb.2008.12.017
8. Besant PG, Attwood P V. (2009) Detection and analysis of protein histidine phosphorylation. Mol Cell Biochem 329:93–106 . doi: 10.1007/s11010-009-0117-2
9. Boyer Pd, Deluca M, Ebner Ke, Hultquist De, Peter Jb (1962) Identification of phosphohistidine in digests from a probable intermediate of oxidative phosphorylation. J Biol Chem 237:PC3306-PC3308
10. Krebs EG, Beavo JA (1979) Phosphorylation-dephosphorylation of enzymes. Annu Rev Biochem 48:923–959 . doi: 10.1146/annurev.bi.48.070179.004423
11. Beenstock J, Mooshayef N, Engelberg D (2016) How do protein kinases take a selfie (Autophosphorylate)? Trends Biochem Sci 41:938–953 . doi: 10.1016/J.TIBS.2016.08.006
12. Wang Z, Cole PA (2014) Catalytic mechanisms and regulation of protein kinases. Methods Enzymol 548:1–21 . doi: 10.1016/B978-0-12-397918-6.00001-X
13. Jia Y, Quinn CM, Kwak S, Talanian R V (2008) Current in vitro kinase assay technologies: the quest for a universal format. Curr Drug Discov Technol 5:59–69
14. Cann ML, McDonald IM, East MP, Johnson GL, Graves LM (2017) Measuring kinase activity-A global challenge. J Cell Biochem 118:3595–3606 . doi: 10.1002/jcb.26103
15. Jia Y, Quinn C, Kwak S, Talanian R (2008) Current in vitro kinase assay technologies:

the quest for a universal format. Curr Drug Discov Technol 5:59–69 . doi: 10.2174/157016308783769414

16. Koresawa M, Okabe T (2004) High-Throughput Screening with Quantitation of ATP Consumption: A Universal Non-Radioisotope, Homogeneous Assay for Protein Kinase. Assay Drug Dev Technol 2:
17. Charter NW, Kauffman L, Singh R, Eglen RM (2006) A Generic, Homogenous Method for Measuring Kinase and Inhibitor Activity via Adenosine 5′-Diphosphate Accumulation. J Biomol Screen 11:390–399 . doi: 10.1177/1087057106286829
18. Yamada S, Nakamura H, Kinoshita E, Kinoshita-Kikuta E, Koike T, Shiro Y (2007) Separation of a phosphorylated histidine protein using phosphate affinity polyacrylamide gel electrophoresis. Anal Biochem 360:160–162 . doi: 10.1016/j.ab.2006.10.005
19. Kinoshita E, Kinoshita-Kikuta E, Sugiyama Y, Fukada Y, Ozeki T, Koike T (2012) Highly sensitive detection of protein phosphorylation by using improved Phos-tag Biotin. Proteomics 12:932–937 . doi: 10.1002/pmic.201100639
20. Jia Y (2008) Current status of HTRF ® technology in kinase assays. Expert Opin Drug Discov 3:1461–1474 . doi: 10.1517/17460440802518171
21. Hemmila I (1999) LANCE™: Homogeneous Assay Platform for HTS. J Biomol Screen 4:303–307 . doi: 10.1177/108705719900400604
22. Avila-Perez M, Vreede J, Tang Y, Bende O, Losi A, Gartner W, Hellingwerf K (2009) In vivo mutational analysis of YtvA from Bacillus subtilis: mechanism of light activation of the general stress response. J Biol Chem 284:24958–24964 . doi: 10.1074/jbc.M109.033316
23. Alexandre MT, Arents JC, van Grondelle R, Hellingwerf KJ, Kennis JT (2007) A base-catalyzed mechanism for dark state recovery in the Avena sativa phototropin-1 LOV2 domain. Biochemistry 46:3129–3137 . doi: 10.1021/bi062074e
24. Möglich A, Moffat K (2010) Engineered photoreceptors as novel optogenetic tools. Photochem Photobiol Sci 9:1286 . doi: 10.1039/c0pp00167h
25. Diensthuber RP, Bommer M, Gleichmann T, Möglich A (2013) Full-length structure of a sensor histidine kinase pinpoints coaxial coiled coils as signal transducers and modulators. Structure 21:1127–1136 . doi: 10.1016/j.str.2013.04.024; 10.1016/j.str.2013.04.024
26. van der Steen JB, Avila-Perez M, Knippert D, Vreugdenhil A, van Alphen P, Hellingwerf KJ (2012) Differentiation of function among the RsbR paralogs in the general stress response of Bacillus subtilis with regard to light perception. J Bacteriol 194(7):1708–1716 . doi: 10.1128/JB.06705-11

4 *In* vivo functioning of the hybrid light dependent yeast histidine protein kinase, Light-Oxygen-Voltage – (LOV)-Sln1, in S*accharomyces cerevisiae*.

Bury AE, Hellingwerf KJ

Abstract

Helical alignment of the α-helical linker of the LOV (light-oxygen-voltage) domain of YtvA from *Bacillus subtilis* with the α-helical linker of the histidine-protein kinase domain of the Sln1 kinase of the phospho-relay system for osmoregulation of *Saccharomyces cerevisiae* has been used to construct a light-modulatable histidine protein kinase. The helical alignment was carried out with conservation of the complete Jα helix of YtvA, as well as of the phosphorylatable histidine residue of the Sln1 kinase, with conservation of the hepta-helical motive of coiled-coil structures, recognizable in the helices of the two separate, constituent, proteins. Introduction of the gene encoding this hybrid histidine protein kinase into cells of *S. cerevisiae* in which the endogenous Sln1 kinase had been deleted, allowed us to modulate gene expression in the yeast cells with (blue) light. This was first demonstrated via the light-induced alteration of the expression level of the mannosyl-transferase Och1, via a translational-fusion approach. As expected, illumination decreased the expression level of Och1; the steady state decrease in saturating levels of blue light was about 40 %. To visualize the *in vivo* functionality of this light-dependent regulation system, we fused the green fluorescent protein (GFP) to another regulatory protein, Hog1, which is also responsive to the Sln1 kinase. Hog1 is phosphorylated by the MAP-kinase-kinase Pbs2, which in turn is under control of the Sln1 kinase, via the phosphoryl transfer domain Ypd1. Fluorescence microscopy was used to show that illumination of cells that contained the combination of the hybrid kinase and the Hog1::GFP fusion protein, led to a persistent increase in the level of nuclear accumulation of Hog1, in contrast to salt stress, which – as expected – showed the well-characterized transient response. The system described in this study will be valuable in future studies on the role of cytoplasmic diffusion in signal transduction in eukaryotic cells.

A condensed version of this chapter has been published as:
Bury A, Hellingwerf KJ. 2018 Design, characterization and *in vivo* functioning of a light-dependent histidine protein kinase in the yeast Saccharomyces cerevisiae. AMB Express. 2018 Apr 2;8(1):53

4.1 Introduction

During the last decade of the previous century, progress in the dynamic resolution of protein structure, in the availability of genomic DNA sequence information, and in the synthetic biology of the heterologous production of complex holo-proteins, has brought our understanding of the molecular basis of cellular signal transduction networks down to the atomic level (see e.g. [1]). This development was aided by the modular nature of many signal transduction proteins, which is particularly notable in the dominant type of prokaryotic signal transduction network, the 'two-component regulatory system', including its more complex variant, the 'phosphorelay system'. [2, 3] In this development photosensory receptor proteins did play an important role because of the ease and accuracy with which these proteins can be (de)activated (for review see e.g. [4, 5]). Understanding the atomic basis of the structural and dynamic aspects of the transitions between the receptor- and the signaling state of signal transduction proteins then led to the development of rational and intuitive guidelines to combine functional (input/output) domains of signal transduction proteins into new functional chimera's, as could be concluded from analyses of their performance both *in vitro* and *in vivo*. [6–8]

These technical developments, and the derived improved insight, have led to the emergence of the interdisciplinary research field of 'optogenetics'. [9–11] This field meanwhile has made radically new and very important contributions to the disciplines of both cell biology [12] and neurobiology. [13] Gradually, these developments now also start to impregnate the field of biotechnology, including the area of sustainability applications of 'direct conversion' [14] with cyanobacteria. [15, 16]

Complete understanding of cellular signal transduction networks, however, not only requires understanding of the dynamics of the structural transitions within the protein components involved, but - particularly for those operating in the larger, i.e. mostly eukaryotic, cells – also resolution of the spatial dimension of such processes. This latter aspect is not only dictated by association/dissociation kinetics of the underlying physicochemical signals (e.g. an electric field or osmotic pressure), signaling molecules and signal-transmission- and output proteins, but also by the processes of classical- and/or anomalous diffusion of all these components, either in the cytoplasm or in the cytoplasmic membrane, with possibly additional effects of molecular crowding.

To resolve (part of) these latter aspects, it would be of great value to have a signal-transduction system available that can be triggered with (a flash of) visible light, and that

initiates relocation of a specific component of that signal transduction network in the cell, like e.g. between subcellular compartments. Here we report the *in vivo* testing of such a system. Our approach is based on the construction of a chimeric histidine protein kinase, composed of the light-oxygen-voltage, LOV, domain of the stressosome protein YtvA from *Bacillus subtilis* [17] as the signal input domain and the histidine-protein kinase domain of the Sln1 kinase [18] of a two-component regulatory system of the yeast *Saccharomyces cerevisiae* as the output domain, for relay of the (light) signal to the downstream components.

The Sln1 kinase of *S. cerevisiae* is part of the osmostress signal transduction network of this yeast (for a brief overview: see figure 3, Introduction Chapter) and has the typical structure of a phospho-relay system. [19, 20] Its input kinase is located in the cytoplasmic membrane of yeast cells and able to convert signals derived from damage of components of their cell wall and of (a) signal(s) derived from osmotic stress, into changes in the level of phosphorylation of the cytoplasmic phosphoryl transfer domain, Ypd1. [21] The level of phosphorylation of Ypd1 modulates nuclear gene expression directly (e.g. of Skn7), and also indirectly - via the MAP kinase pathway of the Ssk system - through the shuttling of the transcriptional regulator Hog1 between the cytoplasmic and nuclear compartment. [22] Via analysis of the spatial distribution of fluorescent reporters in fixed *Saccharomyces* cells, sampled after triggering of either the natural- or an engineered LOV::Sln1-containing signal transduction network, we have been able to show the functionality of the designed chimeric light-dependent histidine protein kinase.

4.2 Materials and methods

4.2.1 Yeast strains, plasmids and cell growth.

The starting strain ΔYLR113W was cultivated on YPD (1% yeast extract, 2% peptone, 2% dextrose) rich medium agar plates, followed by growth in YPD liquid medium, prior to the next steps: knock out of the SLN1 gene and transformation with selected plasmids. All yeast strains used in this study are a derivative of the BY4741 series, see Table 1. All cloning was carried out following the standard protocols. [23] Knock out strains were made by making use of homologous recombination. Primers with 50 bp homologous overlap where used to amplify the knock out cassette with a specific antibiotic resistance gene. Amplified constructs where transformed [24] into selected strains. For selection of the SLN1 knockout strain the minimal complete medium, SCM (2% dextrose, 2g of the specific dropout mix, and yeast nitrogen base with ammonium sulphate) with added nourseothricin sulphate (clonNAT) to a

final concentration 100 µg/ml was used. To select for the continued presence of the plasmids carrying the required customized version of the genes, minimal drop out media were used. All cells were incubated for growth at 30 °C.

4.2.2 **Strains and plasmids**

Table 1: Strains and plasmids used in this investigation

Strain or plasmid	Characteristics	Source or reference
Saccharomyces cerevisiae		
BY4741	*MATa his3Δ1 leu2Δ0 met15Δ0 ura3Δ0*	EUROSCARF
*hog1*Δ	BY4741 *ylr113w*::kanMX4	EUROSCARF
AB004	BY4741 *yil147c*::clonNAT, *ylr113w*::kanMX4, pRS325ActC1LEU, pRS416-HOG1::GFP	This study
AB005	BY4741 *ylr113w*::kanMX4, pRS416-HOG1::GFP	This study
AB006	BY4741 *yil147c*::clonNAT, pRS325ActC1LEU, pRS314-OCH1(-336 to =26)-*lacZ*	This study
AB007	BY4741 pRS314-OCH1(-336 to =26)-*lacZ*	This study
Plasmids		
pRS325ActC1LEU	pRS325II derivate, ACT1 promoter, CYC1 terminator	This study
pRS416-HOG1::GFP	URA3	P. Silver [21]
pJL1416	pRS314-OCH1(-336 to +26)-*lacZ,* URA3	J.S. Fassler [22]

4.2.3 **Microscopy**

Log-phase cultures of the yeast AB005 and AB004 strains, expressing a Hog1::GFP and C1 fusion protein, see table 1 [21], were fixed with 0.37% (v/v) *p*-formaldehyde for 1 hour, washed, re-suspended in phosphate-buffered saline (PBS) pH = 7, and stained with 0.5 µg 4',6'-diamidino-phenylindole (DAPI) per ml culture to visualize the nuclei of the cells. The yeast cells were observed using a Nikon Eclipse Ti inverted microscope (Shinagawa, Tokyo, Japan), equipped with a 100x objective. Fluorescence emission signals of GFP and DAPI were generated using a Lumencor (Beaverton, United States) fluorescent light source and detected at 470 nm and 395 nm, respectively. Images were captured using a Hamamatsu digital camera C11440 (Hamamatsu City, Japan) driven by the Nikon elements AR 4.50.001 software (Shinagawa, Tokyo, Japan). All pictures of cells with a specific fluorophore were acquired using the same exposure time: 100 ms for DAPI and 400 ms for GFP. The pictures were then analyzed using ImageJ software [25] without further manipulation. For analysis, images were exported as .tiff files for import into ImageJ software. For quantitative analysis of the microscopy data, pictures of cells with DAPI-stained nuclei, and with Hog1::GFP expression, were overlapped. Cells with nuclear- and cytoplasmic localization (only cells with > 1.5-fold nuclear accumulation were counted as positive; by definition the others as

cells with cytoplasmic localization) of the Hog1::GFP reporter protein were counted and the percentage of cells with nuclear localization was calculated and plotted.

4.2.4 Activation of the Sln1 kinase domain *in vivo* with (stress) signals

For the application of the standardized osmotic stress signal, 0.4 M NaCl (final concentration) was added to 2 ml cell suspension, growing exponentially in minimal selection medium, at 30 °C, on a rotary shaker in 12 ml glass tubes. [20] Light activation of the hybrid LOV-kinase protein was achieved with blue Light Emitting Diodes (LEDs) with Λ^{max} = 464 nm, with an incident light intensity of 200 µEinstein·m^2·s^{-1}. Cells were fixed with 0.37% (v/v) p-formaldehyde and rapidly frozen for further analysis. [20]

4.2.5 Measurement of the level of expression of reporter enzyme via β-Galactosidase activity

Overnight cultures of recombinant strains of *Saccharomyces cerevisiae* were grown in YPD medium in the dark, starting from a single colony from a plate of the minimal selection medium. The overnight cultures were diluted to OD_{600} = 0.05 on a Biochrom WPA Lightwave II spectrophotometer and allowed to grow in the dark or in the light for 6 hours. Dark were wrapped tightly in tinfoil. Dark samples were taken with minimal red background light intensity ([26]; see above). Samples from illuminated cultures were taken under constant illumination with blue Light Emitting Diodes (LEDs; Λ^{max} = 464 nm) with an incident intensity of 200 µEinstein·m^2·s^{-1}. Samples were immediately transferred to an ice/water mixture and immediately flash frozen with liquid nitrogen for subsequent storage at -80 °C. β-Galactosidase activity was measured in the cells from all samples and expressed in Miller units, based on the average value of at least 8 independently isolated transformants according to reference [27].l

4.3 Results

4.3.1 *In vivo* functionality of the hybrid kinase in the Skn7 signal transduction pathway

As outlined in the Introduction, the Sln1 phospho-relay system has two output pathways, that target the Hog1 and the Skn7 nuclear transcriptional regulator, respectively. The Skn7 pathway is the most direct one of these two because Ypd1 directly phosphorylates Skn7. [22]

We therefore first tested whether or not illumination, via the hybrid kinase C1, could elicit changes in the activity of Skn7. A suitable read-out of the latter is the level of expression of the mannosyl-transferase Och1, via the reporter enzyme β-galactosidase, fused to the former. [18, 22] The results summarized in figure 1 clearly show that this is indeed the case: Switching on saturating intensities of blue light decreases this expression level about two-fold and a decrease is indeed expected as illumination decreases the rate of phosphorylation of the C1 kinase. It is of note that the replacement of the native Sln1 kinase by C1 does give rise to a doubling of the level of Och1 expression, but this is presumably due to the de-regulated expression and/or activity of the truncated kinase domain. The additional control experiment of illuminating wild type cells, clearly shows that without the introduction of the fused LOV domain-containing protein in this assay *S. cerevisiae* does not respond to light (figure 1).

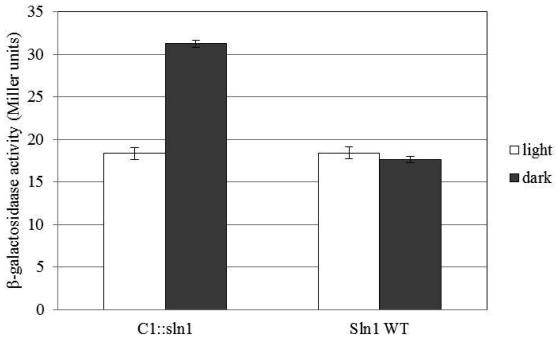

Figure 1. Effect of illumination on the Skn7-dependent expression of the Och1-*lacZ* transcriptional fusion (i.e. the mannosyl-transferase gene fused with the reading frame encoding β-galactosidase) in a *Saccharomyces cerevisiae* strain with the wild-type SLN1 gene – the AB007 strain, and in a strain with SLN1 replaced by the gene encoding the C1-histidine kinase fusion protein – the AB006 strain. Cells were incubated either in the presence of light (white bars) or in the dark (grey bars). The level of expression of the Och1-*lacZ* fusion is deduced from the specific β-galactosidase activity, expressed in Miller units. Error bars indicate standard deviations calculated from three independent biological experiments.

4.3.2 *In vivo* functionality of the hybrid C1 kinase in the HOG1 pathway: Observation of light-induced nuclear shuttling

For this test we used two *S. cerevisiae* strains in which the endogenous Sln1 kinase and the Hog1 regulator protein had been genetically deleted and were replaced by the C1 hybrid kinase and a translational Hog1::GFP fusion protein, (strain AB005 and AB004 table 1), respectively. The first one of these two strains had only the Hog1 gene replaced, and the second strain, both genes. With the resulting two strains stimulus/response experiments were carried out: With the AB005 strain by eliciting an osmostress response, and in the AB004 strain, which now is insensitive to osmostress, the occurrence of a light-response was tested (figures 2 and 3). Through fluorescence microscopy of glutaraldehyde-fixed cells at emission and excitation wavelengths suitable for the analysis of their GFP- and DAPI content, respectively, we then analyzed the subcellular distribution of these two fluorophores, in which of course DAPI reveals the presence of the nuclear compartment, while GFP can be present in both the nucleus and the cytosol. Figure 2 then shows the well-known response of the Hog1 protein in *S. cerevisiae* upon osmostress. [28] An almost equal distribution of the Hog1::GFP fusion protein over the two compartments prior to the stress, followed by a rapid (i.e. within a few minutes) and significant accumulation in the nucleus after this stress. Panel II of figure 2 shows that the same response, i.e. Hog1 accumulation in the nucleus, can be elicited by exposing the yeast cells to saturating intensities of blue light of the yeast strain in which next to Hog1, also the Sln1 kinase has been eliminated and replaced by the C1 hybrid kinase.

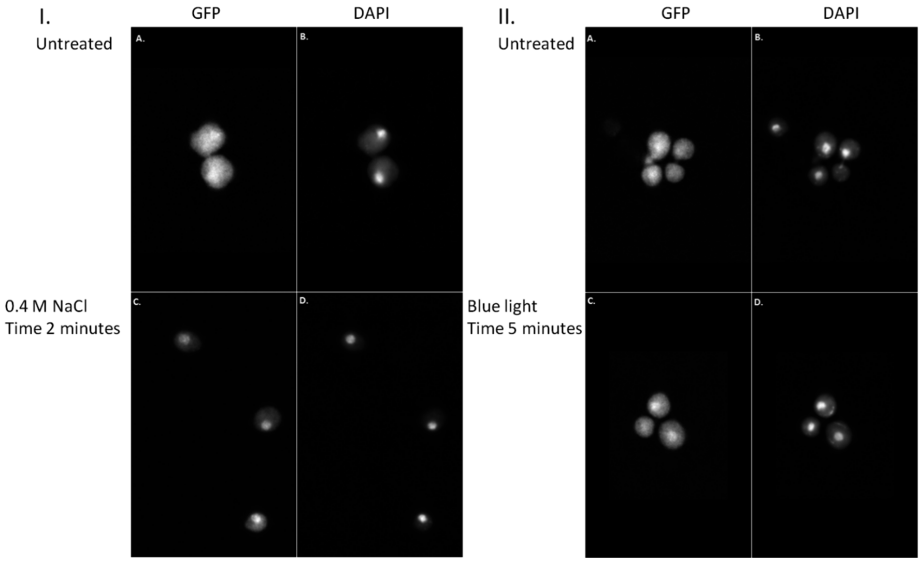

Figure 2. Representative picture of the subcellular localization of the Hog1::GFP fusion protein in response to changes in osmotic pressure (panel I) and after illumination (panel II) of the cells with blue light. Activation of Sln1 signalling was initiated with: (a) a change in osmotic pressure (panel I), elicited by addition of 0.4 M NaCl (final concentration) to the cell suspension, and (b) illumination (panel II) by exposure of the cells to blue light (200 µE incident intensity, 450 nm LED light). The strain used for panel I was AB005 and for panel II AB004, for details see table1.

In figure 3 a quantitative analysis of the dynamics of these two responses (i.e. to osmostress and to illumination) is presented. The osmostress response shows the typical transient response with maximally almost two-fold accumulation of the Hog1::GFP fusion protein in the nucleus after around 5 minutes, and a full relaxation of this concentration gradient at long timescales (e.g. 30 minutes; compare ref [28]).

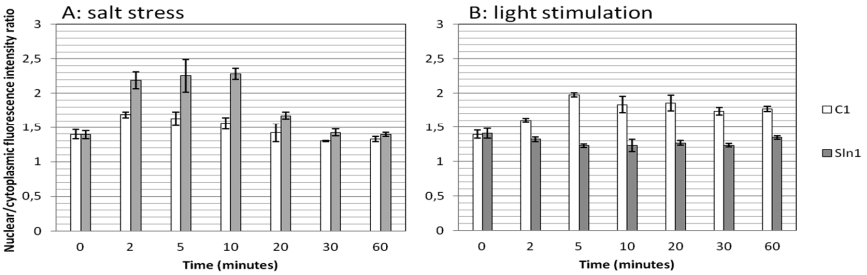

Figure 3. Nucleo-cytoplasmic redistribution of the Hog1::GFP fusion protein after a salt stress (panel A) and after illumination of the cells (panel B). The salt stress (panel A) was applied by addition of 0.4 M NaCl (final concentration) to the cell suspension. In panel B the results are shown of exposure of the cell suspension to blue light (200 µE incident intensity, 450 nm LED light). Samples were taken 0, 2, 5, 10, 20, 30 and 60 minutes after initiation of the experiment. White bars represent the yeast strain with the C1 histidine kinase fusion protein (AB004), and grey bars represent the yeast strain with the native Sln1 histidine kinase (AB005). Error bars represent the standard deviation calculated from three independent experiments, 150 cells were counted for each time point.

The light-induced response in the strain carrying the hybrid C1 kinase (AB004), in contrast, shows the expected persistent response of a light-activatable system in continuous light, but appears to take more time to develop. More detailed analysis, at the level of the individual cells (figure 4) shows that the nuclear accumulation of the fluorescent reporter (i.e. Hog1) in selected cells can increase up to 4-fold (with salt stress) and slightly less (i.e. up to three-fold) with illumination. Consistent with the results displayed in figure 2, also in figure 3 we see the same slower kinetics with light activation. An additionally significant effect visible from this figure is the fact that the functionality of both signal transduction systems depends on the level of expression of the fluorescently labelled Hog1 protein: If the expression level of this protein is increased more than five-fold over minimum expression levels, neither the light- nor and stress-induced nuclear accumulation are detectable anymore.

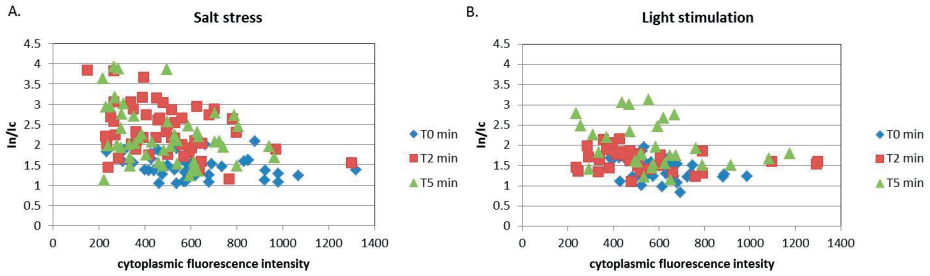

Figure 4. Image analysis of individual *S. cerevisiae* cells exposed to signal transfer that induces nuclear shuttling of a Hog1::GFP fusion protein. Representation of the distribution in the cells of the Hog1::GFP protein against the intensity of the Hog1::GFP fluorescence in the yeast cells before (T0) and at two time points after salt stress with 0.4 M NaCl (final concentration), panel A, and before and after exposure of the cells to blue light (200 µEinstein·m^2·s^{-1} intensity, 450 nm LED light), panel B, after 2 and 5 minutes. In – fluorescence intensity in the nucleus, Ic – fluorescence intensity in the cytoplasm.

4.4 Discussion

Beyond the difference in light sensitivity – the main purpose of the experiment – of the two strains reported on in figure 1, it is clear that the strain with the truncated Sln1 fusion protein shows considerably higher activity in the dark than the unperturbed wild type system. Two possible underlying differences can explain this latter aspect: (i) a higher intrinsic kinase activity of the LOV::Sln1 fusion construct than the authentic Sln1 kinase and (ii) a higher expression level of the fusion kinase. As the kinase is not expressed from its natural promoter, but from the ACT1 promoter, a rather strong, mostly constitutive (but glucose repressible) promoter [29, 30] we think that the fusion kinase may be present at higher concentration than Sln1. Nevertheless, a higher intrinsic activity may also play a role as a similar activation has also been observed in some bacterial two-component kinases. [31, 32]

Absolute numbers, and by inference concentrations, of the molecular components of a signal transduction chain are important, particularly in the two-component systems, e.g. because most kinases in the absence of their cognate signal, display considerable phosphatase activity. The approximately 10 to 100-fold molar excess of response regulator over kinase in most bacterial two-component systems testifies to this (e.g. [33, 34]). The results presented in figure 2 show that both in the natural response system to osmotic stress and in the light

response, mediated by the hybrid kinase, the Hog1/kinase molar ratio is of crucial importance too. If the concentration of the Hog1::GFP reporter protein is increased from its basal level (in cells that presumably contain only a single copy of the expression plasmid) to more than 4 to 5-fold higher, the signal transduction system seems oversaturated with Hog1, and a response to both stimuli is no longer visible. The unperturbed Sln1 signal transduction system functions with 656 and 6780 molecules per cell of Sln1 kinase and the Hog1 transducer, respectively. [35] This corresponds to ~25 nM and 0.5 μM, respectively in non-stimulated cells. Analysis of the average cellular concentration of the Hog1::GFP fusion protein with fluorescence-correlation microscopy (M. Hink et al., unpublished observation; for methodology see [36]) suggests that its abundance – at the basal, pre-stimulus, level – is 0.15 (+/- 0.06; n = 41) μM, i.e. slightly lower but still comparable to that of the Hog1 protein in the wild type, in spite of the differences in promoters used. These results suggest that the concentration of the Hog1 protein in the Sln1 signal transduction pathway is such that overexpression of Hog1 above physiological levels will make the Sln1 signal transduction pathway non-functional.

The results shown in figure 3 and figure 4 suggest that the on-dynamics of the light response is slower than that of the osmostress response. If so, this may have several causes, like a lower degree of kinase modulation by light, or a suboptimal expression ratio of the proteins composing the light-responsive signal transduction pathway. Furthermore, the open bars in figure 3, panel A, do seem to show a very slight remaining stimulation of Hog1 accumulation in the nucleus upon stressing the strain that expresses the light-sensitive, truncated variant of Sln1. This can be explained by weak spill-over of signals from the osmostress-responsive Sho1 system of *S. cerevisiae* into the Sln1 system at the level of the Ssk1 MAP kinase pathway. [37]

The hybrid kinase described in this study is an excellent candidate for future studies on quantitation of the consequences of e.g. localized kinase activation in the cytoplasm, for the dynamics and amplitude of the overall cellular response. This will allow further fine-tuning, e.g. with respect to the role of (anomalous) cytoplasmic diffusion, of systems biology models developed to describe the osmostress response in *S. cerevisiae.* [38, 39] Various super-resolution microscopy techniques are available to facilitate such experiments (e.g. [40, 41]). Also the use of specific subcellular localization tags and/or interaction domains can be exploited for this. [41]

References

1. Ridge KD, Abdulaev NG, Sousa M, Palczewski K (2003) Phototransduction: crystal clear. Trends Biochem Sci 28:479–487 . doi: S0968-0004(03)00172-5
2. Nixon BT, Ronson CW, Ausubel FM (1986) Two-component regulatory systems responsive to environmental stimuli share strongly conserved domains with the nitrogen assimilation regulatory genes ntrB and ntrC. Proc Natl Acad Sci U S A 83:7850–7854
3. Burbulys D, Trach KA, Hoch JA (1991) Initiation of sporulation in B. subtilis is controlled by a multicomponent phosphorelay. Cell 64:545–552 . doi: 0092-8674(91)90238-T
4. van der Horst MA, Hellingwerf KJ (2004) Photoreceptor proteins, "star actors of modern times": a review of the functional dynamics in the structure of representative members of six different photoreceptor families. Acc Chem Res 37:13–20 . doi: 10.1021/ar020219d
5. Hoff WD, Jung KH, Spudich JL (1997) Molecular mechanism of photosignaling by archaeal sensory rhodopsins. Annu Rev Biophys Biomol Struct 26:223–258 . doi: 10.1146/annurev.biophys.26.1.223
6. Levskaya A, Chevalier AA, Tabor JJ, et al (2005) Synthetic biology: engineering Escherichia coli to see light. Nature 438:441–442 . doi: nature04405
7. Wu YI, Frey D, Lungu OI, et al (2009) A genetically encoded photoactivatable Rac controls the motility of living cells. Nature 461:104–108 . doi: 10.1038/nature08241
8. Möglich A, Ayers RA, Moffat K (2009) Design and signaling mechanism of light-regulated histidine kinases. J Mol Biol 385:1433–1444 . doi: 10.1016/j.jmb.2008.12.017
9. Miller G (2006) Optogenetics. Shining new light on neural circuits. Science 314:1674–1676 . doi: 314/5806/1674
10. Ernst OP, Murcia PAS, Daldrop P, et al (2008) Photoactivation of channelrhodopsin. J Biol Chem 283:1637–1643 . doi: M708039200
11. Zhang F, Gradinaru V, Adamantidis AR, et al (2010) Optogenetic interrogation of neural circuits: technology for probing mammalian brain structures. Nat Protoc 5:439–456 . doi: 10.1038/nprot.2009.226
12. Bacchus W, Fussenegger M (2012) The use of light for engineered control and reprogramming of cellular functions. Curr Opin Biotechnol 23:695–702 . doi: 10.1016/j.copbio.2011.12.004
13. Kim CK, Adhikari A, Deisseroth K (2017) Integration of optogenetics with complementary methodologies in systems neuroscience. Nat Rev 18:222–235 . doi: 10.1038/nrn.2017.15
14. Savakis P, Hellingwerf KJ (2015) Engineering cyanobacteria for direct biofuel production from CO2. Curr Opin Biotechnol 33:8–14 . doi: 10.1016/j.copbio.2014.09.007
15. Abe K, Miyake K, Nakamura M, et al (2014) Engineering of a green-light inducible gene expression system in Synechocystis sp. PCC6803. Microb Biotechnol 7:177–183 . doi: 10.1111/1751-7915.12098 [doi]
16. Miyake K, Abe K, Ferri S, et al (2014) A green-light inducible lytic system for cyanobacterial cells. Biotechnol Biofuels 7:56–6834–7–56. eCollection 2014 . doi: 10.1186/1754-6834-7-56
17. van der Steen JB, Avila-Perez M, Knippert D, et al (2012) Differentiation of function among the RsbR paralogs in the general stress response of Bacillus subtilis with regard

to light perception. J Bacteriol 194(7):1708–1716 . doi: 10.1128/JB.06705-11
18. Li S, Dean S, Li Z, et al (2002) The eukaryotic two-component histidine kinase Sln1p regulates OCH1 via the transcription factor, Skn7p. Mol Biol Cell 13:412–424 . doi: 10.1091/mbc.01-09-0434
19. Gao R, Stock AM (2009) Biological insights from structures of two-component proteins. Annu Rev Microbiol 63:133–154 . doi: 10.1146/annurev.micro.091208.073214
20. Fassler JS, West AH (2010) Genetic and biochemical analysis of the SLN1 pathway in Saccharomyces cerevisiae. Methods Enzymol 471:291–317 . doi: 10.1016/S0076-6879(10)71016-8
21. Ferrigno P, Posas F, Koepp D, Saito H, Silver PA (1998) Regulated nucleo/cytoplasmic exchange of HOG1 MAPK requires the importin beta homologs NMD5 and XPO1. EMBO J 17:5606–5614 . doi: 10.1093/emboj/17.19.5606 [doi]
22. Lu JMY, Deschenes RJ, Fassler JS (2003) Saccharomyces cerevisiae Histidine Phosphotransferase Ypd1p Shuttles between the Nucleus and Cytoplasm for SLN1-Dependent Phosphorylation of Ssk1p and Skn7p. Eukaryot Cell 2:1304–1314 . doi: 10.1128/EC.2.6.1304-1314.2003
23. Sambrook J, Fritsch EF, Maniatis T (1989) Molecular Cloning: a Laboratory Manual, 2nd ed
24. Gietz RD, Woods RA (2006) Yeast Transformation by the LiAc/SS Carrier DNA/PEG Method. In: Yeast Protocols. Humana Press, New Jersey, pp 107–120
25. Schindelin J, Arganda-Carreras I, Frise F, et al (2012) Fiji - an Open Source platform for biological image analysis. Nat Methods 9:676–682
26. Avila-Perez M, Hellingwerf KJ, Kort R (2006) Blue light activates the sigmaB-dependent stress response of Bacillus subtilis via YtvA. J Bacteriol 188:6411–6414 . doi: 10.1128/JB.00716-06
27. Miller JH (1972) Experiments in Molecular Genetics. Cold Spring Harb NY
28. Posas F, Wurglermurphy S, Maeda T, et al (1996) Yeast HOG1 MAP Kinase Cascade Is Regulated by a Multistep Phosphorelay Mechanism in the SLN1-YPD1-SSK1 - Two-Component- Osmosensor. Cell 86:865–875 . doi: 10.1016/S0092-8674(00)80162-2
29. Wenzel TJ, Teunissen AW, de Steensma HY (1995) PDA1 mRNA: a standard for quantitation of mRNA in Saccharomyces cerevisiae superior to ACT1 mRNA. Nucleic Acids Res 23:883–884 . doi: l40368 [pii]
30. Planta RJ, Brown AJ, Cadahia JL, et al (1999) Transcript analysis of 250 novel yeast genes from chromosome XIV. Yeast 15:329–350 . doi: 10.1002/(SICI)1097-0061(19990315)15:4<329::AID-YEA360>3.0.CO;2-C
31. Szurmant H, Bu L, 3rd CLB, Hoch JA (2008) An essential sensor histidine kinase controlled by transmembrane helix interactions with its auxiliary proteins. Proc Natl Acad Sci U S A 105:5891–5896 . doi: 10.1073/pnas.0800247105
32. Verhamme D (2002) Signal transfer through the Uhp regulatory system in the signal transduction network of Escherichia coli. University of Amsterdam
33. Yoshida T, Cai S, Inouye M (2002) Interaction of EnvZ, a sensory histidine kinase, with phosphorylated OmpR, the cognate response regulator. Mol Microbiol 46:1283–1294 . doi: 3240 [pii]
34. Wayne KJ, Sham LT, Tsui HC, et al (2010) Localization and cellular amounts of the WalRKJ (VicRKX) two-component regulatory system proteins in serotype 2 Streptococcus pneumoniae. J Bacteriol 192:4388–4394 . doi: 10.1128/JB.00578-10 [doi]
35. Ghaemmaghami S, Huh WK, Bower K, et al (2003) Global analysis of protein

expression in yeast. Nature 425:737–741 . doi: 10.1038/nature02046
36. Maeder CI, Hink MA, Kinkhabwala A, et al (2007) Spatial regulation of Fus3 MAP kinase activity through a reaction-diffusion mechanism in yeast pheromone signalling. Nat Cell Biol 9:1319–1326 . doi: ncb1652
37. Hao N, Behar M, Parnell SC, et al (2007) A systems-biology analysis of feedback inhibition in the Sho1 osmotic-stress-response pathway. Curr Biol 17:659–667 . doi: S0960-9822(07)01021-4
38. Uschner F, Klipp E (2014) Information processing in the adaptation of Saccharomyces cerevisiae to osmotic stress: an analysis of the phosphorelay system. Syst Synth Biol 8:297–306 . doi: 10.1007/s11693-014-9146-6
39. Dexter JP, Xu P, Gunawardena J, McClean MN (2015) Robust network structure of the Sln1-Ypd1-Ssk1 three-component phospho-relay prevents unintended activation of the HOG MAPK pathway in Saccharomyce. BMC Syst Biol 9: 17:
40. Small AR, Parthasarathy R (2014) Superresolution localization methods. Annu Rev Phys Chem 65:107–125 . doi: 10.1146/annurev-physchem-040513-103735 [doi]
41. Schierling B, Pingoud A (2012) Controlling the DNA cleavage activity of light-inducible chimeric endonucleases by bidirectional photoactivation. Bioconjug Chem 23 (6):1105–1109

5 **Analysis of response regulator phosphorylation with 'Phos-tag' SDS-PAGE.**

Bury AE, Arents J, Hellingwerf KJ

Abstract:
Because of the inherent instability of the phospho-di-ester bond between a phosphoryl group and the side chain of aspartic acid, it has been very difficult to monitor the degree of phosphorylation of response regulators of two-component systems, particularly in the *in vivo* environment. In 2006 Kinoshita et al. introduced a new method, the so-called 'Phos-tag' method, to monitor phosphorylation of proteins, which later turned out also to be suited to report the level of phosphorylation of both histidine kinases and response regulators of two-component systems. In this chapter it is described that, despite many attempts, we have not been able to use this method for analysis of the level of phosphorylation of the two response regulators of the Sln1 system, presumably because of a lack of separation of their phosphorylated- and non-phosphorylated form and/or the very unstable nature of the phosphorylated form of these response regulators. During the past few years, a large number of papers has reported on the use of this Phos-tag method for monitoring the level of phosphorylation of an ever-increasing number of response regulators (and also for resolving the pathway of phosphoryl flux through the cognate two-component system). Significantly, however, the latter systems do not include any example of a response regulator derived from a eukaryotic organism. In the discussion paragraph we try to rationalize these observations.

5.1 Introduction

Protein phosphorylation is utilized by all living organisms, to control one or more of a wide range of cellular activities that include signal transduction, apoptosis, gene expression, cell cycle progression, cytoskeletal regulation and energy metabolism. [1–3] Protein phosphorylation is known to occur on the side chain of nine different amino acids (i.e.: Ser, Thr, Tyr, His, Lys, Arg, Asp, Glu and Cys). [4] Of these, phosphoserine, phosphothreonine, and phosphotyrosine are well-known for their involvement in signal transduction in higher eukaryotes by protein kinases. De-regulation of these kinases has been linked to many diseases, including cancer. [4, 5]

Here we focus on the phosphorylation of the histidine- and particularly the aspartate side chain, i.e. the phosphorylation sites relevant for two component systems, including the multicomponent phosphorelay signaling pathways, that are common in bacteria, fungi, and plants. [3, 6] Monitoring the level of phosphorylation of the subsequent protein components in the various two component signal transduction pathways, is crucial for a basic understanding of signal transduction in prokaryotic, as well as in eukaryotic cells. Histidine protein kinases autophosphorylate their conserved histidine in response to a specific stimulus (e.g. binding of an organic acid, absorption of a photon, etc. [3, 7] This event is followed by the intra- or intermolecular transfer of the phosphoryl group [7] to the conserved aspartate of the cognate response regulator (RR) protein or receiver domain (for convenience here we ignore ‘cross-talk’). [3, 8, 9] The stability of phosphohistidines and phosphoaspartates, however, relative to other phosphorylated amino acids, is very low. [10] This makes it difficult to quantitatively assay the amount of these compounds present, let alone to record the flow of phosphoryl groups through a two component signal transduction pathway. [5, 11, 12] Phosphohistidines are particularly labile under acidic conditions, in contrast to the phospho-hydroxy amino acids, phosphoserine and phosphothreonine, which are stable even in a strongly acidic environment. In the presence of 1 M HCl at 100 ^{o}C the half-live of phosphoserine and phosphothreonine is ~18 h, while that of phosphotyrosine is about 5 h. [13] The phosphohistidines 1-phosphohistidine and 3-phosphohistidine have half-lives of 18 and 25 s, respectively, in 1 M HCl at 49 ^{o}C. [14] Phosphoaspartates are even less stable than the phosphohistidines under acidic conditions. At neutral conditions, i.e. in the pH range from 4 to 10 and at 30 ^{o}C, the half-time of phosphoaspartate hydrolysis is about 40 min. Lowering the temperature to 15 ^{o}C increases this half-time to a few hours. [15]

5.1.1 Detection of the level of phosphorylation of response regulators (RR~P levels)

Currently available methods for the detection of the level of phosphorylation of response regulators include both direct methods, based on the use of radiolabelled phosphate, as well as indirect methods, like those in which the difference in migration caused by phosphorylation is analysed with chromatography and/or electrophoresis. [16, 17] In contrast to the substrates/products of the eukaryotic Ser/Thr/Tyr kinases, so far for phospho-aspartate no specific antibodies are available, presumably due to the absence of suitable analogues that can be used as a hapten/antigen. The phosphor-aspartate bond also does not survive in the gas phase of a mass spectrometer. [12] The indirect methods referred to above include methods ranging from the detection of phosphorylation via induction of changes in the intrinsic fluorescence of a target protein, to measurements of the swimming speed of *E. coli*. [18, 19] The direct method with radiolabelled phosphate most often uses the enzymatic reaction of the cognate histidine kinase to transfer radiolabelled phosphoryl groups from [γ-^{32}P]-ATP, via its conserved histidine side chain, to the aspartate of the response regulators. [20] However, also direct labelling with radiolabelled acetyl-phosphate and/or phosphor-amidate can be used for phosphorylation of the response regulators. [18]

5.1.2 Problems in assaying RR~P levels

The role of phosphoaspartate in a two component signal transduction pathway is to relay the input signal, via a phosphorylated histidine (that acts as the phosphoryl donor), to an output domain/protein, like a transcription factor, to initiate transcription of the appropriate gene(s). [7, 20] The response regulators are phosphorylated at aspartate side chains (but note that additional post-translational modifications also occur [22]). The acyl-phosphate bond in phosphoaspartates rapidly hydrolyses spontaneously, under both acidic and alkaline conditions, with a maximal half-live of about 6 h under neutral conditions (see also above).

In the first few years after discovery of the two component systems, only indirect methods were used - based mostly on the detection of the rate of hydrolysis of the phosphoryl donor - to proof that the prototype response regulator, CheY, is phosphorylated at a key aspartate side chain. [6] The aspartate-phosphorylated form of a response regulator often modulates (i.e. effects positively or negatively) transcription [21] and this output response can be ended by auto phosphatase activity of the cognate histidine kinase and/or the response regulator protein, or by an additional (cognate) phosphatase enzyme in the system. [15, 23, 24] Beyond this, the high rate of non-enzymatic hydrolysis of the phosphorylated aspartate allows for

rapid switching off of the output of a signalling pathway, depending on the needs of the cell. [11, 21]

5.1.3 The "Phos-tag" method

In 2006, Prof. Koike's group (Hiroshima University) reported that a specific di-nuclear metal complex (*i.e.*, the 1,3-bis[bis(pyridin-2-ylmethyl) amino]propan-2-olato di-zinc(II) complex) can act, in aqueous solutions and at neutral pH, as a selective phosphate-binding molecule. Hence this complex is also referred to as Phos-tag™. Significantly, Phos-tag™ also has significant affinity for phosphate ions that carry large ligands. [25, 26] Based on this characteristic, a method was developed to detect and quantitate the amount of phosphorylated proteins via the phosphorylation-triggered shift in their electrophoretic mobility during electrophoresis in poly-acrylamide gels that contain the dinuclear Mn^{2+}/Zn^{2+} complex, covalently linked to the poly-acrylamide. [25] This method is loosely referred to as the 'Phos-tag' gel/method. The principle behind this method is thus that phosphorylated proteins move slower in Phos-tag SDS-PAGE than do the corresponding non-phosphorylated molecules, because the phosphoryl group interacts with the Mn^{2+}(Zn^{2+}) Phos-tag ligand in the gel. [27]

Triggered by this exciting finding, a large range of subsequent studies have applied the Phos-tag method for the detection of the level of phosphorylation of the stably phosphorylated components of eukaryotic signal transduction proteins, often even with the resolution of multiple phosphorylation sites (see e.g. [28, 29]). This method was subsequently also applied in the analysis of the level of phosphorylation of the components of bacterial two component systems, [24] be it that this latter approach, however, particularly for the response regulators, was not always successful (see e.g. [30]).

In this study, the light-modulated phosphoryl flow through a designed, chimaeric histidine protein kinase is directed towards the response regulators Ssk1 and Skn7 from *S. cerevisiae*. It would be of interest, therefore, to monitor the level of phosphorylation of these response regulators both *in vitro* and *in vivo*. However, it is relevant to note that so far, the Phos-tag method has not been reported to be successfully applied in the analysis of the level of phosphorylation of eukaryotic response regulators (yet). Here we present our attempts towards this and discuss possible reasons why this approach so far has failed to provide positive results.

5.2 Materials and methods.

5.2.1 Preparation of the recombinant proteins

To construct plasmids for overexpression of the required proteins, the corresponding DNA fragments were prepared by PCR, using genomic DNA of *S. cerevisae*. An ArcA overexpression vector (pETArcA_1) was a gift from Dr. JWA van Beilen [31]. UhpA and Rcp1 overexpression vectors were obtained from the plasmid collection of the Molecular Microbial Physiology Group (University of Amsterdam). Sequences of primers used in this study are listed in table 1. After digestion with the proper restriction enzyme(s) (indicated in italics, see table 1), DNA fragments were ligated into either the pET21 or pQE30 overexpression vector. Each constructed plasmid was transferred into *E. coli* Bl21(DE3) and *E. coli* M15(pREP4), respectively. The host cells were cultivated in the Luria-Bertani medium at 37 ^{o}C, when OD_{600} of the culture reached 0.6, and the target protein overexpression was induced with IPTG. At this point the temperature was lowered to room temperature and growth was allowed to continue with vigorous shaking for approximately 16 hours in darkness. Then cells were harvested by centrifugation and were lysed by sonication in 50 mM Tris-HCl buffer pH = 8, plus 10 mM NaCl, and an EDTA-free protease inhibitor cocktail (complete, EDTA-free, provided by Roche). The C-terminally tagged proteins were purified using nickel affinity chromatography on a HisTrap FF column (GE Healthcare, 5 mL column) (Qiagen, Germany). The list of proteins used in this study is presented in table 2.

Table 1. Sequences of primers used in this study.

Primer name	Primer sequence
pQE30Ypd1FW	5'ccc*ggatcc*atggctagttttcaatcatttgggata 3'
pQE30Ypd1RV	5'ggg*gtcgac*ttataggtttgtgttgtaata 3'
pQE30skn7FW	5' ccc*ggatcc*atgagcttttccaccat 3'
pQE30skn7RV	5'ggg*aagctt*ttatgatagctggttttcttg 3
pQE30ssk1FW	5'ccc*gcatgc*atgctcaattctgcgtta 3'
pQE30ssk1RV	5'ggg*aagctt*ttacaattctatttgagtggg 3'
pET28sln1pHKRV	5'ggg*ctcgag*cgatgcttttagcaacactaaacttga 3'
pET28Sln1pRecFW	5'ccc*catatg*aatgaaacaagtgtcaaaattttggttg3'
pET28sskn7FW	5'ccc*catatg*agcttttccaccataaatagcaacg3'
pET28sskn7RecFW	5'ccc*catatg*agcctaacaccaaatgctcaaaataacac3'
pET28sskn7RV	5' ggg*ctcgag*ctgatagctggttttcttgaagtgtag 3'
pET28ssk1FW	5'ccc*catatg*ctcaattctgcgttactgtgg3'
pET28sskRecFW	5' ccc*catatg*gattttcgaaataaaccagtggcc3'
pET28ssk1RV	5' ggg*ctcgag*ccaattctatttgagtgggcgag 3'
pET28sln1pHKFW	5'ccc*catatg*caacattatgctcttctagaagaaagag3'

Note: primers sequences in italics represent a specific cleavage sites for a restriction enzyme.

Table 2. List of proteins used in the detection of their phosphorylation level, upon *in vitro* phosphorylation, with the Phos-tag electrophoresis method.

Construct	Protein size kDa	Ref
Sln1pHKRec	65	This study
Sln1pHK	43	This study
Sln1pRec	14	This study
C1	80	This study
C2	81	This study
Skn7	62	This study
Skn7Rec	26	This study
Ssk1	71	This study
Ssk1Rec	32	This study
Ypd1	17	This study
ArcA	21	[31]
UhpA	27	[12]
Rcp1	17	W. Laan, unpublished

5.2.2 Preparation of the phosphorylated form of the proteins

For all proteins, the reaction mixture used for phosphorylation was composed of 30 mM HEPES buffer pH 7.5, 10 mM $MgCl_2$, 25 mM acetyl phosphate and 10% (v/v) glycerol. Proteins (0.2 mg/ml) were incubated in 50 µL of a phosphorylation reaction mix at 37 °C. [32] Reactions were stopped at the indicated times by the addition of 12.5 µl of 4-fold concentrated protein loading buffer (0.25 M Tris.HCl, pH = 8.8 % (w/v) SDS, 40 % (v/v) glycerol, 40 mM EDTA, 0.008 % (w/v) bromophenol blue and 4 mM β-mercapto-ethanol.). The samples were placed on ice, without prior boiling, until separation by SDS-polyacrylamide gel electrophoresis. [33–35] The phosphorylation level of the proteins used in this experiment was checked with [γ-^{32}P]-ATP (data not shown).

5.2.3 Phos-tag SDS PAGE

Electrophoresis was performed in 0.75 mm thick 10% (w/v) acrylamide separating gels, in combination with 5% stacking gels. Phos-tag acrylamide, at a concentration of 25 or 50 µM, and the two equivalents of Mn or Zn ions, were added to the separating gel prior to polymerization. [25] Electrophoresis was routinely carried out at the room temperature. In selected experiments the electrophoresis tank was placed in ice to prevent heating of the electrophoresis buffer and gels. Standard electrophoresis was carried out at 40 V for 15 minutes, followed by 140 V for 50 minutes. Modified procedures with lower voltage (80 – 100 V), to minimize heat generation during electrophoresis and to obtain better separation of the proteins, were also tested. Following electrophoresis, the gels were stained overnight with the blue stain solution from Fermentas at 4 °C and de-stained with Millipore water at room temperature.

5.3 Results

5.3.1 Sln1 pathway components used for the in vitro phosphorylation

All the components of the Sln1 pathway were cloned and overexpressed in functional form, based on published procedures [34] and are listed in the table 2. Sln1 overexpression vectors were prepared in 3 forms: (i) the full length protein, (ii) the truncated protein consisting of histidine kinase- and response regulator domain and (iii) only the response regulator domain. Similarly, the two response regulators from Sln1 two component signal transduction pathway (i.e. Ssk1P and Skn7P) were overexpressed both as a full length-, and as a receiver-domain

truncated protein. [34]

5.3.2 **Results of the phosphorylation reaction**

Phosphorylation reactions were carried out under standard conditions [34, 35] (i.e. with 32P detection), and their results were checked with Phos-tag SDS PAGE. Simultaneously ArcA, which is the response regulator from the ArcBA pathway for detection of "electron-acceptor availability" from *Escherichia coli* (see e.g. [31]), was used as the control for a phosphorylated response regulator. Despite many efforts, we have not been able to detect protein bands on the Phos-tag gels that could have represented the phosphorylated form of any of these proteins, except for the control protein ArcA~P. For the latter protein, after electrophoresis on Phos-tag SDS PAGE, two bands were clearly separated: one corresponding to the phosphorylated- and one to the non-phosphorylated form of ArcA (see figure 1, lane 15). Phos-tag- and regular SDS-PAGE gels with lanes separately containing all the components of the Sln1 pathway, as well as ArcA, are presented in this figure 1.

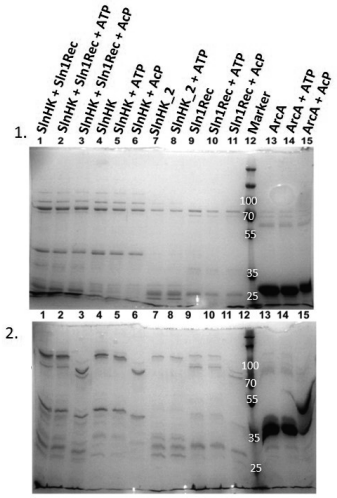

Figure 1. Results of the phosphorylation reaction of the components of the Sln1 pathway, as tested with the Phos-tag method. Acetyl phosphate (AcP) and ATP were used as phosphoryl donors. ArcA was used as the control response regulator. Panel 1 shows an SDS gel without the Phos-tag compound added, panel 2 shows an SDS gel with the added Phos-tag compound.

The initial event in Sln1 signaling is signal-triggered autophosphorylation of its kinase domain. It can therefore not be excluded that the Sln1HK- and Sln1Rec domain, as well as other components of the Sln1 pathway might be overexpressed (even in *E. coli*) already in their phosphorylated form. That then might explain the difficulties in finding both forms of these proteins (i.e. the phosphorylated- and the non-phosphorylated form) in the Phos-tag gels. To investigate this possibility, we incubated samples, containing an appropriate protein, with alkaline phosphatase. The dephosphorylation buffer that we used contained: 0.1 M Tris HCl pH 8.0, 0.05 M $MgCl_2$, 1 M KCl, and 1 U alkaline phosphatase. Samples were incubated for 1 hour at 37°C, and the phosphatase reaction was stopped by mixing a sample with the protein loading buffer for gel electrophoresis. As a control reaction, ArcA was first phosphorylated, after which phosphorylated ArcA was dephosphorylated with alkaline phosphatase. This control confirmed that alkaline phosphatase fully dephosphorylated the proteins tested (data not shown). In the lanes with alkaline phosphatase, the specific band representing a protein with a size of around 45 kDa, is the alkaline phosphatase. Line 2 doesn't contain the alkaline phosphatase and the band corresponding to 45 kDa is a protein co-purifying with the SlnHK. It was not possible, however, to observe any shift in the relative mobility (i.e. R_f value) of any of the Sln1 components in the Phos-tag gels in samples with and without alkaline phosphatase (figure 2).

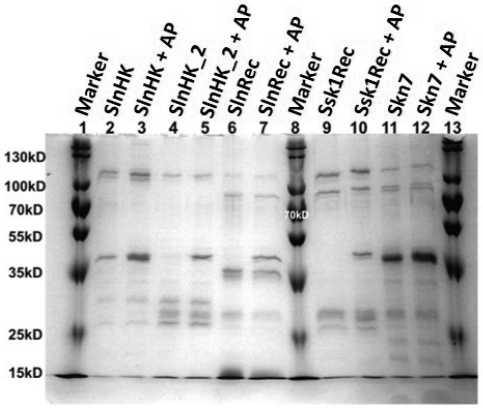

Figure 2. Results of the *in vitro* dephosphorylation of the components of the Sln1 two-component transduction pathway. Shown is a picture of the SDS gel with the added Phos-tag compound.

5.3.3 Use of the Phos-tag method for detection of other phosphorylated response regulators

As the general literature meanwhile contained several reports in which it was reported that the level of phosphorylation of several components of two component systems can be resolved with the Phos-tag approach (see also the Discussion paragraph below) we decided to try the Phos-tag method on two additional response regulators available in the Department. For this the UhpA and Rcp1 response regulators ([12] and W. Laan, unpublished experiments) were overexpressed in *E. coli* and purified similarly to other proteins examined in this study (see Materials and Methods). Phosphorylation of these latter two response regulators, and of ArcA that was used again as a control for effective phosphorylation, was performed under the standard phosphorylation conditions (see Materials and Methods). Both Zn and Mn ions were used, in separate experiments, for the preparation of the Phos-tag gels. Nevertheless, there wasn't any difference observable on Phos tag gels between the samples containing the phosphorylated and non-phosphorylated form of UhpA and Rcp1 on either of them, whereas for ArcA this was clearly possible.

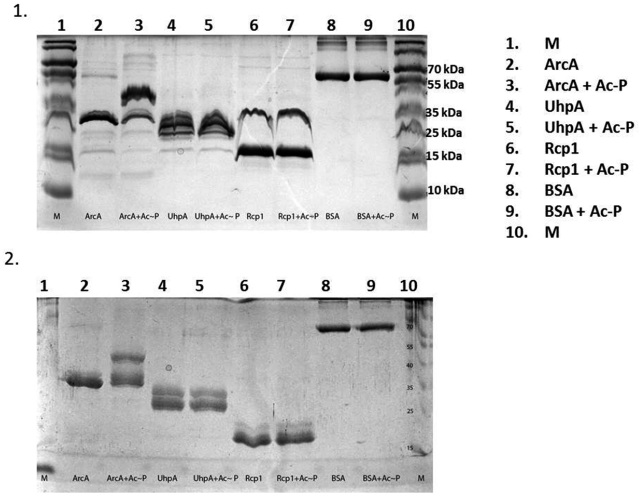

Figure 3. Results of the phosphorylation reaction of the UhpA, Rcp1 and ArcA. Acetyl phosphate was used as a phosphate group donor. ArcA was used as a control. Panel 1 shows the SDS gel with Zn ions and 50 μM Phos-tag compound added; panel 2 shows the SDS gel with Mn ions and the same amount of Phos-tag compound added.

5.4 Discussion.

Since its inception, the Phos-tag method has successfully been used for the separation and/or identification of the phosphorylated form of phosphopeptides [36] and phosphoproteins. [27] Among the latter were various eukaryotic Ser/Thr/Tyr-kinases and even His-kinases. [23, 24] The method has even been applied as an SNP genotyping method. [28] As the decrease of the R_f of a phospho-protein in a Phos-tag SDS-PAGE gel increases with the number of phosphoryl groups, the method could even be used for the identification of the distinct serine phosphorylation states in ovalbumin. [37]

More recently, literature has provided many examples of the successful application of the Phos-tag method to the analysis of the level of phosphorylation of both histidine kinases and of response regulators of (prokaryotic) two component systems (for a review see table 4 and the references therein). In combination with a specific antibody to the protein(s) to be analyzed, this forms a very powerful approach for the functional analyses of two component systems *in vivo*. Strikingly, not a single example of the application of the Phos-tag approach for the analysis of phosphorylation of a response regulator derived from a eukaryotic organism could be found in the scientific literature, which is consistent with the results reported above. In unpublished experiments from the lab of prof. A.H. West, Department of Chemistry and Biochemistry, University of Oklahoma, Norman, Oklahoma, USA, similar observations were made with respect to the Sln1 pathway components from *S. cerevisiae* (A.H. West, personal communication). An alignment of response regulators from prokaryotic and eukaryotic origin, however, has not revealed clear clues as to the explanation for this observation; the observation even may be coincidental.

Not (even) all attempts to use the Phos-tag approach for prokaryotic response regulators were successful, however. Silversmith et al [30] report that their attempts to use of the Phos-tag technology to detect the phosphorylation of response regulators failed. Likewise, we could not detect a change in R_f upon phosphorylation of UhpA and Rcp1. Presumably, the widely-shared habit among researchers of not reporting in the scientific literature on experiments with a negative outcome, may be a reason why not more examples of such failure have been reported. A delicate point in the Phos tag method is the incubation of the target protein(s) with SDS, prior to electrophoresis. Because of the instability of the phosphoaspartates this cannot be done at the conventional high (i.e. 100 ^oC) temperature. Use of much lower temperatures (i.e. from 0 ^oC to room temperature; see section 5.1.2 above), however, increases the risk that the (phosphorylated) protein is incompletely unfolded, which

might hamper separation. Future experiments could be aimed at attempts to compensate for this lowered temperature by using higher SDS concentrations in the sample buffer. Major hydrolysis of the phosphoryl bond in the response regulators during electrophoresis does not appear to be an issue, however, because in all publications the protein under study is always present only in two clearly separated fractions ('bands'); a smear in between these two bands would be expected if hydrolysis during gel electrophoresis would be significant. Another problem may be the change in R_f elicited by response regulator phosphorylation. This change, even for a single phosphorylation event, is quite variable (see e.g. [38] and table 4), and therefore may be undetectably small for some proteins.

Of the examples in which the Phos-tag method was used successfully, Barbieri and Stock employed it to characterize the level of phosphorylation of the *Escherichia coli* response regulator PhoB, both *in vitro* (i.e. by using purified protein), and *in vivo*, by analyzing lysates of cells grown under different conditions of induction of the PhoR/PhoB phosphate assimilation pathway. [20] Different conditions were used for the *in vitro* and *in vivo* tests. Gels were copolymerized with either 75 µM Phos-tag acrylamide and 150 µM $MnCl_2$ for analysis of purified proteins or 25 µM Phos-tag acrylamide and 50 µM $MnCl_2$ for analysis of PhoB from *E. coli* cell lysates. In both *in vivo* and in *in vitro* studies, detection of the phosphorylated and non-phosphorylated from of the PhoB was possible. [20] This goes in line with the general recommendation of the Phos-tag provider.[39] Lower concentrations of the Phos-tag should be use for the cell lysates (*in vivo* testing) when higher for purified proteins (*in vitro* testing). See table 3 for more examples of the concentration ranges of the Phos-tag component used in other studies for the separation of the phosphorylated response regulators.

Table 3 Examples of the conditions used for the detection of the phosphorylated form of the response regulators by Phos-tag method.

Protein	Phos-tag concentration	Type and conc of metal ions	*In vitro* or *in vivo* testing	Ref
CpxR	125 µM	250 µM $MnCl_2$	*In vitro*	[40]
EnvZ	75 µM	150 µM $MnCl_2$	*In vitro*	[41]
EvgA, BarA, ArcB	25 µM	50 µM $MnCl_2$	*In vitro*	[42]
NtrX	35 µM	150 µM ZnCl2	*In vitro*	[43]
SypE, SypA	20 µM	40 µM $MnCl_2$	*In vitro*	[44]
BvgA	75 µM	150 $Zn(NO_3)_2$	*In vitro/in vivo*	[45]
CpxR	35 µM	70 µM $MnCl_2$	*In vivo*	[40]
PhoB	25 µM	50 µM $MnCl_2$	*In vivo*	[46]
RsiB1	25 µM	50 µM $MnCl_2$	*In vivo*	[47]
SypA	25 µM	50 µM $MnCl_2$	*In vivo*	[44]
WalK/WalR	50 µM	100 µM $MnCl_2$	*In vivo*	[48]

Kinoshita and co-workers showed that it is possible to detect the phosphorylated and non-phosphporylated form of FixJ and its cognitive histidine kinase (FixL), using phos-tag SDS-PAGE. They also showed that the phosphorylated form of FixJ was much less stable under acidic conditions than under neutral and alkaline conditions. [35] FixJ is a two-domain response regulator that transduces a signal from the histidine kinase FixL by transferring the phosphoryl group to Asp-54 of the N-terminal receiver domain of FixJ. The C-terminal DNA-binding effector domain of FixJ is then activated, and FixJ increases expression of the target genes *fixK* and *nifA*. [37, 49]

In recent years the very high resolving power of the Phos-tag approach has even allowed the resolution of the pathway of phosphoryl flux within dimers of phospho-relay type histidine kinases. [42, 50] A recent and complicating observation, however, was made on the ClpX protein of *E. coli*: This protein was separated into multiple bands on Phos-tag gels that was fully independent on phosphorylation of an amino acid side chain; [51] the mere presence of a Glu residue in the N-terminus was sufficient to elicit this phenomenon. This observation is another example so often encountered in the molecular sciences (e.g. with measurements of the proton motive force) that scientific claims ideally should be substantiated with at least two independent techniques. Labeling with γ-[^{32}P]-ATP can be used as such an independent probe.

Table 4: Overview of reports of successful separation of the phosphorylated and non-phosphorylated forms of components of two component systems with Phos-tag SDS PAGE

HK	RR	Organism	ΔR_f	Reference
WalK		*Bacillus subtilis*	small separation	[48]
	WalR	*Bacillus subtilis*		[52]
	BvgA	*Bordetella pertussis*	rather large separation	[53]
	NtrX	*Brucella abortus*	very large separation	[43]
	PhyR	*Brucella abortus*		[54]
	NtrX	*Caulobacter crescentus*	large variation	[43]
	RcsB	*Dickeya dadantii*	minimal separation	[55]
	CpxR	*Dickeya dadantii*	variable separation	[40]
CroS		*Enterococcus faecalis*		[56]
	CroR	*Enterococcus faecalis*		[56]
	ArcA	*Escherichia coli*		[57]
	PhoB	*Escherichia coli*		[20, 46, 58]
	PhoP	*Escherichia coli*	small separation	[59]
	EvgA	*Escherichia coli*	actual R_f values provided	[42, 50]
EvgS		*Escherichia coli*		[42, 50]
BarA		*Escherichia coli*		[42, 50]
ArcB		*Escherichia coli*		[42, 50]
EnvZ		*Escherichia coli*		[50]
	MtrA	*Mycobacterium tuberculosis*		[32]
	FrzZ	*Myxococcus xanthus*		[60]
	RprY	*Porphyromonas gingivalis*	RR also acetylated	[61]
	OmpR	*Salmonella enterica*	small separation	[41]
	CtrA	*Sinorhizobium meliloti*		[62]
	DivK	*Sinorhizobium meliloti*	small relative to DivJ	[62]
DivJ		*Sinorhizobium meliloti*		[62]
	RsbiB1	*Sinorhizobium meliloti*		[47]
	CovR	*Streptococcus mutans*	effect of net charge	[63]
	VicR	*Streptococcus pneumonia*		[52]
	RpaA	*Synechococcus elongates*	normal separation	[64]
	RpaB	*Synechococcus elongates*	large separation	[64]
	DrrD	*Thermotoga maritima*		[20]
	RR468	*Thermotoga maritima*		[41]
ThkA		*Thermotoga maritima*		[24]
	DrrB	*Thermotoga maritima*		[32]
	DrrD	*Thermotoga maritima*		[32]
	SypA	*Vibrio fischeri*		[44]

Legend to Table 4: HK – histidine kinase domain, RR – response regulator domain, ΔR_f – shift in the relative mobility during the electrophoresis with the Phos-tag SDS PAGE.

A.

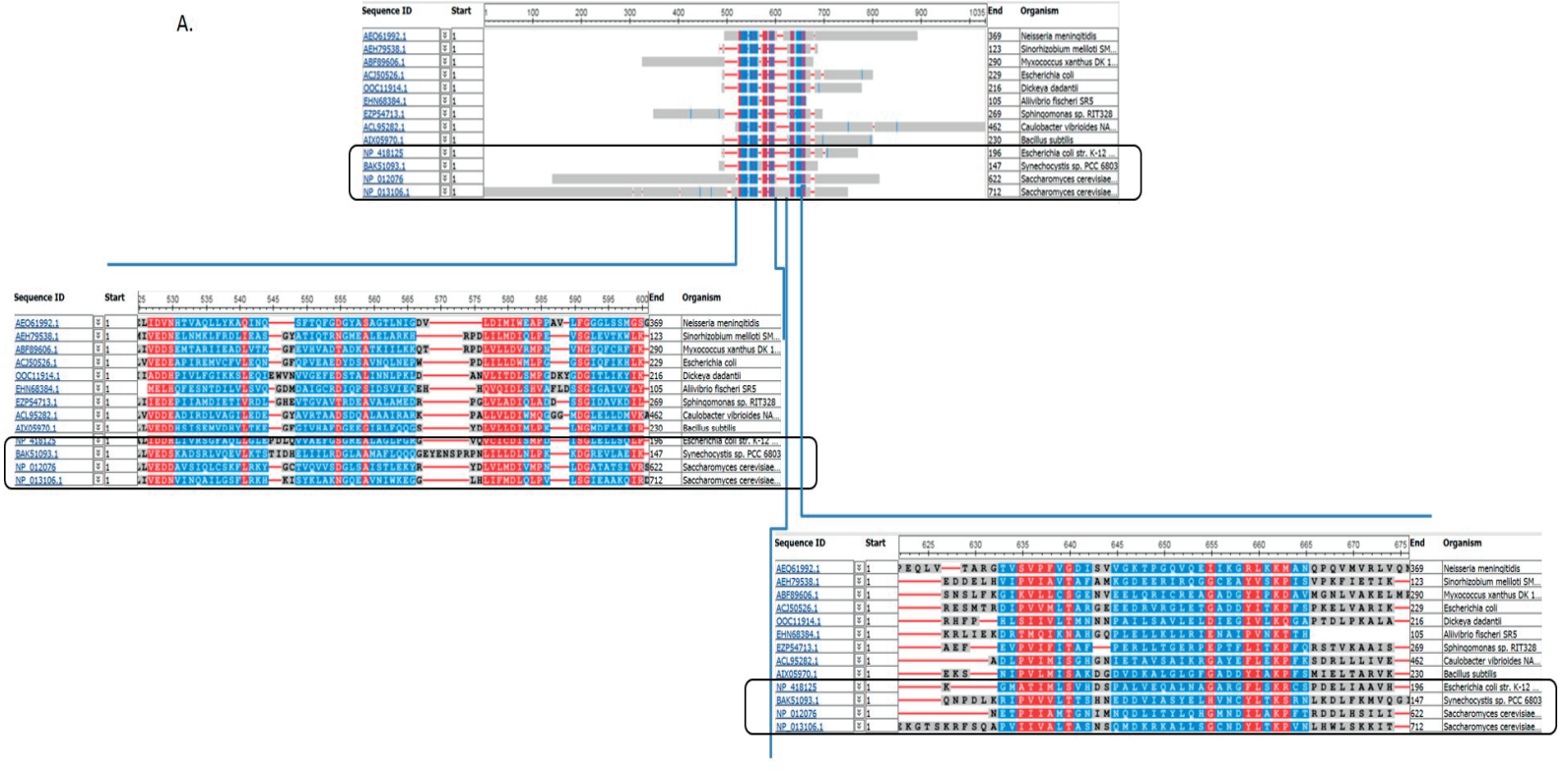
Sequence ID
Start
End
Organism
AEO61992.1
AEH79538.1
ABF89606.1
ACJ50526.1
OOC11914.1
EHN68384.1
EZP54713.1
ACL95282.1
AIX05970.1
NP_418125
BAK51093.1
NP_012076
NP_013106.1
Neisseria meningitidis
Sinorhizobium meliloti SM...
Myxococcus xanthus DK 1...
Escherichia coli
Dickeya dadantii
Allivibrio fischeri SR5
Sphingomonas sp. RIT328
Caulobacter vibrioides NA...
Bacillus subtilis
Escherichia coli str. K-12 ...
Synechocystis sp. PCC 6803
Saccharomyces cerevisiae...

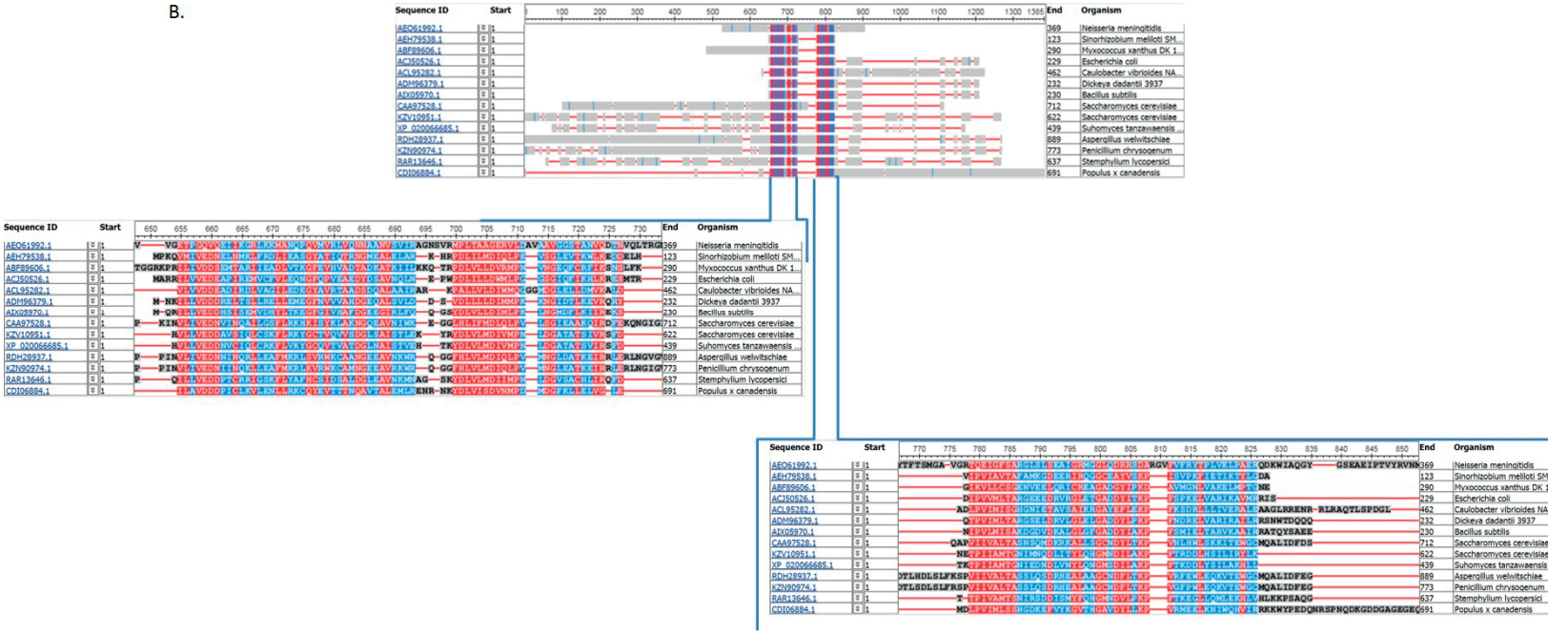

Figure 4. Alignment of the protein sequence of response regulators of which the phosphorylated and non-phosphorylated form were successfully and not-successfully separated by the Phos-tag SDS PAGE method. A. The response regulators in the black frame are amongst those of which the two forms could not be separated by the Phos-tag method (this chapter; see above); the other response regulators are examples of successful detection of this separation, as reported in the literature. The red color indicates highly conserved residues and blue refers to moderately conserved ones. The top alignment represents an overview of the complete sequence of the response regulators. Left and right panels zoom-in on conserved regions. Blue lines indicate which part of the total sequence is enlarged. B. Alignment of the amino acid sequences of seven response regulator from prokaryotic (upper part) and seven from eukaryotic (lower part) organisms. Color coding and highlighting as in A.

As noted above, Asp phosphorylation levels are difficult to quantitate because of their high intrinsic instability. Few techniques are therefore suitable for such assays. One of them is the measurement of phosphorylation-induced changes in intrinsic tryptophan fluorescence. This method can of course be used only for those response regulators that contain a tryptophan of which the fluorescence emission is significantly perturbed by the phosphorylation event (which is not always observed). [10, 20] Yet other techniques allow in some cases detection of the phosphorylation of a specific protein: For some, HPLC analysis allows separation of the phosphorylated and non-phosphorylated form. But also with this approach not every phosphorylated protein can be separated from the non-phosphorylated form. The phosphorylation must induce a change in the solvent-accessible surface of the protein, enabling it to interact differently with the solid and liquid phase during HPLC chromatography. [20, 65] Therefore, it is unlikely that a single separation method will be found that will work for all response regulators, because the response regulators form a very large and quite heterogeneous family of proteins. Figure 4A shows an alignment of several response regulators of which the phosphorylated form was successfully detected with the Phos-tag method and a few that in our hands did not allow this detection. Based on this alignment we could not identify significant differences in the sequence of the listed response regulators of these two classes, that could suggest different behavior during the electrophoresis with the Phos-tag component. Also, a more extensive comparison of prokaryotic and eukaryotic response regulators (figure 4B) did not reveal such features in the region surrounding the Asp phosphorylation site. The overall sequences from eukaryotic origin, however, may suggest that more limited accessibility of the phosphorylated Asp may be a factor that is at the basis of the failure to observe retardation of the phosphorylated form of the protein in that sub-class of eukaryotic response regulator proteins.

References

1. Roskoski R (2015) Invited Review A historical overview of protein kinases and their targeted small molecule inhibitors. Pharmacol Res 100:1–23 . doi: 10.1016/j.phrs.2015.07.010
2. Janiak-Spens F, Sparling JM, Gurfinkel M, West AH (1999) Differential stabilities of phosphorylated response regulator domains reflect functional roles of the yeast osmoregulatory SLN1 and SSK1 proteins. J Bacteriol 181:411–417
3. Stock AM, Robinson VL, Goudreau PN (2000) Two-Component Signal Transduction. Annu Rev Biochem 69:183–215 . doi: 10.1146/annurev.biochem.69.1.183
4. Kee J-M, Muir TW (2012) Chasing Phosphohistidine, an Elusive Sibling in the Phosphoamino Acid Family. ACS Chem Biol 7:44–51 . doi: 10.1021/cb200445w
5. Besant PG, Attwood P V. (2009) Detection and analysis of protein histidine phosphorylation. Mol Cell Biochem 329:93–106 . doi: 10.1007/s11010-009-0117-2
6. Stock JB, Ninfa AJ, Stock AM (1989) Protein phosphorylation and regulation of adaptive responses in bacteria. Microbiol Rev 53:450–490
7. Gao R, Stock AM (2009) Biological insights from structures of two-component proteins. Annu Rev Microbiol 63:133–154 . doi: 10.1146/annurev.micro.091208.073214
8. Nixon BT, Ronson CW, Ausubel FM (1986) Two-component regulatory systems responsive to environmental stimuli share strongly conserved domains with the nitrogen assimilation regulatory genes ntrB and ntrC. Proc Natl Acad Sci U S A 83:7850–7854
9. Li S, Dean S, Li Z, Horecka J, Deschenes RJ, Fassler JS (2002) The eukaryotic two-component histidine kinase Sln1p regulates OCH1 via the transcription factor, Skn7p. Mol Biol Cell 13:412–424 . doi: 10.1091/mbc.01-09-0434
10. Lukat GS, Stock AM, Stock JB (1990) Divalent metal ion binding to the CheY protein and its significance to phosphotransfer in bacterial chemotaxis. Biochemistry 29:5436–42
11. Attwood P V (2013) Histidine kinases from bacteria to humans. Biochem Soc Trans 41:1023–8 . doi: 10.1042/BST20130019
12. Verhamme D (2002) Signal transfer through the Uhp regulatory system in the signal transduction network of Escherichia coli
13. Duclos B, Marcandier S, Cozzone AJ (1991) [2] Chemical properties and separation of phosphoamino acids by thin-layer chromatography and/or electrophoresis. Methods Enzymol 201:10–21 . doi: 10.1016/0076-6879(91)01004-L
14. Hultquist DE (1968) The preparation and characterization of phosphorylated derivatives of histidine. Biochim Biophys Acta - Bioenerg 153:329–340 . doi: 10.1016/0005-2728(68)90078-9
15. Attwood P V., Besant PG, Piggott MJ (2011) Focus on phosphoaspartate and phosphoglutamate. Amino Acids 40:1035–1051 . doi: 10.1007/s00726-010-0738-5
16. Cann ML, McDonald IM, East MP, Johnson GL, Graves LM (2017) Measuring Kinase Activity-A Global Challenge. J Cell Biochem 118:3595–3606 . doi:

10.1002/jcb.26103
17. Jia Y, Quinn CM, Kwak S, Talanian R V (2008) Current in vitro kinase assay technologies: the quest for a universal format. Curr Drug Discov Technol 5:59–69
18. Lukat GS, McCleary WR, Stock AM, Stock JB (1992) Phosphorylation of bacterial response regulator proteins by low molecular weight phospho-donors. Proc Natl Acad Sci U S A 89:718–22 . doi: 10.1073/PNAS.89.2.718
19. Cluzel P, Surette M, Leibler S (2000) An ultrasensitive bacterial motor revealed by monitoring signaling proteins in single cells. Science 287:1652–5
20. Barbieri CM, Stock AM (2008) Universally applicable methods for monitoring response regulator aspartate phosphorylation both in vitro and in vivo using Phos-tag-based reagents. Anal Biochem 376:73–82 . doi: 10.1016/j.ab.2008.02.004
21. West AH, Stock AM (2001) Histidine kinases and response regulator proteins in two-component signaling systems. Trends Biochem Sci 26:369–376 . doi: 10.1016/S0968-0004(01)01852-7
22. Galdieri L, Zhang T, Rogerson D, Lleshi R, Vancura A (2014) Protein acetylation and acetyl coenzyme a metabolism in budding yeast. Eukaryot Cell 13:1472–83 . doi: 10.1128/EC.00189-14
23. Kinoshita-Kikuta E, Aoki Y, Kinoshita E, Koike T (2007) Label-free Kinase Profiling Using Phosphate Affinity Polyacrylamide Gel Electrophoresis. Mol Cell Proteomics 6:356–366 . doi: 10.1074/mcp.T600044-MCP200
24. Yamada S, Nakamura H, Kinoshita E, Kinoshita-Kikuta E, Koike T, Shiro Y (2007) Separation of a phosphorylated histidine protein using phosphate affinity polyacrylamide gel electrophoresis. Anal Biochem 360:160–162 . doi: 10.1016/j.ab.2006.10.005
25. Kinoshita E, Kinoshita-Kikuta E, Takiyama K, Koike T (2006) Phosphate-binding tag, a new tool to visualize phosphorylated proteins. Mol Cell Proteomics 5:749–57 . doi: 10.1074/mcp.T500024-MCP200
26. Kinoshita E, Kinoshita-Kikuta E, Koike T (2009) Separation and detection of large phosphoproteins using Phos-tag SDS-PAGE. Nat Protoc 4:1513–1521 . doi: 10.1038/nprot.2009.154
27. Kinoshita E, Kinoshita-Kikuta E, Sugiyama Y, Fukada Y, Ozeki T, Koike T (2012) Highly sensitive detection of protein phosphorylation by using improved Phos-tag Biotin. Proteomics 12:932–937 . doi: 10.1002/pmic.201100639
28. Kinoshita E, Kinoshita-Kikuta E, Koike T (2007) A single nucleotide polymorphism genotyping method using phosphate-affinity polyacrylamide gel electrophoresis. Anal Biochem 361:294–298 . doi: 10.1016/j.ab.2006.11.032
29. Kinoshita-Kikuta E, Kinoshita E, Koike T (2012) Separation and identification of four distinct serine-phosphorylation states of ovalbumin by Phos-tag affinity electrophoresis. Electrophoresis 33:849–855 . doi: 10.1002/elps.201100518
30. Silversmith RE, Bourret RB (2018) Fluorescence Measurement of Kinetics of CheY Autophosphorylation with Small Molecule Phosphodonors. Humana Press, New York, NY, pp 321–335
31. van Beilen JWA, Hellingwerf KJ (2016) All Three Endogenous Quinone Species of

Escherichia coli Are Involved in Controlling the Activity of the Aerobic/Anaerobic Response Regulator ArcA. Front Microbiol 7:1339 . doi: 10.3389/fmicb.2016.01339

32. Barbieri CM, Mack TR, Robinson VL, Miller MT, Stock AM (2010) Regulation of response regulator autophosphorylation through interdomain contacts. J Biol Chem 285:32325–35 . doi: 10.1074/jbc.M110.157164
33. McCleary WR, Stock JB (1994) Acetyl phosphate and the activation of two-component response regulators. J Biol Chem 269:31567–72
34. Fassler JS, West AH (2010) Genetic and biochemical analysis of the SLN1 pathway in Saccharomyces cerevisiae. Methods Enzymol 471:291–317 . doi: 10.1016/S0076-6879(10)71016-8 [doi]
35. Alvarez AF, Georgellis D (2010) In Vitro and In Vivo Analysis of the ArcB/A Redox Signaling Pathway. Methods Enzymol 471:205–228 . doi: 10.1016/S0076-6879(10)71012-0
36. Kinoshita E, Kinoshita-Kikuta E, Takiyama K, Koike T (2006) Phosphate-binding tag, a new tool to visualize phosphorylated proteins. Mol Cell Proteomics 5:749–757 . doi: 10.1074/mcp.T500024-MCP200
37. Kinoshita E, Kinoshita-Kikuta E, Matsubara M, Yamada S, Nakamura H, Shiro Y, Aoki Y, Okita K, Koike T (2008) Separation of phosphoprotein isotypes having the same number of phosphate groups using phosphate-affinity SDS-PAGE. Proteomics 8:2994–3003 . doi: 10.1002/pmic.200800243
38. Pini F, Frage B, Ferri L, De Nisco NJ, Mohapatra SS, Taddei L, Fioravanti A, Dewitte F, Galardini M, Brilli M, Villeret V, Bazzicalupo M, Mengoni A, Walker GC, Becker A, Biondi EG (2013) The DivJ, CbrA and PleC system controls DivK phosphorylation and symbiosis in Sinorhizobium meliloti. Mol Microbiol 90:54–71 . doi: 10.1111/mmi.12347
39. Phos-tag TM-based Mobility Shift Detection of Phosphorylated Proteins, ver. 12 2014/8, product information
40. Bontemps-Gallo S, Madec E, Lacroix J-M (2015) The two-component system CpxAR is essential for virulence in the phytopathogen bacteria Dickeya dadantii EC3937. Environ Microbiol 17:4415–28 . doi: 10.1111/1462-2920.12874
41. Liu Y, Rose J, Huang S, Hu Y, Wu Q, Wang D, Li C, Liu M, Zhou P, Jiang L (2017) A pH-gated conformational switch regulates the phosphatase activity of bifunctional HisKA-family histidine kinases. Nat Commun 8:2104 . doi: 10.1038/s41467-017-02310-9
42. Kinoshita-Kikuta E, Kinoshita E, Eguchi Y, Yanagihara S, Edahiro K, Inoue Y, Taniguchi M, Yoshida M, Yamamoto K, Takahashi H, Sawasaki T, Utsumi R, Koike T (2015) Functional Characterization of the Receiver Domain for Phosphorelay Control in Hybrid Sensor Kinases. PLoS One 10:e0132598 . doi: 10.1371/journal.pone.0132598
43. Fernández I, Sycz G, Goldbaum FA, Carrica MDC (2018) Acidic pH triggers the phosphorylation of the response regulator NtrX in alphaproteobacteria. PLoS One 13:e0194486 . doi: 10.1371/journal.pone.0194486
44. Morris AR, Visick KL (2013) The response regulator SypE controls biofilm formation

and colonization through phosphorylation of the syp-encoded regulator SypA in Vibrio fischeri. Mol Microbiol 87:509–25 . doi: 10.1111/mmi.12109

45. Chen Q, Boulanger A, Hinton DM, Stibitz S Separation and Detection of Phosphorylated and Nonphosphorylated BvgA, a Bordetella pertussis Response Regulator, in vivo and in vitro Materials and Reagents. doi: 10.21769/BioProtoc.970
46. Gao R, Stock AM (2013) Probing kinase and phosphatase activities of two-component systems in vivo with concentration-dependent phosphorylation profiling. Proc Natl Acad Sci U S A 110:672–7 . doi: 10.1073/pnas.1214587110
47. Sauviac L, Bruand C (2014) A putative bifunctional histidine kinase/phosphatase of the HWE family exerts positive and negative control on the Sinorhizobium meliloti general stress response. J Bacteriol 196:2526–35 . doi: 10.1128/JB.01623-14
48. Fakhruzzaman M, Inukai Y, Yanagida Y, Kino H, Igarashi M, Eguchi Y, Utsumi R (2015) Study on in vivo effects of bacterial histidine kinase inhibitor, Waldiomycin, in Bacillus subtilis and Staphylococcus aureus. J Gen Appl Microbiol 61:177–84 . doi: 10.2323/jgam.61.177
49. Möglich A, Moffat K (2010) Engineered photoreceptors as novel optogenetic tools. Photochem Photobiol Sci 9:1286–1300 . doi: 10.1039/c0pp00167h [doi]
50. Kinoshita-Kikuta E, Kinoshita E, Eguchi Y, Koike T (2016) Validation of Cis and Trans Modes in Multistep Phosphotransfer Signaling of Bacterial Tripartite Sensor Kinases by Using Phos-Tag SDS-PAGE. PLoS One 11:e0148294 . doi: 10.1371/journal.pone.0148294
51. Kinoshita E, Kinoshita-Kikuta E, Karata K, Kawano T, Nishiyama A, Yamato M, Koike T (2017) Specific glutamic acid residues in targeted proteins induce exaggerated retardations in Phos-tag SDS-PAGE migration. Electrophoresis 38:1139–1146 . doi: 10.1002/elps.201600520
52. Wayne KJ, Sham LT, Tsui HC, Gutu AD, Barendt SM, Keen SK, Winkler ME (2010) Localization and cellular amounts of the WalRKJ (VicRKX) two-component regulatory system proteins in serotype 2 Streptococcus pneumoniae. J Bacteriol 192:4388–4394 . doi: 10.1128/JB.00578-10 [doi]
53. Boulanger A, Chen Q, Hinton DM, Stibitz S (2013) In vivo phosphorylation dynamics of the Bordetella pertussis virulence-controlling response regulator BvgA. Mol Microbiol 88:156–72 . doi: 10.1111/mmi.12177
54. Luebke JL, Eaton DS, Sachleben JR, Crosson S (2018) Allosteric control of a bacterial stress response system by an anti-σ factor. Mol Microbiol 107:164–179 . doi: 10.1111/mmi.13868
55. Madec E, Bontemps-Gallo S, Lacroix J-M (2014) Increased phosphorylation of the RcsB regulator of the RcsCDB phosphorelay in strains of Dickeya dadantii devoid of osmoregulated periplasmic glucans revealed by Phos-tag gel analysis. Microbiology 160:2763–2770 . doi: 10.1099/mic.0.081273-0
56. Kellogg SL, Kristich CJ (2018) Convergence of PASTA kinase and two-component signaling in response to cell wall stress in Enterococcus faecalis. J Bacteriol 200:e00086-18 . doi: 10.1128/JB.00086-18
57. Rolfe MD, Ter Beek A, Graham AI, Trotter EW, Asif HMS, Sanguinetti G, de Mattos

JT, Poole RK, Green J (2011) Transcript profiling and inference of Escherichia coli K-12 ArcA activity across the range of physiologically relevant oxygen concentrations. J Biol Chem 286:10147–54 . doi: 10.1074/jbc.M110.211144

58. Gao R, Stock AM (2017) Quantitative Kinetic Analyses of Shutting Off a Two-Component System. MBio 8: . doi: 10.1128/mBio.00412-17
59. Ishii E, Eguchi Y, Utsumi R (2013) Mechanism of Activation of PhoQ/PhoP Two-Component Signal Transduction by SafA, an Auxiliary Protein of PhoQ Histidine Kinase in *Escherichia coli*. Biosci Biotechnol Biochem 77:814–819 . doi: 10.1271/bbb.120970
60. Kaimer C, Zusman DR (2013) Phosphorylation-dependent localization of the response regulator FrzZ signals cell reversals in Myxococcus xanthus. Mol Microbiol 88:740–53 . doi: 10.1111/mmi.12219
61. Li Y, Krishnan K, Duncan MJ (2018) Post-translational regulation of a Porphyromonas gingivalis regulator. J Oral Microbiol 10:1487743 . doi: 10.1080/20002297.2018.1487743
62. Pini F, Frage B, Ferri L, De Nisco NJ, Mohapatra SS, Taddei L, Fioravanti A, Dewitte F, Galardini M, Brilli M, Villeret V, Bazzicalupo M, Mengoni A, Walker GC, Becker A, Biondi EG (2013) The DivJ, CbrA and PleC system controls DivK phosphorylation and symbiosis in Sinorhizobium meliloti. Mol Microbiol 90:54–71 . doi: 10.1111/mmi.12347
63. Khara P, Mohapatra SS, Biswas I (2018) Role of CovR phosphorylation in gene transcription in Streptococcus mutans. Microbiology 164:704–715 . doi: 10.1099/mic.0.000641
64. Piechura JR, Amarnath K, O'Shea EK (2017) Natural changes in light interact with circadian regulation at promoters to control gene expression in cyanobacteria. Elife 6: . doi: 10.7554/eLife.32032
65. Head CG, Tardy A, Kenney LJ (1998) Relative binding affinities of OmpR and OmpR-phosphate at the ompF and ompC regulatory sites 1 1Edited by R. Ebright. J Mol Biol 281:857–870 . doi: 10.1006/jmbi.1998.1985

6 General discussion

Bury AE, Hellingwerf KJ

The primary goal of the work presented in this thesis was to provide a unique tool that may increase our quantitative understanding of the mechanism of cytoplasmic diffusion in signal transduction (networks) in eukaryotic cells, in the form of a chimeric, light-dependent, cytoplasmic signal transduction device in the yeast *Saccharomyces cerevisiae*. In chapter 2 we further characterize the *in vivo* redox transitions of a flavin-containing photo-sensory receptor domain for such a chimeric device. Chapter 3 describes the design and functional characterization of the intended chimera: A light-sensitive histidine protein kinase, derived from the Sln1 kinase of *S. cerevisiae,* translationally fused in a coiled-coil motif with the LOV domain of the stressosome component YtvA from *Bacillus subtilis*. In chapter 4 we describe tests that show the *in vivo* functionality of this light-sensitive histidine protein kinase. This orthogonal photo-transduction system can be used to either study the activation or repression of gene expression in *S. cerevisiae*, depending on the specific promoter/gene combination that is used as a read-out. Furthermore, the device can also be used to initiate nuclear accumulation of a selected signal transduction protein with blue incident illumination. In chapter 5 we go into detail on one of the methods for functional testing of the phosphorylation of the histidine kinases and their cognate response regulator(s), the so-called Phos-tag method.

In each of these chapters the results obtained have been discussed in light of available information from the literature. Nevertheless, a few more general points were not addressed in these chapters and therefore they will be discussed below:

6.1.1 **Robustness of the LOV domain as an advantage for this study**

A key aspect of metabolic processes can be summarized as ‘moving electrons between molecules’, with the simultaneous release of free energy. Part of this (free) energy can be captured (while some is released as entropy and/or heat), as the transferred electrons move from a high-energy to a lower energy state. [1] Many enzymes contain cofactors like NAD(P)H, FADH, quinones, heam groups, etc., that can be easily and safely reduced and oxidized. Among these, flavins, that play a role as a cofactor in flavoenzymes, support one-electron and two-electrons transfer processes, involving the N1, C4a and N5 position of their isoallaxazine ring.[2] Beyond involvement in metabolic enzymes, in several proteinaceous cellular sensing devices, the redox state of a bound flavin is involved in the generation of the functional output signal of that particular sensing system. The resting state of the flavin can be the oxidized as well as the reduced form (and in rare cases even the flavin semiquinone

state), depending on the physiological redox environment in the cell. These flavin-containing sensor proteins can be triggered either by redox-active metabolites or by blue light, absorbed by the particular resting state of the flavin (for the semiquinone form these quanta even can have a wavelength that extends into the green and red part of the spectrum). Flavoproteins that act as photosensors are first of all found in the subfamily of LOV domains of the Per-Arnt-Sim (PAS) domain family. Also the other members of this subfamily are known to respond to changes in cellular redox conditions, light exposure or energy. [3, 4] Furthermore, two additional types of apo-protein fold have the capacity to bind flavin and capture photons for signal transduction, i.e. BLUF domains and cryptochromes. In chapter 2 we showed that the most reducing conditions of the cytoplasm of *E. coli* that we could achieve, did not lead to measurable reduction of the LOV domain of LovK *in vivo*. Recent studies of cryptochrome 2 (Cry2) from *Arabidopsis thaliana* revealed that binding of ATP does have an enhancing effect on photoreduction of Cry2 *in vitro* and *in vivo*. [5] This observation is in line with the conclusions drawn in chapter 2, i.e. that the cryptochromes might be more sensitive to the redox conditions inside the cells than LovK. This observation may lead in the future to combining light- and redox-signaling in a single, cryptochrome dependent pathway.

In making chimeric light-sensing systems one can discriminate two extreme situations: First one would like to have a system in which the light-sensitive domain is sensitive only to light signals. Once the functionality of such a system has been proven and characterized *in vivo*, it is of interest to move to the next level of complexity, i.e. to design a chimera that responds to multiple signals, like the combination of photons and redox signals. For this it is advantageous to have a light-sensing domain with a high redox midpoint potential. In principle, Cry and BLUF domains would qualify best for this, but both types have disadvantages: (i) for both a less well defined engineering strategy is available to link the light-sensitive domain to the output kinase domain; and (ii) representatives of these two families presumably have less attractive stability-, solubility- and chromophore-binding properties.

The midpoint potential of the Lov domains of AsLov2 and YtvA is too negative to be able to expect *in vivo* modulation of their redox state (i.e. < -300 mV). Therefore the LOV domain of LovK became of interest because of its reported midpoint potential of – 254 mV. [6] Although we could not exactly reproduce this value (chapter 2), indeed the midpoint potential of this LOV domain is significantly higher than that of the LOV domain of YtvA (compare ref [7]). Therefore, it would be of interest to perform additional attempts to observe

redox modulation of this particular LovK chimera. As the LovK domain is able to form stable fusion proteins with STAS domains (chapter 2) such tests can now also be carried out in *Bacillus subtilis*, in which such redox transitions could be probed directly spectroscopically, but also via the read-out of the stressosome response, [8] including the color-dependence of this response, particularly in mutants in which YtvA (variants) are incorporated into functional stressosomes. The fact that this organism uses menaquinones in its electron transfer chain, [9] is an extra incentive for such tests.

As mentioned before the YtvA is a functional light sensitive part of the stressosome, multiprotein complex responsible for the general stress response in the *Bacillus subtilis*. Stressosomes comprise the RsbR and RsbS proteins, that both contain a STAS domain. Stress conditions cause phosphorylation of RsbR and RsbS by the kinase RsbT. [10] It was shown that the STAS domain of the YtvA includes a conserved motif that can be involved in GTP binding. Series of experiments involving the BODIPY-GTP proved the capability of YtvA to bind GTP, that can be exchanged for ATP. One could conclude that YtvA could play a role in the sensing of the GTP- or ATP level, [11] or recruit the nucleotides for the kinase activity of the above-mentioned RsbT. [8] However, the most recent study shows that binding of the BODIPY-GTP to YtvA was unspecific. [12, 13] In our lab the NTPase activity of YtvA in its full length form, as well as of truncated versions without the STAS domain and the linker region, was also tested. These experiments confirmed lack of the NTPase activity of YtvA (data not shown).

6.1.2 **Relation between BLUF and LOV domains**

The suitability of LOV domains for integrated sensing of light and redox signals is also suggested by the observation that it is possible to change the signaling mechanism from the adduct formation, in LOV domains, to electron transfer (as it occurs in BLUF domains), by changing the amino acids inside the hydrogen binding pattern in the chromophore binding pocket of the respective apo proteins. [14, 15] Yee at al proposed that this might suggest that the evolutionary history of these domains is such that the LOV domains were fist sensing the redox state of the cells, while adding the Cys into the hydrogen pocket made them less sensitive to the redox changes and more sensitive to blue light. [14] This was shown in the reverse experiment of Suzuki and coworkers. In their hands the BLUF domain in which electron transfer is the basal mechanism of signal propagation, started to operate like a LOV

domain by the insertion of a key Cys residue at the position that corresponds to its position in the LOV domains. [16]

6.2 Light – a very versatile language for intercellular communication

Light is crucial for (culturing) many forms of life on earth. Beyond that, light has become an essential tool that is used to interrogate and manipulate biological systems. It has proven to be an efficient spatiotemporal trigger for many biological processes; moreover, it is cheap and highly tunable with respect to intensity, duration, color, and mode of polarization. As it was described in the General Introduction chapter, in addition to natural photoactive proteins, plenty of chimaeric photosensory devices are available. Here we would like to focus on the input, light sensing, domain of such chimaera's and their suitability for use in the broad field of optogenetics. Our studies are focused on the use of LOV domains. In Chapter 2 we describe the robustness of the LovK domain from *Caulobacter crescentus* and in Chapters 3 and 4 the LOV domain of YtvA from *Bacillus subtilis* was used to design a light-activatable two component signal transduction pathway in the yeast *Saccharomyces cerevisiae*. Nevertheless, there are various other light sensitive domains available that could be used in such studies. An example is a BLUF domain, instead of the LOV domain. The absorption spectrum of these two domains is approximately the same, because both are based on the optical properties of the isoalloxazine ring system the flavins (i.e. from 350 -500 nm). In BLUF domains this cofactor presumably will be mostly FAD, [17] in contrast to the FMN from LOV domains. Because of the larger size of the BLUF domains, they might not be properly folded, nor be stable after overexpression in the form of a chimeric histidine kinase. Significant negative features were reported in the use of BLUF domains as heterologously expressed light gated adenylate cyclases (i.e. the PACα and PACβ from the unicellular flagellate *Euglena gracialis*): quite low stability of the heterologously expressed proteins, significant dark activity and only moderate activation by illumination. [18] Alternative possibilities would be to use the light sensing domain of cryptochromes or phytochromes. Of these two families the cryptochromes also use the abundant cofactor FAD. These sensors therefore absorb a similar range wavelength of the absorbed light as BLUF and LOV domains. Disadvantages that were found by others by using Cry domains for light triggering of protein interaction was the need to carefully control the expression level of the Cry domain and its generally slow off kinetics. [19] If one would want to try to use phytochromes for

light activation, the first obstacle will be the necessity of incorporation of the phycocyanobilin chromophore which is not found in animal cells (note that for many bacteriophytochromes, the abundant biliverdin can be used instead). Secondly, the expression level of the Phy domain needs to be carefully controlled. In spite of these complications, phytochrome domains have been successfully used for light-gated regulation of diverse biological processes, including transcription, [20] splicing [21] and small GTPases in living cells [22] and *in vitro* control of actin assembly. [23]

The choice of the photosensory domain and the way of connecting it to an output domain is also dictated by the function we expect this new fusion protein to play in the cells. It is possible to control various events by stimulation of a light sensing fusion protein like for example: regulation of protein localization, and alteration of protein-protein interactions that might be used for light regulated gene expression. A target protein - fused to a photoreceptor domain - can be translocated to the membrane through light-induced interaction between the photoreceptor domain and its membrane-tethered binding partner. Light-induced interaction between the photoreceptor and its binding partner also allows one to drive the association of a DNA-binding domain with an activation domain of a transcription factor. Such an event will initiate transcription. Chapter 4 shows the introduction of a light dependent two component signal transduction pathway in *S. cerevisiae*. This was achieved by fusion of the light sensing LOV domain with the histidine kinase domain from the Sln1 pathway. Similar approaches to make 'blind' organisms sensitive to light were presented also in many other studies. [6, 24–28] One of the recent examples was presented by Hori and coworkers. Adding a photo-responsive ability to the ArcB-ArcA (anoxic redox control) two component signal transduction pathway of *E. coli* by fusion of a cyanobacterial photoreceptor domain from CcaS with an *E. coli* intracellular HK domain of ArcB to construct chimeric HKs. The CcaS contains a GAF domain with a conserved Cys that covalently binds phycocyanobilin that undergoes the photo-isomerization. Downstream of the GAF domain are two PAS domains, with PAC domains in between, followed by HisKA and HitPase domains. ArcB consists of the PAS domain, followed by a HisKA domain, a HitPase domain, a RAC domain and an HPT domain. A series of fusion proteins were made, out of which the ArcaS9 was the only one that shows light sensitivity; actually, it showed dual sensing, for light-color-dependent signalling and sensing of aerobic-anaerobic transitions. This construct contains the GAF and PAS domain from CcaS and HisKA and HitPase domain from ArcB. The authors show that the crucial factor in the design is the length of the linker between the light sensing domain

and the histidine kinase domain. Constructs with the same domain arrangement like ArcaS9, but with a shorter linker between the CcaS- and ArcB-derived parts, did not show the light sensitivity. [29]

During the past few years also new types of photo-sensing domains have been discovered, like UVR8, [30] aureochromes, [31] vitamin B12-containing receptors, [32] RsbP, [33] etc. These new domains offer little advantage, however, over those already available, except maybe for the extension to the very short wavelengths offered by UVR8. However, for each of these domains a productive mode of domain coupling will have to be resolved before they can be used for the construction of chimera's.

6.3 Spatial design of biochemical regulation networks

Recent developments in the life sciences go into the direction in which many scientific disciplines interlace together. Quick progress in understanding of many basic life processes by interdisciplinary consortia has been possible in recent years by tight interaction/cooperation between quantitative experiments and computational theory. The field of the life sciences suffered, however, because not enough knowledge about molecular interactions in living organisms was available. Although we are still at the beginning of the understanding of all inter-dependency and correlations that are present in and dictate the functioning of the living world, the current state of knowledge allows us to draw very detailed conclusions about life processes, based on the theoretical and experimental data available in the field of the physical systems biology, to the extent that serious attempts are now under way to build-up cellular life from its molecular constituents *in vitro*. [34]

Mathematical models of biochemical regulation networks generally have to consider both (de)binding events and molecular diffusion processes. Initially, mainly classical Brownian motion was used to describe the diffusion processes. More recently, also anomalous modes of diffusion are taken into account. [35, 36] For recent review see. [37] Current developments of the techniques used for the analysis of the (anomalous) diffusion allow modelers to formulate more precise descriptions, based on the experimental data. Methods like fluorescence recovery after photobleaching (FRAP) [38, 39] and fluorescence correlation spectroscopy (FCS) [40, 41], and fluorescence loss in photobleaching (FLIP) [42] play an important role in these developments. Implementation of a light-activatable two component signal transduction pathway provides another possibility for the study of diffusion of a signal

in the crowded cytoplasm of a eukaryotic cell. Spatiotemporally localized activation of these components by LED- or laser-light, makes available an even more advanced tool to investigate signal diffusion in a biochemical regulation network, mimicking real-life processes in (multi)cellular systems with spatial differentiation of cellular function.

6.4 Concluding remarks and future prospects

Our study introduces another tool for investigation of signal diffusion in a biochemical regulation network through the design and characterization of a light stimulated histidine kinase that consists of the LOV domain from YtvA from *Bacillus subtilis* and the histidine kinase domain Sln1 from *Saccharomysec cerevisiae*. We showed that blue light can be used as a trigger for modulation of the phosphorylation events in this engineered two component signal transduction pathway in a eukaryotic cell. At the same time, we showed the robustness of LOV domains and their capability in use for designing of fusion proteins for signal transduction that can be triggered with (blue) light. Local, i.e. sub-cellular, activation of such designed pathways in *S. cerevisiae* cells would be a great supplement for more detailed experimental tests of computational models for signal transduction in the eukaryotic cytoplasm, triggered by local light stimulation. Membrane anchoring may be used in future experiments along these lines to reduce the dimensionality of the problem, and to align models with the outcome of such experiments. This optogenetic approach, which is an extensively growing branch of the life sciences, has the potential to bring the understanding of (cellular) life to the next level.

References

1. Berg JM, Tymoczko JL, Stryer L (2011) Biochemistry. WH Freeman and company
2. Fraaije MW, Mattevi A (2000) Flavoenzymes: diverse catalysts with recurrent features. Trends Biochem Sci 25:126–132 . doi: 10.1016/S0968-0004(99)01533-9
3. Taylor BL, Zhulin IB (1999) PAS domains: internal sensors of oxygen, redox potential, and light. Microbiol Mol Biol Rev 63:479–506
4. Key J, Hefti M, Purcell EB, Moffat K (2007) Structure of the Redox Sensor Domain of Azotobacter Vinelandii nifl at Atomic Resolution: Signaling, Dimerization, and Mechanism. Biochemistry 46:3614-3623 doi: 10.1021/bi0620407
5. Eckel M, Steinchen W, Batschauer A (2018) ATP boosts lit state formation and activity of Arabidopsis cryptochrome 2. Plant J. doi: 10.1111/tpj.14039
6. Purcell EB, McDonald CA, Palfey BA, Crosson S (2010) An analysis of the solution structure and signaling mechanism of LovK, a sensor histidine kinase integrating light and redox signals. Biochemistry 49:6761–6770 . doi: 10.1021/bi1006404
7. Arents JC, Perez MA, Hendriks J, Hellingwerf KJ (2011) On the midpoint potential of the FAD chromophore in a BLUF-domain containing photoreceptor protein. FEBS Lett 585:167–172 . doi: 10.1016/j.febslet.2010.11.035
8. Avila-Perez M, Vreede J, Tang Y, et al (2009) In vivo mutational analysis of YtvA from Bacillus subtilis: mechanism of light activation of the general stress response. J Biol Chem 284:24958–24964 . doi: 10.1074/jbc.M109.033316
9. Azarkina N, Konstantinov AA (2002) Stimulation of menaquinone-dependent electron transfer in the respiratory chain of Bacillus subtilis by membrane energization. J Bacteriol 184:5339–47 . doi: 10.1128/JB.184.19.5339-5347.2002
10. van der Steen JB, Avila-Perez M, Knippert D, et al (2012) Differentiation of function among the RsbR paralogs in the general stress response of Bacillus subtilis with regard to light perception. J Bacteriol 194(7):1708–1716 . doi: 10.1128/JB.06705-11
11. Buttani V, Losi A, Polverini E, Gärtner W (2006) Blue news: NTP binding properties of the blue-light sensitive YtvA protein from *Bacillus subtilis*. FEBS Lett 580:3818–3822 . doi: 10.1016/j.febslet.2006.06.007
12. Nakasone Y, Hellingwerf KJ (2011) On the Binding of BODIPY-GTP by the Photosensory Protein YtvA from the Common Soil Bacterium Bacillus subtilis†. Photochem Photobiol 87:542–547 . doi: 10.1111/j.1751-1097.2011.00919.x
13. Dorn M, Jurk M, Schmieder P (2012) Blue News Update: BODIPY-GTP Binds to the Blue-Light Receptor YtvA While GTP Does Not. PLoS One 7:e29201 . doi: 10.1371/journal.pone.0029201
14. Yee EF, Diensthuber RP, Vaidya AT, et al (2015) Signal transduction in light-oxygen-voltage receptors lacking the adduct-forming cysteine residue. Nat Commun 6:10079 . doi: 10.1038/ncomms10079 [doi]
15. Magerl K, Stambolic I, Dick B (2017) Switching from adduct formation to electron transfer in a light–oxygen–voltage domain containing the reactive cysteine. Phys Chem Chem Phys 19:10808–10819 . doi: 10.1039/C6CP08370F
16. Suzuki H, Okajima K, Ikeuchi M, Noguchi T (2008) LOV-Like Flavin-Cys Adduct Formation by Introducing a Cys Residue in the BLUF Domain of TePixD. J Am Chem

Soc 130:12884–12885 . doi: 10.1021/ja805363u
17. Laan W, Gauden M, Yeremenko S, et al (2005) On the Mechanism of Activation of the BLUF Domain of AppA. doi: 10.1021/BI051367P
18. Schröder-Lang S, Schwärzel M, Seifert R, et al (2007) Fast manipulation of cellular cAMP level by light in vivo. Nat Methods 4:39–42 . doi: 10.1038/nmeth975
19. Kennedy MJ, Hughes RM, Peteya LA, et al (2010) Rapid blue-light-mediated induction of protein interactions in living cells. Nat Methods 7:973–975 . doi: 10.1038/nmeth.1524 [doi]
20. Shimizu-Sato S, Huq E, Tepperman JM, Quail PH (2002) A light-switchable gene promoter system. Nat Biotechnol 20:1041–1044 . doi: 10.1038/nbt734 [doi]
21. Tyszkiewicz AB, Muir TW (2008) Activation of protein splicing with light in yeast. Nat Methods 5:303–305 . doi: 10.1038/nmeth.1189
22. Levskaya A, Weiner OD, Lim WA, Voigt CA (2009) Spatiotemporal control of cell signalling using a light-switchable protein interaction. Nature 461: . doi: 10.1038/nature08446
23. Leung DW, Otomo C, Chory J, Rosen MK (2008) Genetically encoded photoswitching of actin assembly through the Cdc42-WASP-Arp2/3 complex pathway. Proc Natl Acad Sci U S A 105:12797–802 . doi: 10.1073/pnas.0801232105
24. Möglich A, Ayers RA, Moffat K (2009) Design and signaling mechanism of light-regulated histidine kinases. J Mol Biol 385:1433–1444 . doi: 10.1016/j.jmb.2008.12.017
25. Correa F, Ko WH, Ocasio V, et al Blue light regulated two-component systems: enzymatic and functional analyses of light-oxygen-voltage (LOV)-histidine kinases and downstream response regulators. 2014
26. Fraikin GY, Strakhovskaya MG, Rubin AB (2013) Biological photoreceptors of light-dependent regulatory processes. BiochemistryBiokhimiia 78:1238–1253 . doi: 10.1134/S0006297913110047 [doi]
27. Abe K, Miyake K, Nakamura M, et al (2014) Engineering of a green-light inducible gene expression system in Synechocystis sp. PCC6803. Microb Biotechnol 7:177–183 . doi: 10.1111/1751-7915.12098 [doi]
28. Cao Z, Buttani V, Losi A, Gartner W (2008) A blue light inducible two-component signal transduction system in the plant pathogen Pseudomonas syringae pv. tomato. Biophys J 94:897–905 . doi: 10.1529/biophysj.107.108977
29. Hori M, Oka S, Sugie Y, et al (2017) Construction of a photo-responsive chimeric histidine kinase in <i>Escherichia coli</i> J Gen Appl Microbiol 63:44–50 . doi: 10.2323/jgam.2016.07.005
30. Yang X, Montano S, Ren Z (2015) How Does Photoreceptor UVR8 Perceive a UV-B Signal? Photochem Photobiol 91:993–1003 . doi: 10.1111/php.12470
31. Matiiv AB, Chekunova EM (2018) Aureochromes – Blue Light Receptors. Biochem 83:662–673 . doi: 10.1134/S0006297918060044
32. Jost M, Fernández-Zapata J, Polanco MC, et al (2015) Structural basis for gene regulation by a B12-dependent photoreceptor. Nature 526:536–41 . doi: 10.1038/nature14950

33. Avila-Pérez M, van der Steen JB, Kort R, Hellingwerf KJ (2010) Red light activates the sigmaB-mediated general stress response of Bacillus subtilis via the energy branch of the upstream signaling cascade. J Bacteriol 192:755–62 . doi: 10.1128/JB.00826-09
34. Desai A, Dogterom M (2010) Cell structure and dynamics Editorial overview Arshad Desai and Marileen Dogterom. Curr Opin Cell Biol 22:1–3 . doi: 10.1016/j.ceb.2010.01.003
35. Guo M, Gelman H, Gruebele M (2014) Coupled Protein Diffusion and Folding in the Cell. PLoS One 9:e113040 . doi: 10.1371/journal.pone.0113040
36. Ramadurai S, Duurkens R, Krasnikov V V., Poolman B (2010) Lateral diffusion of membrane proteins: Consequences of hydrophobic mismatch and lipid composition. Biophys J. doi: 10.1016/j.bpj.2010.06.036
37. Kong M, Van Houten B (2017) Rad4 recognition-at-a-distance: Physical basis of conformation-specific anomalous diffusion of DNA repair proteins. Prog Biophys Mol Biol 127:93–104 . doi: 10.1016/j.pbiomolbio.2016.12.004
38. Schlimpert S, Klein EA, Briegel A, et al (2012) General Protein Diffusion Barriers Create Compartments within Bacterial Cells. Cell 151:1270–1282 . doi: 10.1016/j.cell.2012.10.046
39. Kühn T, Ihalainen TO, Hyväluoma J, et al (2011) Protein Diffusion in Mammalian Cell Cytoplasm. PLoS One 6:e22962 . doi: 10.1371/journal.pone.0022962
40. Banks DS, Fradin C (2005) Anomalous diffusion of proteins due to molecular crowding. Biophys J. doi: 10.1529/biophysj.104.051078
41. Wachsmuth M, Waldeck W, Langowski J (2000) Anomalous diffusion of fluorescent probes inside living cell nuclei investigated by spatially-resolved fluorescence correlation spectroscopy. J Mol Biol 298:677–689 . doi: 10.1006/jmbi.2000.3692
42. Wüstner D, Solanko LM, Lund FW, et al (2012) Quantitative fluorescence loss in photobleaching for analysis of protein transport and aggregation. BMC Bioinformatics 13:296 . doi: 10.1186/1471-2105-13-296

Summary

The primary goal of the work presented in this thesis was to provide a unique tool that may increase our understanding of the mechanism of cytoplasmic diffusion in signal transduction (networks) in eukaryotic cells, in the form of a chimeric, light-dependent, cytoplasmic signal transduction device in the yeast *Saccharomyces cerevisiae*.

Chapter 1 gives a general introduction to the optogenetics field, as well an insight into the issues connected to signal diffusion in the spatially differentiated eukaryotic cells.

In chapter 2 we further characterize the *in vivo* redox transitions of a flavin-containing photo-sensory receptor domain for such a chimeric device. We provide further evidence for the overlap of the ranges of the redox midpoint potential of the flavin in a specific photoreceptor protein and the redox potential of key intracellular redox-active metabolites, and demonstrate that the redox state and photochemical activity of LOV domains can be recorded *in vivo* in *Escherichia coli*. Significantly, so far *in vivo* reduction of LOV domains under physiological conditions was not observed.

Chapter 3 describes the design and functional characterization of the intended chimera: A light-sensitive histidine protein kinase, derived from the Sln1 kinase of *S. cerevisiae,* translationally fused in a coiled-coil motif with the LOV domain of the stressosome component YtvA from *Bacillus subtilis*. In most chimeras exposure to blue light decreased the rate of autophosphorylation, but rational engineering also allowed the construction of a light-stimulated histidine protein fusion kinase.

In chapter 4 we describe tests that show the *in vivo* functionality of one of the light-sensitive histidine protein kinases, C9, in which exposure to blue light leads to a decrease of its autophosphorylation activity. This orthogonal photo-transduction system can be used to both activate and repress gene expression in *S. cerevisiae*, depending on the specific promoter that is targeted. Furthermore, the device can also be used to initiate nuclear accumulation of a selected signal transduction protein with incident blue light.

In chapter 5 we go into detail on one of the methods for functional testing of the phosphorylation of histidine kinases and their cognate response regulator(s), the so-called Phos-tag method. In this chapter it is described that, despite many attempts, we have not been able to use this method for analysis of the level of phosphorylation of the two response regulators of the Sln1 system, presumably because of a lack of separation of their phosphorylated- and non-phosphorylated form and/or the very unstable nature of the

phosphorylated form of these response regulators. Screening of the recent literature revealed that until now Phos-tag separation of the two forms, i.e. the phosphorylated and non-phosphorylated form, of a eukaryotic response regulator has not yet been reported.

Finally, in the chapter 6 we discuss a few more relevant points that were not highlighted in the discussions of the earlier chapters, predominantly in the light of recent advances in the field of signal diffusion and the design of the light sensing fusion proteins.

Samenvatting

Het belangrijkste doel van het werk dat beschreven is in dit proefschrift is de constructie van een uniek moleculair hulpmiddel dat gebruikt kan worden om ons begrip van diffusie van eiwitten, en eiwit netwerken, in het cytoplasma van eucaryote cellen, op een hoger plan te brengen. Dit hulpmiddel zou moeten bestaan uit een fusie eiwit, opgebouwd uit een lichtgevoelig input domein translationeel gefuseerd met een cytoplasmatisch histidine-specifiek eiwit kinase uit de bakkersgist *Saccharomyces cerevisiae*.

Hoofdstuk 1 is een algemene inleiding in de achtergrondkennis die beschikbaar was rond dit onderwerp bij de start van het onderzoek. Met name wordt ingegaan op issues die te maken hebben met (i) biologische signaaloverdracht, (ii) cytoplasmatische diffusie in ruimtelijk gedifferentieerde cellen (eucaryote) cellen en (iii) optogenetika. Dit laatste is een recent ontstaan onderzoeksveld waar het ontwerpen en gebruik van fusie eiwitten centraal staat, waarin met (zichtbaar) licht de output functie van het eiwit (zoals bijvoorbeeld een kinase activiteit) gemoduleerd kan worden.

In hoofdstuk 2 wordt een karakterisering gepresenteerd van de redox transities van de flavine chromofoor van zo'n fusie-eiwit, in dit geval bestaande uit het LOV-domein van LovK en STAS-domein van een stressosoom eiwit van *B. subtilis*. We laten zien dat de redox transitie van dit flavine plaatsvindt bij een redox potentiaal die dicht ligt bij de redox potentiaal waarbij een aantal belangrijke intracellulaire metabolieten ook zo'n overgang vertonen. Bovendien laten we zien dat de redox toestand van de chromofoor van zo'n LOV-domein ook waargenomen kan worden *in vivo*, i.e. wanneer het eiwit zich bevindt in het cytoplasma van *Escherichia coli*. Maar onder geen van de geteste condities vond een overgang van deze flavine chromofoor naar de (volledig) gereduceerde toestand plaats.

In hoofdstuk 3 wordt het ontwerpen, de constructie en synthese, en de *in vitro* biochemische karakterisering gepresenteerd van de beoogde functionele fusie eiwitten. Deze bestaan uit een N-terminaal LOV-domein (van het stressosoom eiwit YtvA uit *Bacillus subtilis*), translationeel gefuseerd, via een coiled-coil linker structuur, met het Sln1 histidine kinase domein van het osmostress respons systeem van *S. cerevisie*. In de meeste van deze fusie eiwitten zorgt blootstelling aan blauw licht voor een verlaging van de histidine kinase activiteit. Maar via rationele engineering van de lengte van de coiled-coil linker structuur is ook een licht-moduleerbaar kinase verkregen waarin belichting leidt tot een verhoging van de kinase activiteit.

Hoofdstuk 4 beschrijft *in vivo* tests van de functionaliteit van één van de geconstrueerde kinases beschreven in hoofdstuk 3, C9, het fusie eiwit waarin belichting aanleiding gaf tot de sterkste verlaging van de autokinase (i.e. 'zelf-fosforylering' m.b.v. ATP) activiteit. Dit orthogonale licht-afhankelijke systeem kan in *Saccharomyces cerevisiae* zowel gebruikt worden om genexpressie te stimuleren, alsook om repressie van genexpressie te bewerkstelligen, via een specifieke keus van de respectievelijke target promotor. Daarenboven kan dit geconstrueerde hybride kinase ook gebruikt worden om de accumulatie van signaaltransductie componenten in de kern van de gistcellen met een puls van blauw licht te in gang te zetten.

In hoofdstuk 5 wordt in detail ingegaan op de toepassing van een recent geïntroduceerde methode (de 'Phos-tag' methode) om te meten in welke mate specifieke eiwitten, zoals de kinases en response regulators van twee-componenten systemen, gefosforyleerd zijn (op respectievelijk de zijketen van een histidine en een asparaginezuur in de katalytisch centrum van deze twee eiwitten). We beschrijven een serie experimenten waaruit we moeten concluderen dat, ondanks vele pogingen, het niet gelukt is om met deze techniek de fosforyleringsgraad van de beide response regulatoren van het Sln1 systeem van *S. cerevisiae* te bepalen, terwijl dit voor het controle eiwit, ArcA, wel mogelijk was. Mogelijke verklaringen hiervoor moeten gezocht worden in problemen om de gefosforyleerde en niet-gefosforyleerde vorm van deze eiwitten op een SDS-PAA gel van elkaar te scheiden, of in de intrinsieke instabiliteit van de fosfo-aspartyl binding. Uit een screening van de recente literatuur bleek dat toepassing van deze phos tag methode nog voor geen enkele eucaryote response regulator gerapporteerd is.

Tot slot worden in hoofdstuk 6 een aantal zaken die uit de uitgevoerde experimenten naar voren kwamen, en die nog niet in de discussie paragraaf van de afzonderlijke hoofdstukken aan de orde gekomen waren, bediscussieerd in het licht van de kennis die hieromtrent beschikbaar is in de recente wetenschappelijke literatuur. Dit betreft vooral zaken die te maken hebben met de diffusie van signaal moleculen in het cytoplasma van eucaryote cellen en het ontwerp van lichtgevoelige fusie-eiwitten waarmee dit proces verder bestudeerd kan worden via in ruimte en tijd gelimiteerde belichting.

Streszczenie

Głównym celem tej pracy było stworzenie narzędzia umożliwiającego lepsze zrozumienie dyfuzji sygnału w komórkach eukariotycznych. Aby go zrealizować zaprojektowano chimeryczne, światłoczułe białko, które jest aktywne w cytoplazmie komórek drożdży *Saccharomyces cerevisiae.*

Rozdział 1 zawiera ogólne wprowadzenie do działu optogenetyki oraz detale z zakresu dyfuzji sygnału w przestrzennie zróżnicowanych komórkach eukariotycznych.

W rozdziale 2 scharakteryzowane zostały przemiany *in vivo* fotoreceptorów redox zawierających flawiny używanych w projektowanych chimerycznych białkach. Następnie przedstawione zostały zakresy potencjałów redox białek flawinowych w poszczególnych fotoreceptorach oraz potencjały redox głównych redox-aktywnych metabolitów komórkowych. Zaprezentowane zostało, iż potencjał redox oraz aktywność fotochemiczna domeny LOV mogą być badane *in vivo* w komórkach *Escherichia coli.* Jak dotąd redukcja domeny LOV *in vivo* wykonywana w warunkach fizjologicznych nie została zaobserwowana.

Rozdział 3 opisuje projektowanie i funkcjonalną charakterystykę przedstawionej chimery białkowej: światłoczułej kinazy histydynowej pochodzącej z kinazy Sln1 z *Sachcaromyces cerevisiae,* połączonej poprzez motyw alfa helisy z LOV domeną będącą częścią YtvA. Ytva wchodzi w skład stresosomu w komórkach *Bacillus subtillis*. Większość zaprojektowanych białkowych chimer, po ekspozycji na niebieskie światło wykazywała redukcję w poziomie autofosforylacji. Racjonalne projektowanie połączenia tych dwóch domen, LOV i kinazy Sln1, pozwoliło na zaprojektowanie światłoczułej kinazy histydynowej.

W rozdziale 4 prezentowane są *in vivo* testy przedstawiające funkcjonalność jednej ze światłoczułych kinaz histydynowych, C9, gdzie ekspozycja na niebieskie światło powoduje obniżenie poziomu autofosforylacji. Taki ortogonalny foto-transdukcyjny system może zostać wykorzystany zarówno do aktywacji jak i represji transkrypcji genów w *S. cerevisiae*, w zależności od użytego specyficznego promotora. Poza tym urządzenie to może zostać użyte do indukcji akumulacji wybranego białka należącego do danej sieci transduckyjnej poprzez światło niebieskie.

W rozdziale 5 opisana została w szczegółowy sposób jedną z metod stosowanych do funkcjonalnego testowania poziomu fosforylacji kinaz histydynowych oraz ich biełek regulatorowych, tak zwaną metoda Phos-tag. W tym rozdziale opisane zostało, iż pomimo

wielu prób nie byliśmy w stanie użyć tej metody do analizy poziomu fosforylacji dwóch białek regulatorowych szlaku Sln1. Z powodu braku separacji ufosforylowanej i nie ufosforylowanej formy oraz niestabilność tych regulatorów w ufosforylowanej formie. Przegląd aktualnej literatury nie wyłonił przykładów użycia tej metody do separacji ufosforylowanej i nie ufosforylowanej formy regulatorów eukariotycznych.

Na zakończenie, w rozdziale 6 omówione zostało kilka istotnych zagadnień, które nie zostały opisane w poprzednich rozdziałach, głównie z zakresu dyfuzji sygnału oraz projektowania światło-zależnych białek fuzyjnych.

Publications

Bury A, Hellingwerf KJ (in press) Development of a light-dependent protein histidine kinase. Springer Protocols

Bury A, Hellingwerf KJ (2018) Design, characterization and in vivo functioning of a light-dependent histidine protein kinase in the yeast Saccharomyces cerevisiae. AMB Express 8:53 . doi: 10.1186/s13568-018-0582-7

Bury A, Hellingwerf KJ (2014) On the In Vivo Redox State of Flavin-Containing Photosensory Receptor Proteins. In: Methods in molecular biology (Clifton, N.J.). pp 177–190

van der Horst MA, van Lieshout JFT, Bury A, Hartog AF, Wever R (2012) Sulfation of Various Alcoholic Groups by an Arylsulfate Sulfotransferase from *Desulfitobacterium hafniense* and Synthesis of Estradiol Sulfate. Adv Synth Catal 354:3501–3508 . doi: 10.1002/adsc.201200564

Persoon IF, Hoogenkamp MA, Bury A, Wesselink PR, Hartog AF, Wever R, Crielaard W (2013) Antimicrobial effect of a modified vanadium chloroperoxidase on Enterococcus faecalis biofilms at root canal pH. J Endod. Aug;39(8):1035-8. doi: 10.1016/j.joen.2013.04.038

Abbreviations

ABBREVIATION	EXPLANATION
AMP	adenosine monophosphate
ARG	arginine
ASP	aspartate
ATP	adenosine triphosphate
BLUF	blue-light using FAD
CA	catalitic domain
CFP	cyan fluorescent protein
CLONNAT	neuroserothricine sulphate
CYS	cysteine
DAPI	4',6'-diamidino-phenylindole
DHP	dimerization domain
DNA	deoxyribonucleic acid
EDTA	ethylenediaminetetraacetic acid
EM	electrochemical midpoint potential
FAD	flavin adenine dinucleotide (oxidised)
FADH	flavin adenine dinucleotide (reduced)
FCS	fluorescence correlation spectroscopy
FLIP	fluorescence loss in photobleaching
FMN	flavin adenine nucleotide
FRAP	fluorescence recovery after photobleaching
FRET	(forster resonance energy transfer)
GFP	green fluorescent protein
GLU	glutamine
GMP	guanosine monophosphate
GTP	guanosine triphosphate
HIS	histidine
HK	histidine kinase
HPLC	high-performance liquid chromatograph
HTH	helix-turn-helix
IPTG	isopropyl β-d-thiogalactopyranoside
LED	light emitting diodes
LOV	light oxygen voltage
LYS	lysine
MAPKI	mitogen-activated protein kinase
NAD	nicotinamide adenine dinucleotide (oxidised)
NADH	nicotinamide adenine dinucleotide (reduced)
NADP	nicotinamide adenine dinucleotide phosphate (oxidised)
NADPH	nicotinamide adenine dinucleotide phosphate (reduced)
OCH1	mannosyl-transferase
OD	optical density
PAS	per-arnt-sim
PB	production broth
PBS	phosphate-buffered saline
PEG	polyethylene glycol
PHOS-TAG	1,3-bis[bis(pyridin-2-ylmethyl) amino] propan-2-olato di-zinc(ii) complex
R	response regulator
RAC	receiver domain
SDS-PAGE	sodium dodecyl sulfate–polyacrylamide gel electrophoresis
SER	serine
STAS	sulphate transporter anti-σ antagonist
STORM	stochastic optical reconstruction microscopy
THR	threonine
TYR	tyrosyne
UV	ultra violet
YFP	yellow fluorescent protein
YPD	yeast extract peptone dextrose medium

Acknowledgements

This book ends my very, very, very long journey to obtain PhD. During these years I have met many people. The completion of this book would not be possible without a contribution of many of them. Some did not contribute directly to this thesis but their presence during these years made the journey pleasant.

Firstly, I would like to write thanks words to ma promoter and supervisor, Klaas Hellingwerf. Klaas, thank you for giving me the opportunity to work in the Molecular Microbial Physiology Group. Thank you for sharing your experience and knowledge. Thank you for supporting me also when my life decisions seemed to be a surprise for you. In many moments I doubted if I'll ever write this section of the thesis, thanks to your support I can now write this final page. Besides, I especially appreciate your assistance in completing and shaping my manuscript. Thank you for your endless patience. Your dedication and passion for science are inspiring.

I convey a special thanks to the members of my defense committee for accepting my invitation and spending time reading my thesis and giving valuable feedback.

My sincere gratitude goes to Ron Wever, my first boss at the University of Amsterdam. The experience I got by working in your group gave me a lot of strength. You always encourage me to aim higher. Here my thoughts go also to Louis, I could always count on your expertise with all the chemistry question I had. Also, Lara and Teunie, you encouraged me to start my PhD journey. Going back in time a bit further I would like to mention here also my supervisor during the master study, Urszula Guzik. Your optimistic attitude, passion and deep knowledge where very inspiring.

Back to Amsterdam, and the MMP group. First of all, many thanks to Dennis and Jos to managing the lab. Taking care for every desperate: it doesn't work, but I need it for yesterday. Jos, you are the calmest and warmest person I have ever met. I highly appreciate your expertise in the lab, finishing up last experiments, as well as many discussions about life in general.

Kind words should go to all my roommates: Aniek, Jeroen, Jos, Marijka, Martijn, Orawan, Pascal, Patricia, Que, Rosanne, Vinod and other members of the MMB and Molecular Biology and Microbial Food Safety Groups. Thanks for creating friendly, warm and work stimulating atmosphere both in the office and in the lab.

Something that I'll always remember are the discussions during the lunch break followed by coffee. The level of curiosity of the topics and easiness in switching the topics from the rocket fuel to defecation habits of elephants only proves the grate of all big minds that contributed to these discussions: Alice, Clemens, Andreas, Jeroen, Nadine, Orawan, Pascal, Philipp, Soraya, and all the others…

Alice, Nadine and Orawan thanks for support on the Amsterdam Crew group.

Would like to also say a word to my current workmates at the AMC: Alicia, Eric, Jolien, Karen, Karlijne, Sabina, Tugce, thanks for listening to my complains and frustrations.

Last but not least: Chcę podziękować mojej rodzinie (mamie i tacie, babciom, rodzeństwu) za wspieranie mnie w moich decyzjach. Mamo, tato dziękuję za to, że zawsze dawaliście mi możliwość wyboru. Magda i Bartek, dziękuję za motywowanie mnie do dalszej pracy i Waszą przeprowadzkę do Amsterdamu. Szymek za nieustające pytanie, jak mi idzie pisanie i przypominanie o oddechu.

Grzesiek, dziękuję, że towarzysz mi już tyle lat.

Marysia i Hania, w końcu w weekendy będę dla was.

Sincerely,

Aleksandra